

Electrotonic Properties of Axons and Dendrites

Gordon M. Shepherd

We have seen, in Chapter 3, that most neurons are characterized by elaborate dendritic trees and by single axons having complex branching patterns. With this structural apparatus, neurons carry out five basic functions (Fig. 5.1):

1. Reception of synaptic inputs (mostly in dendrites; to some extent in cell bodies; in some cases in axon terminals)
2. Generation of intrinsic activity at any given site on the neuron through voltage-dependent membrane properties and internal second-messenger mechanisms
3. Integration of synaptic responses with intrinsic membrane activity
4. Generation of patterns of impulse discharges in axon, cell body, and dendrites, encoding outputs from the cell
5. Distribution of synaptic outputs (mostly from axon arborizations; in some cases from cell bodies and dendrites).

In addition to specific interactions through synaptic inputs and outputs, neurons may receive and send nonsynaptic signals through chemical messengers (e.g., hormones) and electrical fields.

A fundamental goal of neuroscience is to develop quantitative descriptions of how each region of the neuron mediates its operations and how these operations are coordinated within the neuron so that it can function as an integrated information-processing unit. Such quantitative description is the necessary basis for understanding the functional organization of the neuron. It is also the basis for constructing realistic models to test hypotheses and simulate the roles of neurons, neural systems, and networks in information processing and behavior.

This chapter deals mainly with the spread of activity within and between neuronal regions. Subsequent chapters will focus on specific properties—membrane receptors, internal receptors, synaptically gated membrane channels, intrinsic voltage-gated channels, and second-messenger systems—that mediate the neuron's operations. Slow spread of activity is by diffusion or active transport; rapid spread is by electric current. Many factors determine this rapid spread at any given point in a neuron; the most basic are the passive **electrotonic** properties.

The origins of our understanding of electrotonic properties were succinctly described by Wilfrid Rall,¹ whose brief account (adapted in Box 5.1)^{2–16} highlights the interesting fact that our understanding of electrotonus has arisen from a merging of the study of the flow of current in nerve cells and muscle with the development of cable theory for transmission through electrical cables on the ocean floor. As mentioned in Box 5.1, electrotonic theory was first applied mathematically to the nervous system in the late 19th century for the simplest case of spread of electric current through a single nerve fiber. By the 1930s and 1940s, it was applied to simple invertebrate (crab and squid) axons—the first steps toward the development of the Hodgkin–Huxley equations for the impulse in the axon. The analytical approach is impractical for the complexity of dendritic systems, but the development of computational compartmental models by Rall,^{17–21} beginning in the 1960s, opened the way to **compartmental models**. Together with the analytical methods, these models have provided a sound basis for a theory of dendritic function.^{21,22} A variety of software packages now make it possible for even a beginning student to explore functional properties and construct realistic neuron models.^{23–26} We therefore present modern elec-

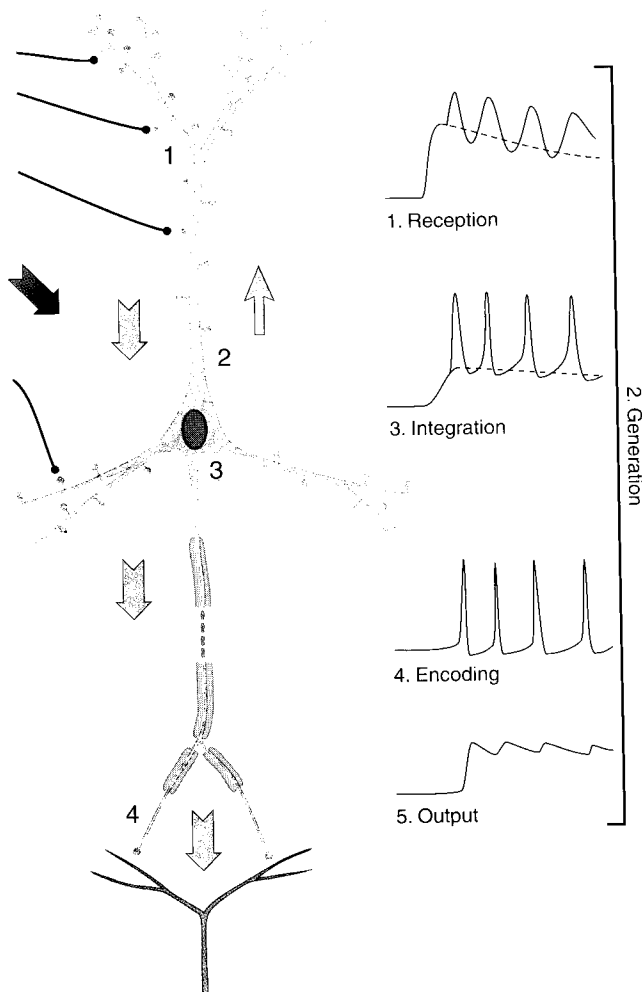


FIGURE 5.1 Nerve cells have four main regions and five main functions. Electrotonic potential spread is fundamental for coordinating the regions and their functions.

trotonic theory within the context of constructing these compartmental models.

SPREAD OF STEADY-STATE SIGNALS

Modern Electrotonic Theory Depends on Simplifying Assumptions

The successful application of cable theory to nerve cells requires that it be based as closely as possible on the structural and functional properties of neuronal processes. The problem confronting the neuroscientist is that most of these processes are quite complicated. As discussed in Chapter 4, a segment of axon or dendrite may be filled with various organelles, bounded by a plasma membrane with its own complex structure

and irregular outline (Fig. 5.2A), and surrounded by myriad neighboring processes. Constructing a model of the spread of electric current through a segment of the neuron therefore requires some carefully chosen simplifying assumptions. These assumptions allow the construction of an **equivalent circuit** of the electrical properties of such a segment. The critical assumptions are as follows^{1,22,27,28}:

1. *Segments are cylinders.* A segment is assumed to be a cylinder with constant radius. This is the simplest assumption; however, compartmental simulations can readily incorporate different geometrical shapes with differing radii if needed (Fig. 5.2B).
2. *The electrotonic potential is due to a change in the membrane potential.* At any instant of time, the "resting" membrane potential (E_r) at any point on the neuron can be changed by several means: injection of current into the cell, extracellular stimulation that causes current to cross the membrane, and a change in membrane conductance (caused by a driving force different from that responsible for the membrane potential). Electric current then begins to flow between that point and the rest of the neuron, in accord with the equation

$$V = V_m - E_r,$$

where V is the electrotonic potential and V_m is the changed membrane potential. Modern neurobiologists recognize that the membrane potential is rarely at rest. In practice, "resting" potential means the membrane potential at any given instant of time other than during an action potential or rapid synaptic potential.

3. *Electrotonic current is ohmic.* All passive electrotonic current flow is assumed to be ohmic—that is, in accord with the simple linear equation

$$E = IR,$$

where E is the potential, I is the current, and R is the resistance. This relation is largely inferred from macroscopic measurements of the conductance of solutions having the composition of the intracellular medium, but is rarely measured directly for a given nerve process. Also largely untested is the likelihood that at the smallest dimensions (0.1- μm diameter or less), the processes and their internal organelles may acquire submicroscopic electrochemical properties that deviate significantly from macroscopic fluid conductance values; compartmental models permit the incorporation of estimates of these properties.

BOX 5.1

THE ORIGINS OF ELECTROTONUS

The mathematical treatment of axonal electrotonus began in the 1870s with the work of Hermann,^{2,3} supported by Weber's⁴ mathematical analysis of the external field in the surrounding volume conductor. Hermann recognized the mathematical analogy of this problem with the problems in heat conduction, but the analogy with Kelvin's treatment of the submarine telegraph cable in the 1850s^{5,6} was first recognized by Hoorweg in 1898.⁷ This cable analogy was developed independently by Cremer^{8,9} and by Hermann¹⁰ early in the 20th century and has been widely used since that time. These mathematical analogies

are important because of the extensive literature devoted to both general mathematical methods and special solutions applicable to problems of this kind.¹¹ Important papers on the steady-state distributions of axonal electrotonus are those of Rushton^{12,13} and of Cole and Hodgkin,¹⁴ published in the 1920s and 1930s. The two most useful mathematical presentations of axonal electrotonus (including consideration of transients) are those provided by Hodgkin and Rushton¹⁵ and by Davis and Lorente de No¹⁶ in the 1940s. (From Rall, 1958¹)

Wilfrid Rall

4. *In the steady state, membrane capacitance is ignored.* The simplest case of electrotonic spread assumes spread from the point of a **steady-state change** (due to injected current, a change in synaptic conductance, or a change in voltage-gated conductance), so that time-varying properties due to

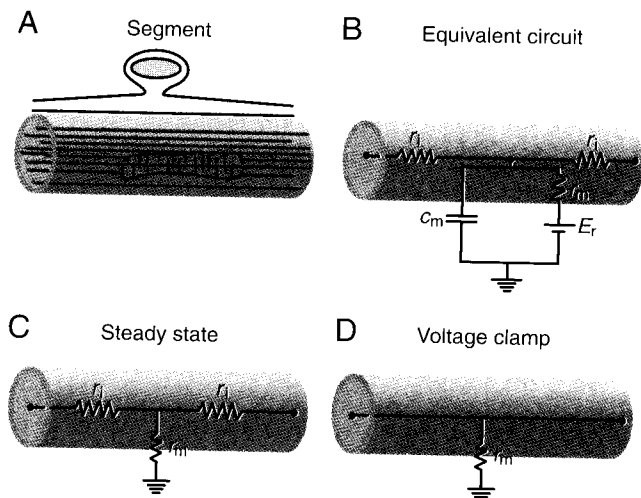


FIGURE 5.2 Construction of a compartmental model of the passive electrical properties of a nerve-cell process begins with (A) identification of a segment of the process and its organelles followed by (B) abstraction of an equivalent electrical circuit based on the membrane capacitance (c_m), membrane resistance (r_m), resting membrane potential (E_r), and internal resistance (r_i); (C) abstraction of the circuit for steady-state electrotonus, in which c_m and E_r can be ignored. (D) The space clamp used in voltage-clamp analysis reduces the equivalent circuit even further to only the membrane resistance (r_m), usually depicted as the membrane conductances (g) for different ions. In a compartmental modeling program, the equivalent circuit parameters are scaled to the size of each segment.

the capacitance of the membrane can be ignored (Fig. 5.2C).

5. *The resting membrane potential can usually be ignored.* In the simplest case, we consider the spread of electrotonic potential (V) relative to a uniform resting potential (E_r), so that the value of the resting potential can be ignored. Where the resting membrane potential may vary spatially, V must be defined for each segment as $V_m - E_r$.
6. *Electrotonic current divides between internal and membrane resistances.* In the steady state, at any point on a process, current divides into two local resistance paths: further within the process through an internal (axial) resistance (r_i) or across the membrane through a membrane resistance (r_m) (see Fig. 5.2C).
7. *Axial current is inversely proportional to diameter.* Within the volume of the process, current is assumed to be distributed equally (the resistance across the process, in the Y and Z axes, is essentially zero). Because resistances in parallel sum to decrease the overall resistance, axial current (I) is inversely proportional to cross-sectional area ($I \propto 1/A \propto 1/\pi r^2$); thus, a thicker process has a lower overall axial resistance than does a thinner process. Because the axial resistance (r_i) is assumed to be uniform throughout the process, the total cross-sectional axial resistance of a segment is represented by a single resistance,

$$r_i = \frac{R_i}{A},$$

where r_i is the internal resistance per unit length of cylinder (in ohms per centimeter of axial

length), R_i is the specific internal resistance (in ohms centimeter, or Ω cm), and $A (= \pi r^2)$ is the cross-sectional area. The internal structure of a process may contain membranous or filamentous organelles that can raise the effective internal resistance or provide high-conductance submicroscopic pathways that can lower it. In voltage-clamp experiments, the space clamp eliminates current through r_i , so that the only current remaining is through r_m , thereby permitting isolation and analysis of different ionic membrane conductances (Fig. 5.2D).

8. *Membrane current is inversely proportional to membrane surface area.* For a unit length of cylinder, the membrane current (i_m) and the membrane resistance (r_m) are assumed to be uniform over the entire surface. Thus, by the same rule of the summing of parallel resistances, the membrane current is inversely proportional to the membrane area of the segment, so that a thicker process has a lower overall membrane resistance. Thus,

$$r_m = \frac{R_m}{c},$$

where r_m is the membrane resistance for unit length of cylinder (in Ω cm of axial length), R_m is the specific membrane resistance (in Ω cm²), and $c (= 2\pi r)$ is the circumference. For a segment, the entire membrane resistance is regarded as concentrated at one point; that is, there is no axial current flow within a segment but only between segments (see Fig. 5.2C).

Modern compartmental simulations recognize that membrane current passes through ion channels in the membrane and that the density and types of these channels vary in different processes and indeed may vary locally in different segments and branches. These differences are readily incorporated into compartmental representations of the processes.

9. *The external medium along the process is assumed to have zero resistivity.* In contrast with the internal axial resistivity (r_i), which is relatively high because of the small dimensions of most nerve processes, the external medium has a relatively low resistivity for current because of its large volume. For this reason, the resistivity of the paths either along a process or to ground is regarded as negligible, and the potential outside the membrane is assumed to be everywhere equivalent to ground (see Fig. 5.2C). This greatly simplifies the equations that describe the spread of electrotonic potentials inside and along the membrane.

Modern compartmental models can simulate any arbitrary distribution of properties, includ-

ing significant values for extracellular resistance. Particular cases in which external resistivity may be very large, such as the special membrane caps around synapses on the cell body or axon hillock of a neuron, can be addressed by suitable representation in the simulations. However, for most simulations, the assumption of negligible external resistance is a useful simplifying first approximation.

10. *Driving forces on membrane conductances are assumed to be constant.* It is usually assumed that ion concentrations across the membrane are constant during activity. However, changes in ion concentrations with activity may occur, particularly in constricted extracellular or intracellular compartments; these changes may cause deviations from the assumptions of constant driving forces for the membrane currents, as well as the assumption of uniform E_r . For example, accumulations of extracellular K^+ may change local E_r ,²⁹ and intracellular accumulations of ions within the tiny volumes of spine heads may change the driving force on synaptic currents.³⁰ These special properties are easily included in most compartmental models.
11. *Cables have different boundary conditions.* In classical cable theory, a cable such as one used for long-distance telecommunication is very long and can be considered of infinite length (one customarily assumes a semi-infinite cable with $V = 0$ at $x = 0$ and only positive values of length x). This assumption carries over to the application of cable theory to long axons, but most dendrites are relatively short. This imposes **boundary conditions** on the solutions of the cable equations, and these boundary conditions have very important effects on electrotonic spread. In highly branched dendritic trees, they are difficult to deal with analytically but are readily represented in compartmental models.

In summary, even the simplest representation of the passive spread of electrotonic potential during a steady-state input to a neuron requires a number of specific assumptions. We will see that an understanding of these assumptions is critical to describing electrotonic spread under the different conditions that the nervous system presents.

Electrotonic Spread Depends on the Characteristic Length (λ)

Let us first consider the spread of electrotonic potential under steady-state conditions. Using the preceding assumptions, we represent a segment of a process as

an internal resistance r_i connected both to the r_i of the next segment and through the membrane resistance r_m to ground (see Fig. 5.2C). In standard cable theory, the steady-state spread of electrotonic potential along this process is described by

$$V = \frac{r_m}{r_i} \cdot \frac{d^2V}{dx^2}. \quad (5.1)$$

This equation states that if there is a steady-state current input at point $x = 0$, the electrotonic potential (V) spreading along the cable is proportional to the second derivative of the potential (d^2V) with respect to distance and the ratio of the membrane resistance (r_m) to the internal resistance (r_i) over that distance. A solution of this equation for a cable of infinite extension for positive values of x gives

$$V = V_0 e^{-x/\lambda}, \quad (5.2)$$

where lambda (λ) is defined as the square root of r_m/r_i (in centimeters) and V_0 is the value of V at $x = 0$.

Inspection of this equation shows that when $x = \lambda$, the ratio of V to the V_0 is $e^{-1} = 1/e = 0.37$. Thus, λ is a critical parameter defining the length over which the electrotonic potential spreading along an infinite cable with given values for internal and membrane resistance decays (is attenuated) to a value of 0.37 of the value at the site of the input. It is accordingly referred to as the **characteristic length** (space constant, or length constant) of the cable. The higher the value of the specific membrane resistance (R_m), the higher the value of r_m for that segment, the larger the value for λ , and the greater the spread (the less the attenuation) of electrotonic potential through that segment (Fig. 5.3). Specific membrane resistance (R_m) is thus an important variable in determining the spread of activity in a neuron. Most of the passive electrotonic current may be carried by K^+ "leak" channels, which are open at "rest" and are largely responsible for holding the cell at its resting potential. However, as mentioned earlier, many cells or regions within a cell are seldom at "rest" but are constantly active, in which case electrotonic current is carried by a variety of open channels. Thus, the effective R_m can vary from values of less than $1000 \Omega \text{ cm}^2$ to more than $100,000 \Omega \text{ cm}^2$ in different neurons and in different parts of a neuron. Note that λ varies with the square root of R_m , and so a 100-fold difference in R_m translates into only a 10-fold difference in λ .

Conversely, the higher the value of the specific internal resistance (R_i), the higher the value of r_i for that segment, the smaller the value of λ , and the less the spread of electrotonic potential through that segment (see Fig. 5.3). Traditionally, the value of R_i has been believed to be in the range of approximately $50\text{--}100 \Omega \text{ cm}$ based on muscle cells and the squid axon. In mammalian neurons, estimates now tend toward a

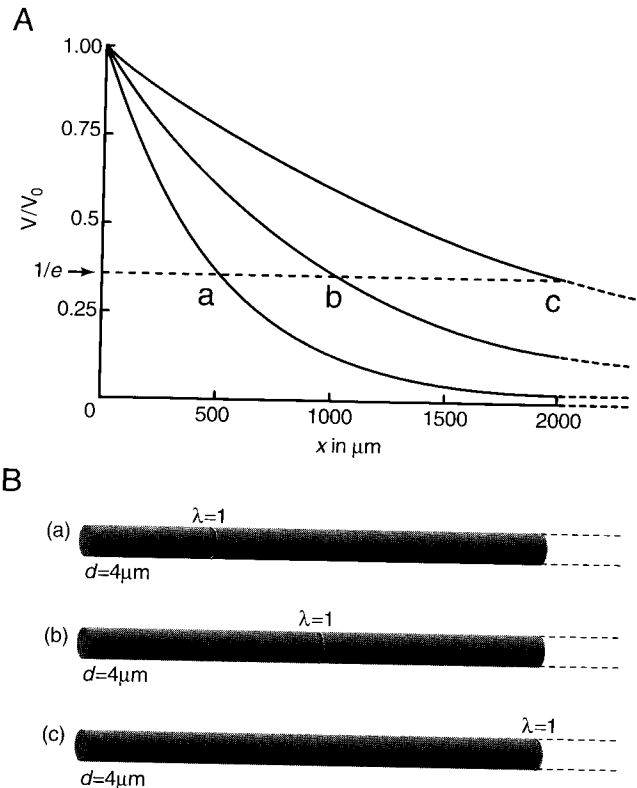


FIGURE 5.3 The space constant governing the spread of electrotonic potential through a nerve-cell process depends on the square root of the ratio between the specific membrane resistance (R_m) and the specific internal resistance (R_i). (A) Potential profiles for processes with three different values of λ . (B) Dotted lines represent the location of λ on each of the three processes.

value of $200 \Omega \text{ cm}$. This limited range may suggest that R_i is less important than R_m in controlling passive current spread in a neuron. The square-root relation further reduces the sensitivity of λ to R_i . However, as noted in assumption 7 in the preceding section, the membranous and filamentous organelles in the cytoplasm may alter the effective R_i . The presence of these organelles in very thin processes, such as distal dendritic branches, spine stems, and axon preterminals, may thus have potentially significant effects on the spread of electrotonic current through them. Furthermore, the relative significance of R_i and R_m greatly depends on the length of a given process, as will be seen shortly.

Electrotonic Spread Depends on the Diameter of a Process

The space constant (λ) depends not only on the internal and membrane resistance, but also on the diameter of a process. Thus, from the relations between r_m and R_m , and r_i and R_i , discussed in the preceding section,

$$\lambda = \sqrt{\frac{r_m}{r_i}} = \sqrt{\frac{R_m}{R_i} \cdot \frac{d}{4}}. \quad (5.3)$$

Neuronal processes vary widely in diameter. In the mammalian nervous system, the thinnest processes are the distal branches of dendrites, the necks of some dendritic spines, and the cilia of some sensory cells; these processes may have diameters of only $0.1 \mu\text{m}$ or less (the thinnest processes in the nervous system are approximately $0.02 \mu\text{m}$). In contrast, the largest processes in the mammal are the largest myelinated axons and the largest dendritic trunks, which may be from

20 to $25 \mu\text{m}$. This means that the range of diameters is approximately three orders of magnitude. Note, again, that the relation to λ is the square root; thus, over a 10-fold difference in diameter, the difference in λ is only about 3-fold (Fig. 5.4).

Electrotonic Properties Must Be Assessed in Relation to the Lengths of Neuronal Processes

As noted earlier, application of classical cable theory to neuronal processes assumes that the processes are

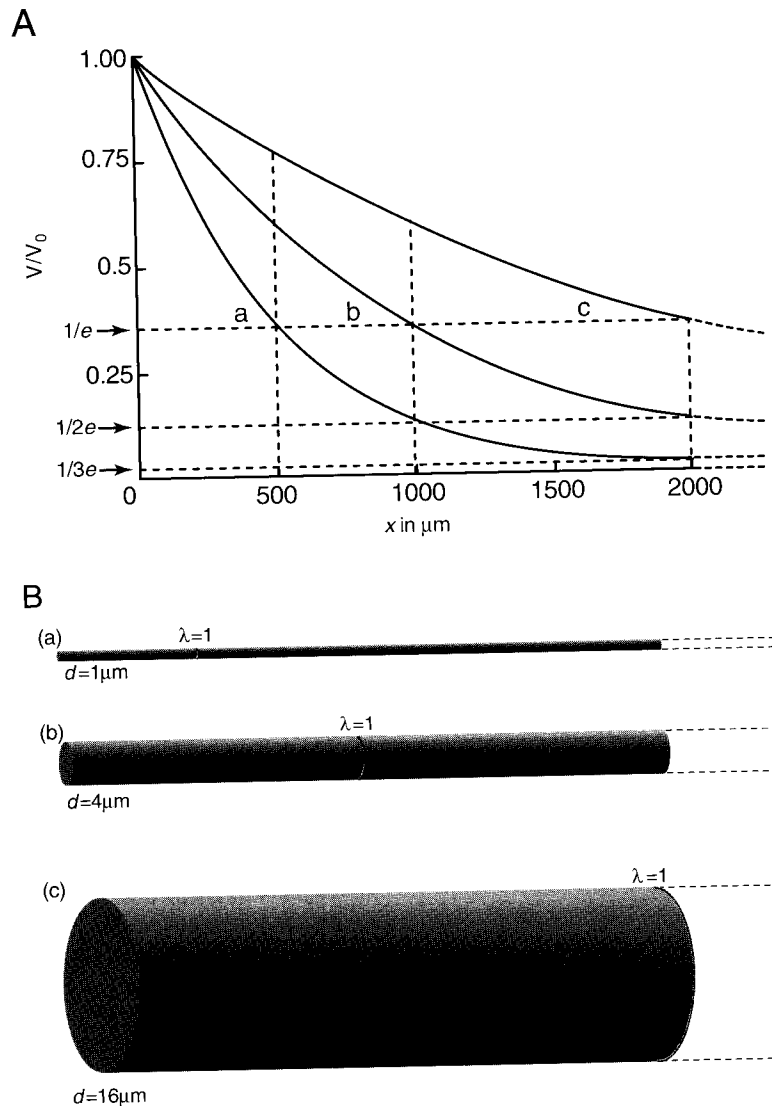


FIGURE 5.4 The space constant governing the spread of electrotonic potential through a nerve-cell process also depends on the square root of the diameter of the process. (A) Potential profiles for processes with three different diameters but fixed values of R_i and R_m . (B) The three axon profiles in (A). Note that to double λ , the diameter must be quadrupled.

infinitely long. However, because neuronal processes have finite lengths, the length of a given process must be compared with λ to assess the extent to which λ accurately describes the actual electrotonic spread in that process. For example, one of the largest processes in any nervous system, the squid giant axon, has a diameter of approximately 1 mm. For this axon, R_m has been estimated as $600 \Omega \text{ cm}^2$ (a very low value compared to most values of R_m in mammals), and R_i is approximately $80 \Omega \text{ cm}$, the value of Ringer solution (note that the very large diameter is counterbalanced by the very low R_m). Putting these values into Eq. (5.3) gives a λ of approximately 4.5 mm. The real length of the giant axon is several centimeters; to relate real length to characteristic length, we define **electrotonic length**^{1,20,27} as

$$L = x / \lambda. \quad (5.4)$$

Thus, if $x = 30 \text{ mm}$, then $L = 30 \text{ mm} / 4.5 \text{ mm} = 7$; that is, the real length of the giant axon is seven characteristic lengths. However, by only three characteristic lengths, the electrotonic potential decays to only a small percentage of the original value (see Fig. 5.4); so for this case the assumption of an infinite length is justified. A reason often given for why the nervous system needs impulses is that impulses enable it to overcome the severe attenuation of passively spreading potentials that occurs over the considerable lengths required for transmission of signals by axons.

The relative importance of R_i and R_m in controlling current spread depends on the length of a segment relative to its characteristic length λ . Consider, for example, a neuronal process (large axon or dendrite) $10 \mu\text{m}$ in diameter, with $R_i = 100 \Omega \text{ cm}$ and $R_m = 10,000 \Omega \text{ cm}^2$.²² By the preceding definitions, the longitudinal resistance r_i per unit length (1 cm) would equal $130 \text{ M}\Omega$, whereas the membrane resistance r_m would be only $3 \text{ M}\Omega$. Thus, the relatively low specific internal resistance has a relatively large effect over the unit distance (1 cm) because of the small diameter of the nerve process. Such a process would have a characteristic length of $1500 \mu\text{m}$, where, by definition, $r_m = r_i$, and the current would be equally divided between the two. At shorter distances, more current tends to flow through r_i as the membrane area is reduced (and r_m thereby increases); this becomes an important factor in shaping current flow through small dendritic branches and dendritic spines (as will be seen shortly and in Chap. 13).

Summary

Passive spread of electrical potential along the cell membrane underlies all types of electrical signaling in

the neuron. It is thus the foundation for understanding how the diverse functions of the neuron are coordinated within the neuron, so that the neuron can generate, receive, encode, and send signals in interacting with its neighboring neurons and glial cells.

Electrotonic spread shares properties with electrical transmission through electrical cables; the study of cable transmission for over a century has put these properties on a sound quantitative basis. The theoretical basis for extension of cable theory to complex dendritic trees has been developed in parallel with compartmental modeling methods for simulating dendritic signal processing.

Steady-state electrotonus in dendrites depends on passive resistance, branch diameter, and impedance matching at branch points. Local electrotonic currents underlie the continuous spread of the impulse in unmyelinated axons and the discontinuous spread from node to node in myelinated axons. In dendrites, synaptic potentials are delayed and attenuated by passive membrane properties, exquisitely dependent on the electrotonic properties.

SPREAD OF TRANSIENT SIGNALS

Electrotonic Spread of Transient Signals Depends on Membrane Capacitance

Until now, we have considered only the passive spread of steady-state inputs. However, the essence of many neural signals is that they change rapidly. Fast impulses characteristically last from 1 to 5 ms, and fast synaptic potentials last from 5 to 30 ms. How do the electrotonic properties affect spread of these rapid signals?

Rapid signal spread depends not only on all of the factors discussed thus far, but also on the membrane capacitance (c_m), which is due to the lipid moiety of the plasma membrane. Classically, the value of the specific membrane capacitance (C_m) has been 1 microfarad per square centimeter ($1 \mu\text{F cm}^{-2}$). However, a value of $0.6\text{--}0.75 \mu\text{F cm}^{-2}$ is now preferred for the lipid moiety itself, the remainder being due to gating charges on membrane proteins.²²

The simplest case demonstrating the effect of the membrane capacitance on transient signals is that of a cell body with no processes (a very unrealistic assumption, but a simple starting point). In the equivalent electrical circuit for a neural process, the membrane capacitance is placed in parallel with the ohmic components of the membrane conductance and the driving potentials for ion flows through those conductances (see Fig. 5.2B). Again neglecting the resting membrane

potential, we take as an example the injection of a current step into a soma; in this case, the time course of the current spread to ground is described by the sum of the capacitive and resistive current (plus the input current, I_{pulse}):

$$C \frac{dV_m}{dt} + \frac{V_m}{R} = I_{\text{pulse}}. \quad (5.5)$$

By rearrangement,

$$RC \frac{dV_m}{dt} + V_m = I_{\text{pulse}} \cdot R, \quad (5.6)$$

where $RC = \tau$ (τ is the **time constant** of the membrane).

A solution of this equation is

$$V_m(T) = I_{\text{pulse}} R (1 - e^{-T}), \quad (5.7)$$

where $T = t/\tau$. This gives the initial response of the membrane to an injected current (I) pulse. When the pulse is terminated, the decay of the initial potential (V_0) to rest is given by

$$V_m(T) = V_0 e^{-T}. \quad (5.8)$$

These “on” and “off” transients are shown in Fig. 5.5. The significance of τ is shown in the diagram; it is the time required for the voltage change across the membrane to reach $1/e = 0.37$ of its final value. This time constant of the membrane defines the transient voltage response of a patch of membrane to a current

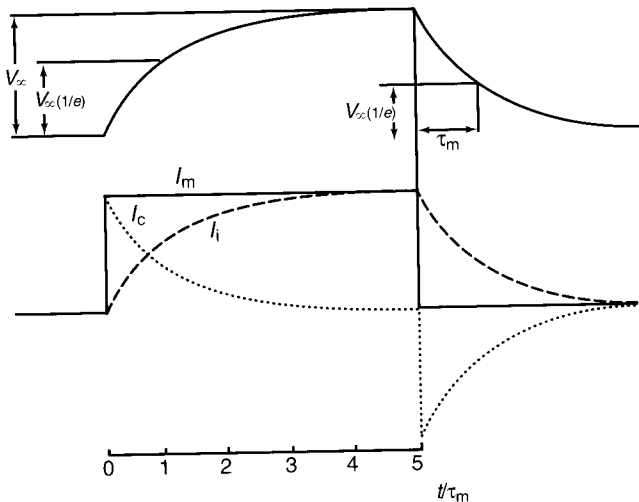


FIGURE 5.5 The equivalent circuit of a single isolated compartment responds to an injected current step by charging and discharging along a time course determined by the time constant τ . In actuality, nerve-cell segments are parts of longer processes (axonal or dendritic) or larger branching trees, so the actual time courses of charging or discharging are modified. Abbreviations: V_{∞} , steady-state voltage; I_m , injected current applied to membrane; I_c , current through the capacitance; I_i , current through the ionic leak conductance; τ_m , membrane time constant.

step in terms of the electrotonic properties of the patch, analogous to the way that the length constant defines the spread of voltage change over distance in terms of the electrotonic properties of a segment.

A Two-Compartment Model Defines the Basic Properties of Signal Spread

These spatial and temporal cable properties can be combined in a two-compartment model³¹ that will apply to the generation and spread of any arbitrary transient signal (Fig. 5.6).

In the simplest case, current is injected into one of the compartments. For a positive current pulse, the positive charge injected into compartment A attempts to flow outward across the membrane, partially opposing the negative charge on the inside of the lipid membrane (this is the charge responsible for the negative resting potential), thereby depolarizing the membrane capacitance (C_m) at that site. At the same time, the charge begins to flow across the membrane through the resistance of the ionic membrane channels (R_m) that are open at that site. The proportion of charge divided between C_m and R_m determines the rate of charge of the membrane—that is, the membrane time constant, τ . However, charge also starts to flow through the internal resistance (R_i) into compartment B, where the same events take place. The charging (and discharging) transient in compartment A departs from the time constant of a single isolated compartment and is faster because of the impedance load (e.g., current sink) of the rest of the cable (represented by compartment B). Thus, the time constant of the system no longer describes the charging transient, which is faster because of the conductance load of one compartment on another (note that this is analogous to the way that the conductance load makes the electrotonic potential more attenuated than the space constant). The system is entirely passive and invariant; the response to a second current pulse sums linearly with that of the first.

Understanding this case is useful because an experimenter often uses electrical currents as stimuli in analyzing nerve function; however, it is not the way in which a neuron normally generates current flows. This usually occurs by means of a localized **conductance change** across the membrane. Consider such a change in the example of compartment A in Fig. 5.6. Assume a change in the ionic conductance for Na^+ , as in the initiation of an action potential or an excitatory postsynaptic potential, producing an inward positive current in compartment A. The charge transferred to the interior surface of the membrane attempts to follow the same paths followed by the injected current just described: opposing the negativity inside the mem-

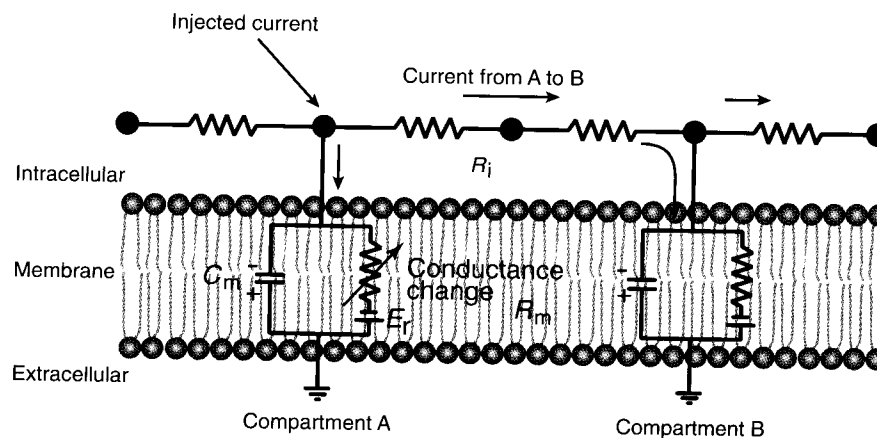


FIGURE 5.6 The equivalent circuit of two neighboring compartments or segments (A and B) of an axon or dendrite shows the pathways for current spread in response to an input (injected current or increase in membrane conductance) at segment A.

brane capacitance; crossing the membrane through the open membrane channels to ground; and spreading through the internal resistance to the next compartment, where the charge flows are similar. Thus, the two cases start with different means of transferring positive charge within the cell, but from that point the current paths and the associated spread of the electrotonic potential are similar. The electrotonic current that spreads between the two segments is also referred to as the **local current**. Note again that the charging transient in compartment A is faster than the time constant of the resting membrane; this difference is due both to the conductance load of compartment B and to the fact that the imposed conductance increase in compartment A reduces the time constant of compartment A (by reducing effective R_m). This illustrates a critical point first emphasized by Rall: changes in membrane conductance alter the system so that it is no longer strictly a linear system even though it is a passive system.¹⁷ Nonlinear summation of synaptic responses is further discussed later in this chapter.

Summary

In addition to the properties underlying steady-state electrotonus, passive spread of transient potentials depends on the membrane capacitance. Initiation of electrotonic spread by intracellular injection of a transient electrical current pulse produces an electrotonic potential that spreads by passive local currents from point to point. It is more attenuated in amplitude than the steady-state case as it spreads along an axon or dendrite, due to the low-pass filtering action of the membrane capacitance. Simultaneous current pulses at that site or other sites produce potentials that add linearly,

because the passive properties are invariant. However, electrotonic potentials produced by a transient conductance change do not sum linearly because of the nonlinear interactions of the conductances.

ELECTROTONIC PROPERTIES UNDERLYING PROPAGATION IN AXONS

Impulses Propagate in Unmyelinated Axons by Means of Local Electrotonic Currents

Let us now consider how knowledge of these electrotonic current properties helps us to understand the propagation of an impulse in an axon. (Details on the ionic mechanisms of the nerve impulse can be found in Chapter 6.) The local current spreading through the internal resistance to the neighboring compartment enables the impulse to spread along the membrane of the axon. The rate of spread is determined by both the passive electrotonic properties and the kinetics of the action potential mechanism. For an unmyelinated axon (i.e., one that is not surrounded by myelin or other membranes that restrict the spread of extracellular current), the relevant passive properties are the specific membrane resistance (R_m), the specific internal resistance (R_i), the diameter (d) of the axon, and the specific membrane capacitance (C_m).

Each of these properties is relevant in specific ways. For brief signals such as the action potential, C_m is critical in controlling the rate of change of the membrane potential. For long processes such as axons, R_i opposes electrotonic current flow as the value of R_i increases beyond the characteristic length, as stated

earlier. This effect is greater in thinner axons, which have shorter characteristic lengths. Finally, R_m is a parameter that can vary widely; in addition, the effective membrane resistance encountered by electrotonic current is greatly increased by myelin sheathing. Thus, each of these parameters must be assessed in order to understand the exquisite effects of passive variables on the rates of impulse spread in axons.

A high value of R_m , for example, forces current further along the membrane, increasing the characteristic length and consequently the spread of electrotonic potential; however, at the same time, it increases the membrane time constant, thus slowing the response of a neighboring compartment to a rapid change. Increasing the diameter of the axon (d) lowers the effective internal resistance of a compartment, thereby also increasing the characteristic length. Because these effects are achieved without a concomitant effect on the time constant, changing the diameter is a direct way of affecting the rate of impulse propagation through changes in passive electrotonic properties. The conduction rate of any given axon depends on the particular combination of these properties.^{32,33} For example, in the squid giant axon, the very large diameter (as large as 1 mm) promotes rapid impulse propagation; the very low value of R_m ($600 \Omega \text{ cm}^2$) lowers the time constant (promoting rapid spread) but also decreases the length constant (limiting the spatial extent of spread).

The effects of these passive properties on impulse velocity also depend on other factors. For example, on the basis of the cable equations, we can show that the conduction velocity should be related to the square root of the diameter.³² However, the density of Na^+ channels in fibers of different diameters is not constant; thus, the binding of saxitoxin molecules, for example, to Na^+ channels varies greatly with diameter, from almost $300 \mu\text{m}^{-2}$ in the squid axon to only $35 \mu\text{m}^{-2}$ in the garfish olfactory nerve.³³ Both active and passive properties must be assessed in order to understand a particular functional property.

Myelinated Axons Have Membrane Wrappings and Booster Sites for Faster Conduction

The evolution of larger brains to control larger bodies and more complex behavior required communication over longer distances within the brain and body. This requirement placed a premium on the ability of axons to conduct impulses as rapidly as possible. As noted in the preceding section, a direct way of increasing the rate of conduction is by increasing the diameter, but larger diameters mean fewer axons within a given space, and complex behavior must be mediated by many axons. Another way of increasing the rate of

conduction is to make the kinetics of the impulse mechanism faster; that is, make the rate of increase in Na^+ conductance with increasing membrane depolarization faster. The Hodgkin–Huxley equations for the impulse in mammalian nerves in fact have this faster rate.

As we have seen, rapid spread of local currents is promoted by an increase in R_m but opposed by an associated increase in the time constant. What is needed is an increase in R_m with a concomitant decrease in C_m . This is brought about by putting more resistances in series with the membrane resistance (resistances in series add) while putting more capacitances in series with the membrane capacitance (capacitances in series add as the reciprocals, much like resistances in parallel, as noted earlier). The way the nervous system does this is through a special satellite cell called a Schwann cell, a type of glial cell. As described in Chapter 4, Schwann cells wrap many layers of their plasma membranes around an axon. The membranes contain special constituents and together are called myelin. Myelinated nerves contain the fastest conducting axons in the nervous system. A general empirical finding known as the Hursh factor³⁴ states that the rate of propagation of an impulse in meters per second is six times the diameter of the axon in micrometers. Thus, the largest axons in the mammalian nervous system are approximately $20 \mu\text{m}$ in diameter, and their conduction rate is approximately 120 m s^{-1} , whereas the thin myelinated axons of about $1 \mu\text{m}$ in diameter have conduction rates of approximately 5 to 10 m s^{-1} .

As discussed in Chapter 4, myelinated axons are not myelinated along their entire length; at regular intervals (approximately 1 mm in peripheral nerves), the myelin covering is interrupted by a node of Ranvier. The node has a complex structure. The density of voltage-sensitive Na^+ channels at the node is high ($10,000 \mu\text{m}^{-2}$), whereas it is very low ($20 \mu\text{m}^{-2}$) in the internodal membrane. This difference in density means that the impulse is actively generated only at the node; the impulse jumps, so to speak, from node to node, and the process is therefore called **saltatory conduction**. In faster-conducting axons, the impulse may extend over considerable lengths; for example, in a $20\text{-}\mu\text{m}$ -diameter axon conducting at 120 m s^{-1} , at any instant of time an impulse of 1-ms duration extends over a 120-mm length of axon, which includes more than 100 nodes of Ranvier. It is therefore more appropriate to think of the impulse as being generated simultaneously by many nodes, which adds to local currents spreading to the next adjacent nodes to activate them. A myelinated axon therefore resembles a passive cable with active booster stations. The specific membrane resistance (R_m) at the node is estimated to be only $50 \Omega \text{ cm}^2$, owing to a large number of open ionic channels at rest. This

value of R_m reduces the time constant of the nodal membrane to approximately 50 ms, which enables the nodal membrane to charge and discharge quickly, greatly aiding rapid impulse generation. For axons of equal cross-sectional area, myelination is estimated to increase the impulse conduction rate 100-fold.

In all axons, a critical relation exists between the amount of local current spreading down an adjacent axon and the threshold for opening Na^+ channels in the membrane of the adjacent axon so that propagation of the impulse can continue. This introduces the notion of a **safety factor**, that is, the amount by which the electrotonic potential exceeds the threshold for activating the impulse. The safety factor must allow for a wide range of operating conditions, including adaptation (during high-frequency firing), fatigue, injury, infection, degeneration, and aging. Normally, an excess of local current ensures an adequate margin of safety against these factors. In the squid axon, the safety factor ranges from 4 to 5. In myelinated axons, an exquisite matching between the internodal electrotonic properties and the nodal active properties ensures that the electrotonic potential reaching a node has an adequate amplitude and the node has sufficient Na^+ channels to generate an impulse that will spread to the next node. The safety factors for myelinated axons range from 5 to 10. Thus, the interaction of passive and active properties underlies the safety factors for impulse propagation in axons. Similar considerations apply to the orthodromic spread of signals in dendritic branches and the backpropagation of impulses from the axon hillock into the soma and dendrites.

Theoretically, the conduction velocity, space constant, and impulse wavelength of myelinated fibers scale linearly with fiber diameter,^{32,33} as indeed is indicated in the aforementioned Hursh factor. This difference between myelinated and unmyelinated fibers in their dependence on diameter is thus related to the scaling of the internodal length. At approximately 1 μm in diameter, the Hursh factor breaks down; at less than 1 μm in diameter, there is an advantage, all other factors being equal, for an axon to be unmyelinated. However, myelinated axons are found down to a diameter of only 0.2 μm , and this has been correlated with shorter internodal distances.³⁵ Thus, conduction velocity in myelinated nerve depends on a complex interplay between passive and active properties.

Summary

Electrotonic potentials are said to *spread* by means of passive local currents, whereas action potentials (impulses) are said to *propagate* by means of active local currents. Impulses propagate continuously through

unmyelinated fibers because the active local currents spread directly to neighboring sites on the membrane. This rate of propagation is directly determined by the electrotonic properties of the fiber. In myelinated fibers, the impulse propagates discontinuously from node to node. The electrotonic properties of both the nodal and internodal regions determine not only the rate of impulse propagation but also the safety factor for impulse transmission.

ELECTROTONIC SPREAD IN DENDRITES

Dendrites are the main neuronal compartment for reception of synaptic inputs. Spread of synaptic responses through the dendritic tree depends critically on the electrotonic properties of the dendrites. Because dendrites are branching structures, understanding the rules governing dendritic electrotonus and the resulting integration of synaptic responses in dendrites is much more difficult than understanding those of simple spread in axons.

Dendritic Electrotonic Spread Depends on Boundary Conditions of Dendritic Termination and Branching

Compared with axons, dendrites are relatively short. Their length is an important factor in assessing their electrotonic properties. Consider, in the mammalian nervous system, a moderately thin dendrite of 1 μm (three orders of magnitude smaller than the squid axon) that has a typical R_m of 60,000 $\Omega \text{ cm}^2$ (two orders of magnitude larger than that of the squid axon) and an R_i of 240 $\Omega \text{ cm}$ (three times the squid value). Inserting these values into the equation for characteristic length (Eq. 5.3) gives a λ of approximately 790 μm . This illustrates that although λ is short in thin dendrites, in absolute terms it is relatively long in comparison with the actual lengths of the dendrites; in other words, because of the relatively high membrane resistance, electrotonic spread of potentials is relatively effective within a dendritic branching tree. This essential property underlies the integration of signals in dendrites. However, with this property, the assumption of infinite length no longer holds; dendritic branches are bounded by their terminations, on the one hand, and the nature of their branching, on the other, and an assessment of the spread of electrotonic potentials through them must take these boundary conditions into account.

This problem is approached most easily by considering two extreme types of termination of a dendritic branch. First, consider that at $x = a$ the branch ends in an infinite resistance. In this case, the axial component of the current can spread no further and must therefore seek the only path to ground, which is across the membrane of the cylinder. This current is added to the current already crossing the membrane; in the equation for Ohm's law ($E = IR$), I is increased, giving a larger E . The membrane will thus be more depolarized up to the terminal point a ; in fact, near point a , axial current is negligible and almost all the current is across the membrane, which amounts to a virtual space clamp near point a (Fig. 5.7). If at point a the infinite resistance is replaced by the more realistic assumption of an end that is sealed with surface membrane, only a small amount of current crosses this membrane and attenuation of electrotonic potential is correspondingly slightly greater; thus, the infinite resistance is a useful approximation for assessing the effects of a sealed end on electrotonic spread in a terminal dendritic branch.

At the other extreme, consider that at point a a small dendritic branch opens out into a very large conduc-

tance. Examples are a very small dendritic branch on a large soma and a small branch or spine on a large dendritic branch. Recall that large processes have their resistances in parallel, which gives low current density and small voltage changes. Therefore, a current spreading through the high resistance of a small branch into a large branch encounters a very low resistance. For steady-state current spread, this situation is referred to as a large **conductance load**; for a transient current, we refer to it as a **low impedance** (which includes the effect of the membrane capacitance). Thus, an **impedance mismatch** exists between the high-impedance thin branch and the lower-impedance thick branch. This mismatch reduces any voltage change due to the current and, in the extreme, effectively clamps the membrane to the resting potential (E_r) at that point. The electrotonic potential is thus attenuated through the branch much more rapidly than would be predicted by the characteristic length (see Fig. 5.7). This does not invalidate λ as a measure of electrotonic properties; rather, it means that, as with the time constant, each cable property must be assessed within the context of the size and branching of the dendrites.

All the different types of branching found in neuronal dendrites lie between these two extremes and give rise to a corresponding range of boundary conditions at $x = a$. Consider a segment of dendrite that divides into two branches at $x = a$. We can appreciate intuitively that the amount of spread of electrotonic potential into the two branches will be governed by the factors just considered. One possibility is that the two branches have very small diameters, so their input impedance is higher than that of the segment; in this case, the situation will tend toward the sealed-end case. In contrast, the segment may give rise to two very fat branches, so the situation will tend toward the large-conductance-load case (see Fig. 5.7).

For many cases of dendritic branching, the input impedance of the branches is in between the two extremes, providing for a reasonable degree of impedance matching between the stem branch and its two daughter branches. This situation thus approximates the infinite-cylinder case, in which by definition the input impedance at one site matches that at its neighboring site along the cylinder. The general rules for impedance matching at branch points were worked out by Rall,^{17,20,21,27} who showed that the input conductance of a dendritic segment varies with the diameter raised to the $\frac{3}{2}$ power; there is electrotonic continuity at a branch point equivalent to the infinitely extended cylinder if the diameter of the segment raised to the $\frac{3}{2}$ power equals the sum of the diameters raised to the $\frac{3}{2}$ power of all the daughter branches. A branching pattern that satisfies this rule is shown in Fig. 5.8. Not

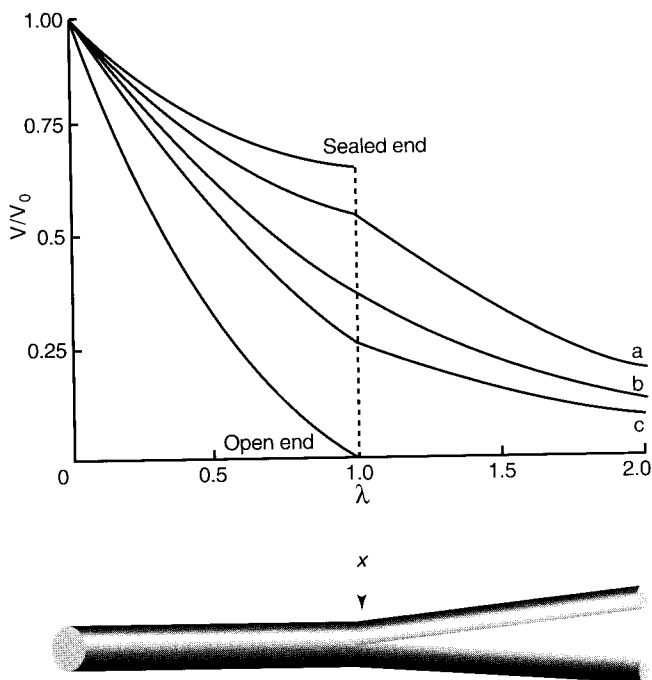


FIGURE 5.7 The spread of electrotonic potential through a short nerve-cell process such as a dendritic branch is governed by the space constant and by the size of the branches; the latter imposes a boundary condition at the branch point. The graph shows three assumptions about the size of the branches relative to the size of the stem, together with the limiting conditions of an open circuit (corresponding to an infinite conductance load) and a closed circuit (corresponding to a sealed tip).

only does the $d^{3/2}$ relation give a rule for constructing an **equivalent cylinder** for a segment and its daughter branches, but iterative application of the rule leads to an equivalent cylinder for an entire dendritic tree if there are similar orders of branching (see Fig. 5.8).

Dendritic Synaptic Potentials Are Delayed and Attenuated by Electrotonic Spread

We are now in a position to assess the effects of cable properties on the time course of the spread of synaptic potentials through dendritic branches and

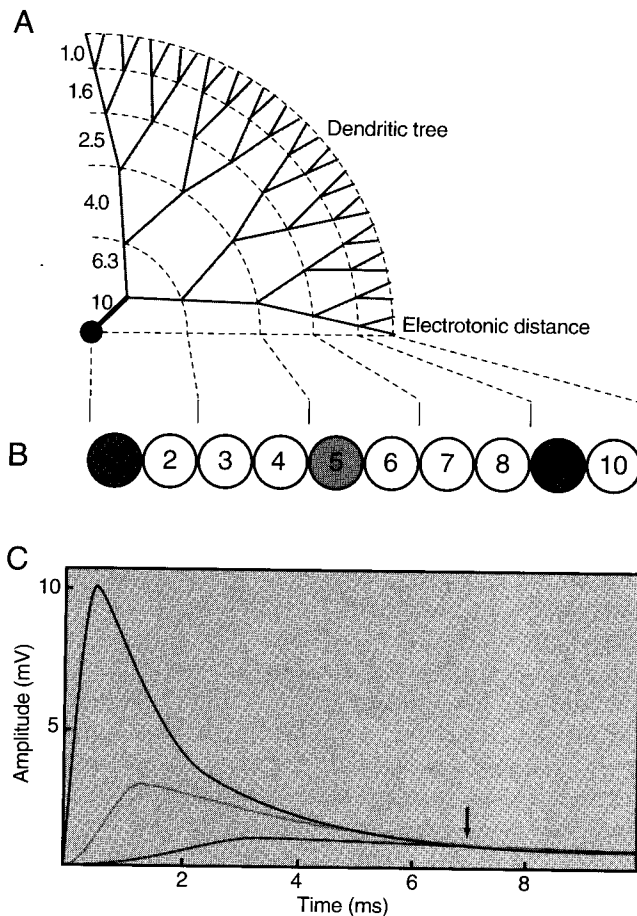


FIGURE 5.8 The spread of electrotonic potentials is accompanied by a delay and an attenuation of amplitude. (A), dendritic diameters (left) satisfy the $\frac{3}{2}$ rule, so that the tree can be portrayed by an equivalent cylinder. An excitatory postsynaptic potential (EPSP) is generated in compartment 1, 5, or 9 (B) while recordings are made from compartment 1. The graph (C) shows the short latency, large amplitude, and rapid transient response in compartment 1 at the site of input, as well as the later, smaller, and slower responses recorded in compartment 1 for the same input to compartments 5 and 9. Despite the initial differences in time course, the responses converge at the arrow to decay together. Based on Rall¹⁷; computer simulation in (C) by K. L. Marton.

trees. The simplest case is a chain of equal compartments; this chain can simulate a single long dendritic branch or it can simulate an entire dendritic tree if the tree satisfies the $d^{3/2}$ branching rule, as described in the preceding section (Fig. 5.8). Consider the case of recording from a soma while delivering a brief excitatory synaptic conductance change to different locations in the dendritic tree. The response to the nearest site is a rapidly rising synaptic potential that peaks near the end of the conductance change and then rapidly decays toward baseline. When the input is delivered to the middle of the chain of compartments, the response in the soma begins only after a delay, rises more slowly, reaches a much lower peak (which is reached after the end of the conductance change in the soma), and decays slowly toward baseline. For input to the terminal compartment, the voltage delay at the soma is so long that the response has scarcely started by the end of the conductance change in the distal dendrite; the response rises slowly to a delayed (several milliseconds) and prolonged plateau that subsides very slowly.

Although the synaptic potentials thus decrease in amplitude as they spread, the rate of spread can be calculated in terms of the half-amplitude at any point. If distance is expressed in units of λ and time in units of τ , then for spread through a semi-infinite cable, we have the simple equation

$$\text{Velocity} = 2 \frac{\lambda}{\tau}. \quad (5.9)$$

Thus, if we ignore boundary effects, for the 10-mm process mentioned earlier in which $\lambda = 1500$ and $\tau = 10$ ms, the velocity of spread would be 0.3 m s^{-1} , or 300 mm s^{-1} . It can be seen that spread can be relatively fast over short distances within a dendritic tree but is very slow in comparison with impulse transmission for an axon of this diameter (60 m s^{-1}). Thus, both the severe decrement and the slow velocity make passive spread by itself ineffective for transmission over long distances.

These general rules of delay and attenuation govern the passive spread of all transient potentials in dendritic branches and trees. From a functional point of view, what matters is the linkage between a response in one part of a branch or branching system and a related site or sites where integration of this signal with other signals takes place. As a rule of thumb, spread within one space constant (see the decrement between compartments 1 and 5 in Fig. 5.8) mediates relatively effective linkage for rapid signal integration, whereas spread over one or two space constants (see the decrement between compartments 1 and 9 in Fig. 5.8) is limited to slower background modulation. In

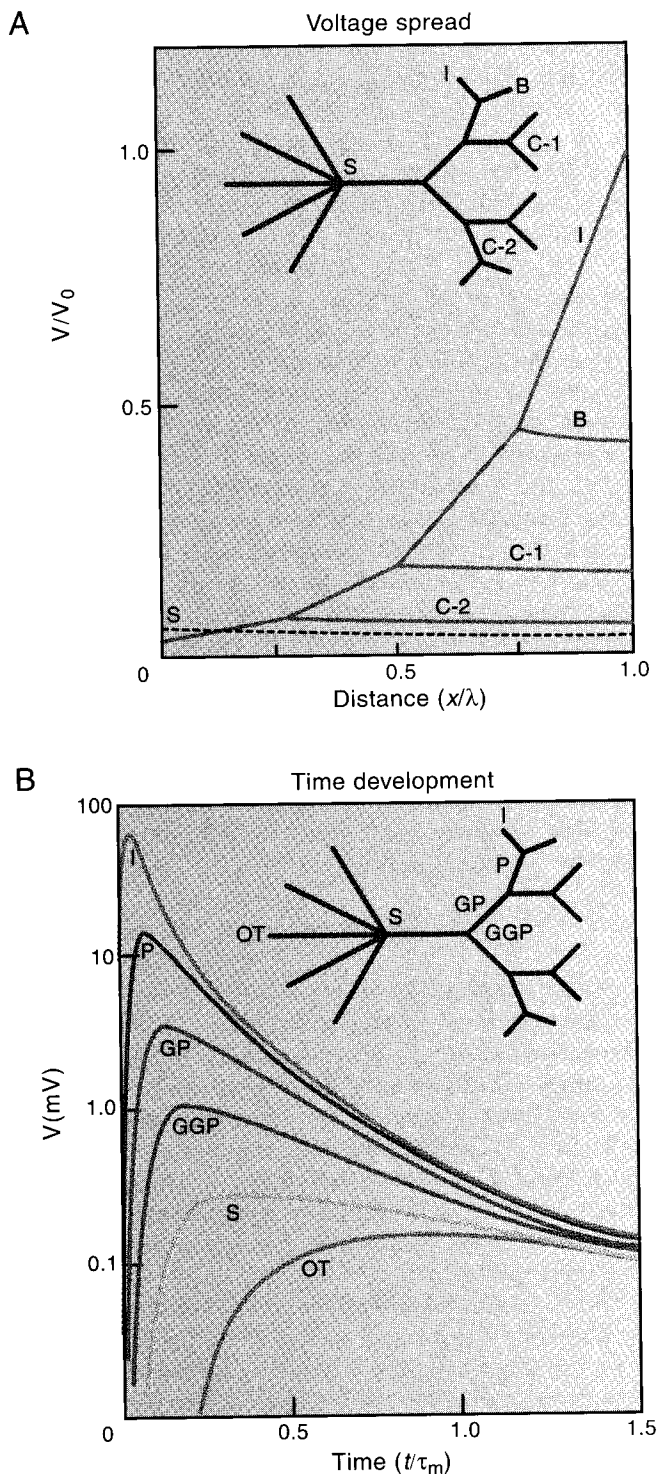


FIGURE 5.9 (A) For steady-state inputs (I) to a distal dendritic branch, the electrotonic potential spreads through the dendritic tree with large decrements into the parent branch (due to the large conductance load) but small decrements into neighboring branches B, C-1, and C-2 (due to the small conductance loads). The resulting potential in the soma (S) is much reduced, as is the response to the same input delivered directly to the soma (because of the low input resistance at the soma and the large conductance load of the dendritic

real dendrites, these limitations are often overcome through boosting the signals by voltage-gated properties (see Chap. 13).

The spread of electrotonic potential from a locus of input involves the equalization of charge on the membrane throughout the system. After cessation of the input, a time is reached when charge has become equalized and the entire system is equipotential; from this time on, the remaining electrotonic potential decays equally at every point in the system. This time is indicated by the vertical arrow in Fig. 5.8C. Before this time, the decaying transients are governed by **equalizing time constants**, indicating electrotonic spread, which can be identified by "peeling" on semilogarithmic plots of the potentials.²⁰ After this time, the decay of electrotonic potential is governed solely by the membrane time constant, τ . In experimental recordings of synaptic potentials, the overall electrotonic length of the dendritic system, considered an "equivalent cylinder," can be estimated from measurements of the membrane time constant and the equalizing time constants. The electrotonic lengths of the dendritic trees of many neuron types lie between 0.3 and 1.5.

What is the spread of the postsynaptic potential throughout the system when a synaptic input is delivered to a single terminal dendritic branch (Fig. 5.9)?^{36,37} Let us begin by considering a steady-state potential. Two main factors are involved. First, in the terminal branch, both the effective membrane resistance and the internal resistance are very large; hence, the branch has a very **high input resistance**, which produces a very large voltage change for any given synaptic conductance change. Balanced against this high input resistance is a second factor: the small branch has a very large **conductance load** on it because of the rest of the dendritic tree. As a result, there is a steep decrement in the electrotonic potential spreading from the branch through the tree to the cell body (see Fig. 5.9A). For comparison, a direct input to the soma produces only a small potential change there because of the relatively very low input resistance at that site.

For a transient synaptic input, a third factor—the **membrane capacitance**—must be taken into account. The small surface area of a terminal branch has little capacitance, and so the amplitude of a transient response differs little from a steady-state response in

tree). (B) For transient inputs (I) to a distal branch, the transient electrotonic potentials decrease sharply in amplitude and are delayed and slower as they spread toward the soma through the parent (P), grandparent (GP), and great-grandparent (GGP) branches, eventually reaching the soma (S) and output trunk (OT). Modified from Segev²⁸ based on Rall and Rinzel.^{36,37}

the branch. However, in spreading out from a small process (such as a distal dendritic twig or spine), the transient synaptic potential is attenuated by the impedance mismatch between the process and the rest of the dendritic tree. Spread of the transient through the dendritic tree is further attenuated by the need to charge the capacitance of the dendritic membrane and is slowed by the time taken for the charging. The amount of slowing is so precise that the relative distance of a synapse in the dendritic tree from the soma can be calculated from experimental measurements in the soma of the time to peak of the recorded synaptic potential.^{20,38} For these reasons, the peak of a synaptic potential spreading from the distal dendrites toward the soma may be severely attenuated, severalfold more than for the case of steady-state attenuation. However, the integrated response (the area under the transient voltage) is approximately equivalent to the steady-state amplitude, indicating that there is only a small loss of total charge (see Fig. 5.9B).

The Electrotonic Structure of the Neuron Changes Dynamically

These considerations show that, compared with the anatomical structure of a dendritic system, which is relatively fixed, the electrotonic properties have complex and subtle effects on signal integration. The effects depend on multiple factors, including the directions of signal spread, inhomogeneities in passive properties, rates of signal transfer, and interactions between synaptic or active conductances, to name a few. The effects can be illustrated in a graphic fashion for the entire soma–dendritic system by taking a stained neuron and replacing it with a representation based on its electrotonic properties. This is termed a morpho-electrotonic transform (MET)³⁹ or neuromorphic transform.⁴⁰

The method is illustrated in Fig. 5.10 for a CA1 hippocampal pyramidal cell. The problem is to compare the spread of a signal from the soma to the dendrites (voltage out, V_{out}) with spread from the dendrites to the soma (voltage in, V_{in}). On the left is the stained neuron, giving rise to a long apical dendrite with many branches and shorter basal dendrites and their branches. On the right, lower diagram, is an electrotonic representation of the neuron for signals spreading from the distal dendrites toward the soma. As shown in Fig. 5.9, there is severe decrement from each distal branch, so that apical and basal dendritic trees have electrotonic lengths of approximately 3 and 2, respectively. By comparison, on the right, upper diagram, is an electrotonic representation of this neuron for a signal spreading from the soma to the dendrites. The basal dendrites have shrunk to almost nothing, indicating

that they are nearly isopotential. This is because they are relatively short compared with their electrotonic lengths and because the sealed-end boundary condition greatly reduces the decrement of electrotonic potential through them (see Fig. 5.7). The apical dendrite has shrunk to an electrotonic length of approximately 1. This analysis helps in understanding that distal synaptic responses decrease considerably in spreading to the soma, which active properties can help to overcome, as we shall see in Chapter 13. On the other hand, signals at the soma “see” a relatively compact dendritic tree.

The analysis in Fig. 5.10 applies to spread of steady-state or very slowly changing signals. What about spread of rapid signals? We have seen that the membrane capacitance makes the dendrites act as a low-pass filter, further reducing rapid signals. The electrotonic transforms can include this effect, as shown in Fig. 5.11. On the left, the electrotonic representation of a pyramidal neuron is shown for a slow (100 Hz) current injected in the soma. The form is similar to that of the cell in Fig. 5.10, with tiny, virtually isopotential basal dendrites, and a longer apical dendritic tree of electrotonic length of approximately 1.5. By comparison, a rapid (500 Hz) signal is severely attenuated in spreading into the dendrites, as shown by the basal dendrites with L of approximately 1 and the apical dendritic tree electrotonic lengths of 4–5. Thus, a somatic action potential could backpropagate into the basal dendrites rather effectively, but would require active properties to invade very far into the apical dendrites. There is direct evidence for these properties underlying backpropagating action potentials in apical dendrites (Chapter 13).

The electrotonic structure of a neuron is not necessarily fixed, but may vary under synaptic control. An example is shown in Fig. 5.12 for the case of a medium spiny cell in the basal ganglia. During low levels of resting excitatory synaptic input, the electrotonic transform of this cell type is relatively large (left) because of the action of a specific K^+ current in the dendrites that holds them relatively hyperpolarized (see arrow at -90 mV). When synaptic excitation increases, the K^+ current is deactivated, reducing the membrane conductance and thereby increasing the input resistance of the cell; the dendritic tree becomes more compact electrotonically (middle) so that synaptic inputs are more effective in activating the cell. As the cell responds to the synaptic excitation, the resulting depolarization activates other K^+ currents, which expand the electrotonic structure again (right). This example illustrates how cable properties and voltage-gated properties interact to control the integrative actions of the neuron.

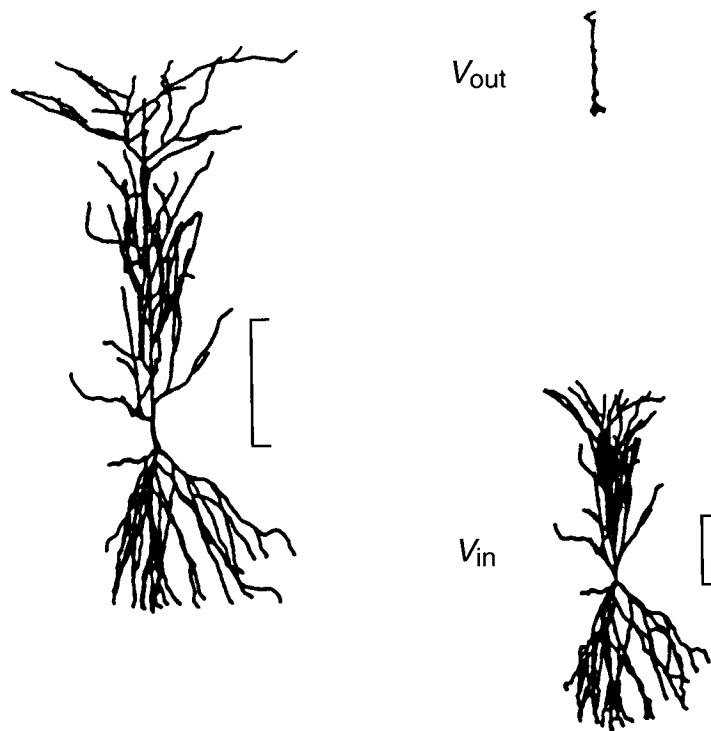


FIGURE 5.10 The electrotonic structure of a neuron varies with the direction of spread of signals. (Left) Stained CA1 pyramidal neuron. (Right) Electrotonic transform of the stained morphology for the case of a voltage spreading toward the cell body (below, V_{in}) and away from the cell body (above, V_{out}). Calibration, 1 electrotonic length. See text. From Carnevale *et al.*⁴⁰

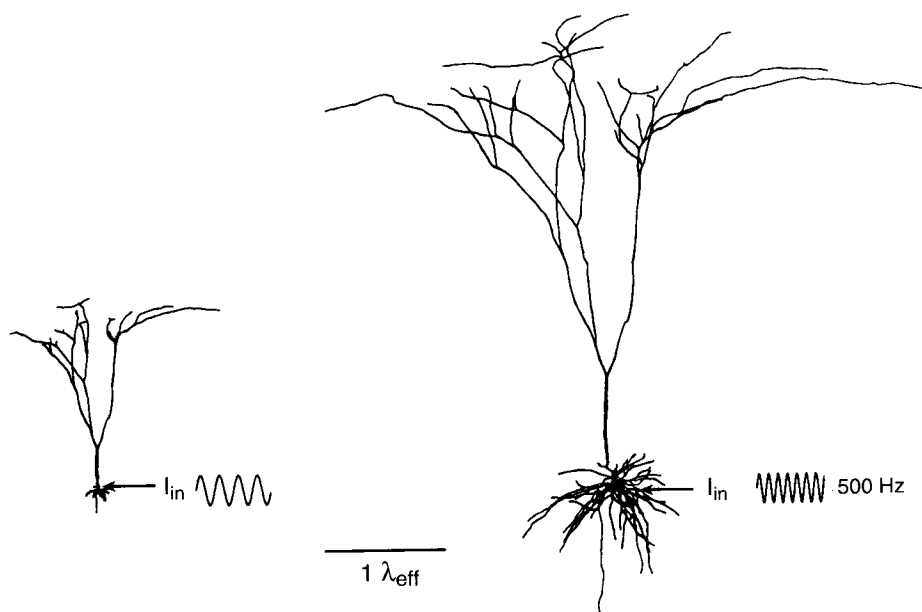


FIGURE 5.11 The electrotonic structure of a neuron varies with the rapidity of signals. (Left) Electrotonic transform of a pyramidal neuron in response to a sinusoidal current of 100 Hz injected into the soma (i.e., this is an example of V_{out}). (Right) Electrotonic transform of same cell in response to 500 Hz. Calibration, 1 electrotonic length. See text. From Zador *et al.*³⁹

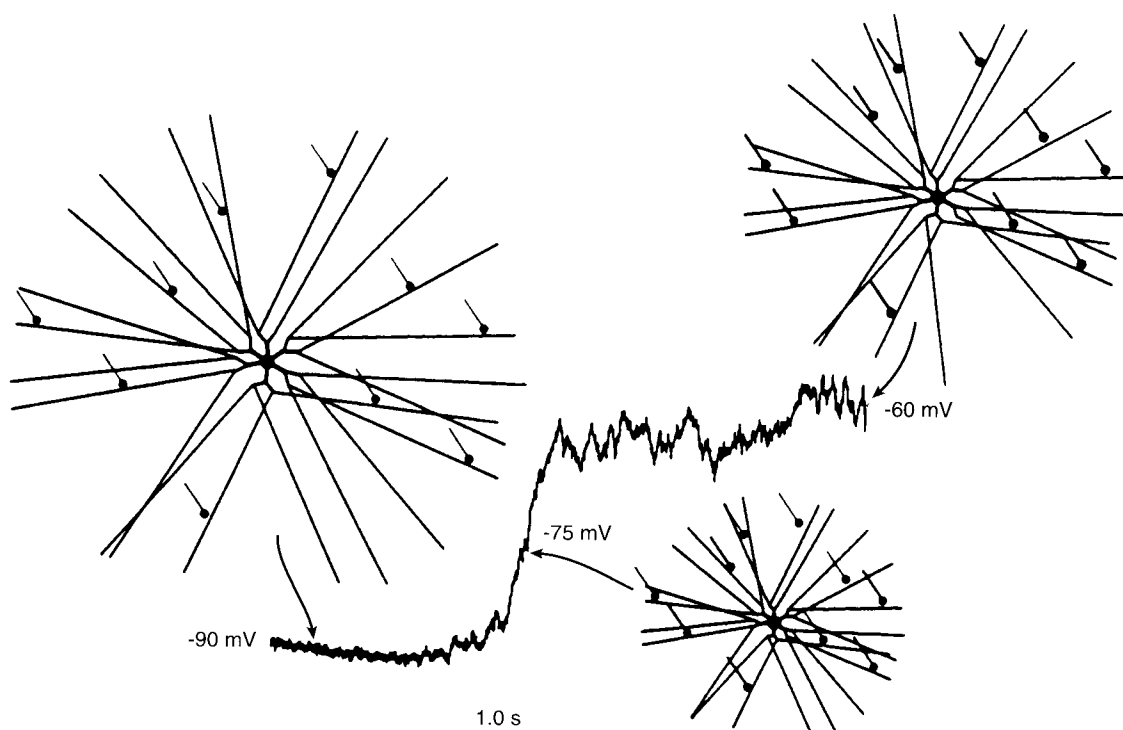


FIGURE 5.12 The electrotonic structure of a neuron can vary with shifts in the resting membrane potential. In this medium spiny cell, the electrotonic transform varies with the resting membrane potential, which in turn reflects the combination of resting voltage-gated K^+ currents and excitatory synaptic currents. See text. From Wilson.⁴¹

Synaptic Conductances in Dendrites Tend to Interact Nonlinearly

It is often assumed that synaptic responses sum linearly, but this is not generally true. In an electrical cable, responses to simultaneous current inputs sum linearly because the cable properties remain invariant at all times; this type of case was considered in Fig. 5.6. However, as noted in regard to that case, synaptic responses in real neurons generate current by means of changes in the membrane conductance at the synapse. In addition to generating current, the change in synaptic conductance alters the overall membrane resistance of that segment and with it the input resistance, thereby changing the electrotonic properties of the whole system. As pointed out by Rall, excitatory and inhibitory conductance changes involve "a change in a conductance which is an element of the system; the system itself is perturbed; the value of a constant coefficient in the linear differential equation is changed; hence the simple superposition rules do not hold."¹⁷

This effect is easily illustrated by the two-compartment model of Fig. 5.6. Consider a synaptic input to compartment A, which decreases the membrane resis-

tance of that compartment. Now consider a simultaneous synaptic input to compartment B, which has the same effect on the membrane resistance of that compartment. The internal current flowing between the two compartments will then encounter a much lower impedance and hence have much less effect on the membrane potential than would have been the case for current injection. The integration of these two responses will therefore give a smaller summed potential than the summation of the two responses taken individually. This effect is referred to as **occlusion**. In essence, each compartment partially short circuits the other through a larger conductance load, thus reducing the combined response.

These properties mean that synaptic integration in dendrites in general is not linear even for purely passive electrotonic properties. The further apart the synaptic sites, the fewer the interactions between the conductances, and the more linear the summation becomes (see Fig. 5.13). These nonlinear properties of passive dendrites combined with the nonlinear properties of voltage-gated channels at local sites on the membrane contribute to the complexity of signal processing that takes place in dendrites, as will be discussed in Chapter 13.

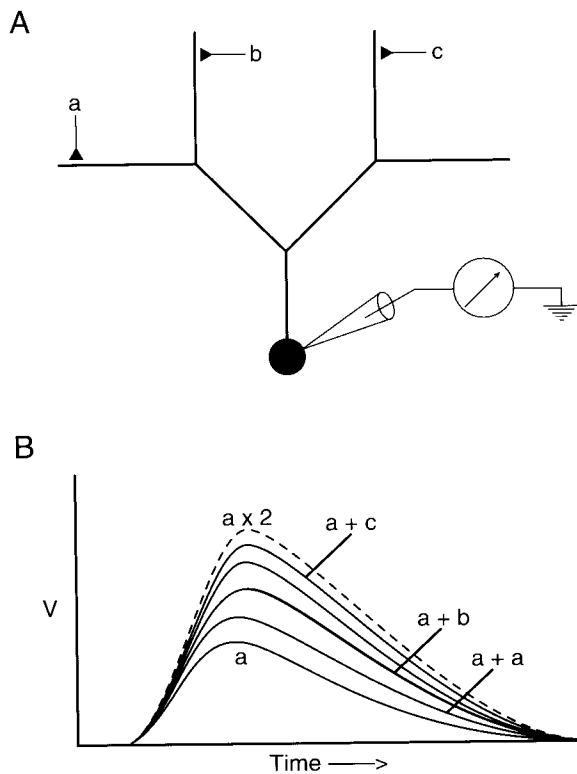


FIGURE 5.13 Schematic diagram of a dendritic tree to illustrate graded effects of nonlinear interactions between synaptic conductances. (A) Three sites of synaptic input (a–c) are shown, with recording site in the soma. (B) The voltage response (V) is shown for the response to a single input at a, the theoretical linear summation for two inputs at a ($a \times 2$), and the gradual reduction in summation from c to a due to increasing shunting between the conductances. See text. From Shepherd and Koch.³¹

The Significance of Active Conductances in Dendrites Depends on Their Relation to Cable Properties

In electrophysiological recordings from the cell body, dendritic synaptic responses often appear small and slow. However, at their sites of origin in the dendrites, the responses tend to have a large amplitude (because of the high input resistances of the thin distal dendrites) and a rapid time course (because of the small membrane capacitance), as the electrotonic simulations in Fig. 5.9 suggest. These properties have important implications for the signal processing that takes place in dendrites. In particular, the fact that the distal dendrites contain sites of voltage-gated channels means that local integration, local boosting, and local threshold operations can take place. These most distal responses need spread no further than to neighboring local active sites to be boosted by these sites; thus, a rapid integrative sequence of these actions ultimately produces significant effects on signal integration at the

cell body. These properties will be considered further in Chapter 13.

In addition to their role in orthodromic signal processing, the cable properties of the neuron are also important for controlling the spread of synaptic potentials from the dendrites through the soma to the site of impulse initiation in the axon hillock initial segment and for backpropagation of an impulse into the soma–dendritic compartments, where it can activate dendritic outputs and interact with the active properties involved in signal processing. These properties will be discussed further in Chapter 13.

Dendritic Spines Form Electrotonic and Biochemical Compartments

The rules governing electrotonic interactions within a dendritic tree also apply at the level of the smallest process of a nerve cell, called a **spine**. This may vary from a bump on a dendritic branch to a twig to a lollipop-shaped process several micrometers long (Fig. 5.14). A dendritic spine usually receives a single excitatory synapse; an axonal spine characteristically receives an inhibitory synapse.

Spines receive most of the excitatory inputs to pyramidal neurons in the cerebral cortex and to Purkinje cells in the cerebellum, as well as to a variety of other neuron types, so an understanding of their properties is critical for understanding brain function.^{43–46} As with the whole dendritic tree, one begins with their electrotonic properties. Given the rules we have built earlier in this chapter, by simple inspection of spine morphol-

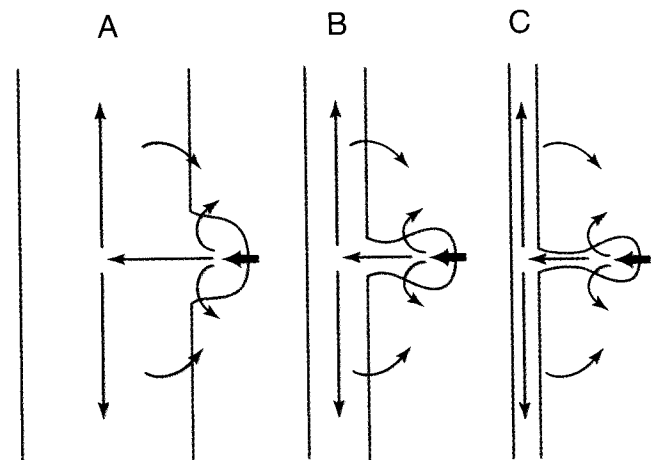


FIGURE 5.14 Diagrams illustrating different types of spines and the current flows generated by a synaptic input. (A) Stubby spine arising from a thick process. (B) Moderately elongated spine from a medium diameter branch. (C) Spine with a long stem originating from a thin branch. Parallel considerations apply to diffusion between the spine head and dendritic branch. Modified from Shepherd.⁴²

ogy as shown in Fig. 5.14, we can postulate several distinctive features that may have important functional implications. First, the smaller the size and the narrower the stem, the higher the input resistance; this gives a large amplitude synaptic potential for a given synaptic conductance. A large depolarizing EPSP could have powerful effects on the local environment within the spine. Second, the small size also means a small capacitance, implying that synaptic (and any active) potentials may be rapid; this means that spines on dendrites can potentially be involved in rapid information transmission. Third, there is an impedance mismatch between the spine head and its parent dendrite; this means that potentials spreading from the spine to the dendrite will suffer considerable decrement, unless there are active properties of the dendrite or of neighboring spines to boost the signal. Fourth, the other side of this impedance mismatch is that potentials spreading through the dendrite will spread into the spine with little decrement; thus, the spine will tend to follow the potential of its dendrite, except for the transient large amplitude responses to its own synaptic input. This means that a spine can serve as a coincidence detector for nearby synaptic responses or for a back-propagating impulse.

In addition to its electrotonic properties, the spine may have interesting parallel biochemical properties. This is because the same cable equations that govern electrotonic properties also have their counterparts in describing the diffusion of substances (as well as the flow of heat). Thus, as already noted, accumulations of only small numbers of ions are needed within the tiny volumes of spine heads to change the driving force on an ion species or to effect significant changes in the concentrations of subsequent second messengers. For this reason, interest in the biochemical properties of spines is increasing. This interest will undoubtedly intensify as the ability to image ion fluxes, such as for Ca^{2+} , and measure other molecular properties of individual spines increases in the near future. The interpretation of those results for the integrative properties of the neuron will require considerations in the biochemical domain that parallel those we have discussed in the electrotonic domain.

The range of properties and possible functions of spines are discussed further in Chapter 13.

Rational Analysis of Dendritic Integration Reveals the True Computational Power of the Neuron

The field of dendritic integration is still relatively young, having been established about 1960. However, as this chapter explains, a number of properties have

emerged that enable us to begin to identify some general principles. Some of the main insights are summarized in the following list adapted from Segev.²⁸ Most of these insights can be seen to build on the principles presented in this chapter. Together, these principles constitute rules for dendritic integration that can be the basis for rational analysis of dendritic functions and serve as a guide for the construction of more realistic network models that will incorporate the true computational power and complexity of the individual neuron.

1. Because of its dendritic tree, the neuron is not isopotential in response to individual synaptic inputs. Compared with the soma, the dendritic tree is relatively compact; there are significant local electrotonic gradients in dendrites.
2. Dendritic attenuation implies the need for multiple synchronous excitatory synaptic inputs to sum and reach threshold for impulse activation at the axonal initial segment. The large local dendritic depolarization and attenuation through the dendritic tree imply that the tree is functionally separated into semiautonomous subunits.
3. In spreading through the dendrites to the soma, the amplitude of transient potentials undergoes severe attenuation, but the attenuation of the total charge is relatively small.
4. Linear system theory predicts that the voltage change at a given recording location will be the same for local current injection into different sites in a passive dendritic tree. However, the same current or conductance change in thin distal dendrites produces a larger change in membrane potential and a steeper attenuation than does a similar change in thick proximal dendrites and the cell body; thus attenuation between different points along the soma-dendritic axis is asymmetrical.
5. In addition to being attenuated, transient synaptic potentials are delayed and become broader as they spread through the dendritic tree. This means that there are multiple time windows for synaptic integration within the dendritic tree.
6. With the exception of the most distal inputs, the delay of a spreading synaptic potential is small compared with the membrane time constant. Thus, for most synapses, the significant time window for somatic integration is the time constant of the somatic membrane.
7. Synaptic inputs tend to sum nonlinearly because of interactions between their conductances. Linear summation is therefore enhanced by spatial distribution of synaptic inputs within the dendritic tree.

8. Inhibitory synapses are most effective when positioned between a more distal excitatory input and a proximal dendrite or soma. In this position, an inhibitory input can "veto" excitatory responses in more distal parts of the dendritic tree.
9. Because of synaptic delay and attenuation, activation of synaptic inputs in a temporal sequence from distal to proximal in the dendritic tree produces a larger summated potential at the soma than a sequence from proximal to distal. Output from neurons with these arrangements is thus inherently directionally selective.
10. The passive membrane properties of the dendritic tree are the net effect of background activity and specific inputs. By changing the net membrane conductance, background synaptic activity can dynamically modulate the input-output operations of the neuron.

Summary

In addition to being dependent on membrane properties, spread of electrotonic potentials in branching dendritic trees is dependent on the boundary conditions set by the modes of branching and termination within the tree. In general, other parts of the dendritic tree constitute a conductance load on activity at a given site; the spread of activity from that site is determined by the impedance match or mismatch between that site and the neighboring sites. Rules governing these impedance relations have been worked out relative to the case in which the sum of the daughter branch diameters raised to the $\frac{3}{2}$ power is equal to that of the parent branch, in which case the system of branches is an "equivalent cylinder," resembling a single continuous cable. Many dendritic trees approximate this relation, thus providing a starting point in analyzing synaptic integration within them.

Synchronous synaptic potentials in several branches spread relatively effectively through most dendritic trees. Responses in individual branches may be relatively isolated because of the decrement of passive spread and require local active boosting for effective communication with the rest of the tree. Passive spread can be characterized in terms of several measures, including characteristic length of the equivalent cylinder. There is scaling within individual branches, such that in finer branches electrotonic spread is relatively effective over their shorter lengths. Integration of synaptic potentials in passive dendrites is fundamentally nonlinear, because of interactions between the synaptic conductances. The rules for electrotonic spread in dendrites are the basis for understanding the contributions of active properties of dendrites.

References

1. Rall, W. (1958). Dendritic current distribution and whole neuron properties. *Nav. Med. Res. Inst. Res. Rep.* **NM 0105.01.02**: 479–525.
2. Hermann, L. (1872). *Arch. Gesamte Physiol. Menschen Tiere* **6**: 312.
3. Hermann, L. (1879). *Handbuch der Physiologie* (L. Hermann, ed.), Vogel, Leipzig.
4. Weber, H. (1873). Über die stationären strömungen der elektricität in cylindren. *J. Reine Angewandte Math.* **76**(1): 1–20.
5. Kelvin, W. T. (1855). On the theory of the electric telegraph. *Proc. R. Soc. London* **7**: 382–399.
6. Kelvin, W. T. (1856). On the theory of the electric telegraph. *Philos. Mag.* [4] **11**: 146–160.
7. Hoorweg, J. L. (1898). Ueber die elektrischen Eigenschaften der Nerven. *Arch. Gesamte Physiol. Menschen Tiere* **71**: 128.
8. Cremer, M. (1899). Zum kernleiterproblem. *Z. Biol.* **37**: 550–553.
9. Cremer, M. (1909). Die allgemeine physiologie ner nerven. In *Handbuch der Physiologie des Menschen*, p. 793. Vieweg, Braunschweig.
10. Hermann, L. (1905). Beiträge zur physiologie und physik des nerven. *Arch. Gesamte Physiol. Menschen Tiere* **109**: 95.
11. Carslaw, H. S., and Jaeger, J. C. (1959). *Conduction of Heat in Solids*. Oxford University Press, London.
12. Rushton, W. A. H. (1927). The effect upon the threshold for nervous excitation of the length of nerve exposed and the angle between current and nerve. *J. Physiol. (London)* **63**: 357.
13. Rushton, W. A. H. (1934). A physical analysis of the relation between threshold and interpolar length in the electric excitation of medullated nerve. *J. Physiol. (London)* **82**: 332–352.
14. Cole, K. C., and Hodgkin, A. L. (1939). Membrane and protoplasm resistance in the squid giant axon. *J. Gen. Physiol.* **22**: 671–687.
15. Hodgkin, A. L., and Rushton, W. A. H. (1946). The electrical constants of a crustacean nerve fibre. *Proc. R. Soc. London, Ser. B* **133**: 444–447.
16. Davis, L., and Lorente de Nó, R. (1947). Contribution to the mathematical theory of electrotonus. *Stud. Rockefeller Inst. Med. Res.* **131**: 50–62.
17. Rall, W. (1964). Theoretical significance of dendritic trees for neuronal input-output relations. In *Neural Theory and Modelling* (R. F. Reiss, ed.), pp. 73–97. Stanford University Press, Stanford, CA.
18. Rall, W. (1967). Distinguishing theoretical synaptic potentials computed for different soma-dendritic distributions of synaptic input. *J. Neurophysiol.* **30**: 1138–1168.
19. Rall, W., and Shepherd, G. M. (1968). Theoretical reconstruction of field potentials and dendrodendritic synaptic interactions in olfactory bulb. *J. Neurophysiol.* **31**(6): 884–915.
20. Rall, W. (1977). Core conductor theory and cable properties of neurons. In *The Nervous System: Cellular Biology of Neurons* (E. R. Kandel, ed.), Vol. 1: pp. 39–97. Am. Physiol. Soc., Bethesda, MD.
21. Segev, I., Rinzel, J., and Shepherd, G. M., eds. (1995). *The Theoretical Foundation of Dendritic Function*. MIT Press, Cambridge, MA.
22. Jack, J. J. B., Noble, D., and Tsien, R. W. (1975). *Electrical Current Flow in Excitable Cells*. Oxford University Press (Clarendon), London.
23. Shepherd, G. M., and Brayton, R. K. (1979). Computer simulation of a dendrodendritic synaptic circuit for self- and lateral-inhibition in the olfactory bulb. *Brain Res.* **175**: 377–382.
24. Hines, M. (1984). Efficient computation of branched nerve equations. *Int. J. Bio-Med. Comput.* **15**: 69–76.
25. Bower, J., and Beeman, D., eds. (1995). *The Book of Genesis*. Springer-Verlag (Telos), New York.
26. Ziv, I., Baxter, D. A., and Byrne, J. H. (1994). Simulator for neural

- networks and action potentials: description and application. *J. Neurophysiol.* **71**: 294–308.
27. Rall, W. (1959). Branching dendritic trees and motoneuron membrane resistivity. *Exp. Neurol.* **1**: 491–527.
 28. Segev, I. (1995). Cable and compartmental models of dendritic trees. In *The Book of Genesis* (J. M. Bower and D. Beeman, eds.), pp. 53–82. Springer-Verlag (Telos), New York.
 29. Pongracz, F., Poolos, N. P., Kocsis, J. D., and Shepherd, G. M. (1992). A model of NMDA receptor-mediated activity in dendrites of hippocampal CA1 pyramidal neurons. *J. Neurophysiol.* **68**(6): 2248–2259.
 30. Qian, N., and Sejnowski, T. J. (1989). An electro-diffusion model for computing membrane potentials and ionic concentrations in branching dendrites, spines and axons. *Biol. Cybernet.* **62**: 1–15.
 31. Shepherd, G. M., and Koch, C. (1990). Dendritic electrotonus and synaptic integration. In *The Synaptic Organization of the Brain* (G. M. Shepherd, ed.), 3rd ed., pp. 439–574. Oxford University Press, New York.
 32. Rushton, W. A. H. (1951). A theory of the effects of fibre size in medullated nerve. *J. Physiol. (London)* **115**: 101–122.
 33. Ritchie, J. M. (1995). Physiology of axons. In *The Axon: Structure, Function, and Pathophysiology* (S. G. Waxman, J. D. Kocsis, and P. K. Stys, eds.), pp. 68–69. Oxford University Press, New York.
 34. Hursh, J. B. (1939). Conduction velocity and diameter of nerve fibers. *Am. J. Physiol.* **127**: 131–139.
 35. Waxman, S. G., and Bennett, M. V. L. (1972). Relative conduction velocities of small myelinated and nonmyelinated fibres in the central nervous system. *Nat., New Biol.* **238**: 217.
 36. Rall, W., and Rinzel, J. (1973). Branch input resistance and steady attenuation for input to one branch of a dendritic neuron model. *Biophys. J.* **13**: 648–688.
 37. Rinzel, J., and Rall, W. (1974). Transient response in a dendritic neuron model for current injected at one branch. *Biophys. J.* **14**: 759–790.
 38. Johnston, D., and Wu, S. M.-S. (1995). *Foundations of Cellular Neurophysiology*. MIT Press, Cambridge, MA.
 39. Zador, A. M., Agmon-Snir, H., and Segev, I. (1995). The morphoelectrotonic transform: A graphical approach to dendritic function. *J. Neurosci.* **15**: 1169–1682.
 40. Carnevale, N. T., Tsai, K. Y., Claiborne, B. J., and Brown, T. H. (1997). Comparative electrotonic analysis of 3 classes of rat hippocampal neurons. *J. Neurophysiol.*, in press.
 41. Wilson, C. J. (1998). Basal ganglia. In *The Synaptic Organization of the Brain*. (G. M. Shepherd, ed.), 4th ed., pp. 329–376. Oxford Univ. Press, New York.
 42. Shepherd, G. M. (1974). *The Synaptic Organization of the Brain*. Oxford Univ. Press, New York.
 43. Shepherd, G. M. (1996). The dendritic spine: A multifunctional integrative unit. *J. Neurophysiol.* **75**: 2197–2210.
 44. Zador, A., and Koch, C. (1994). Linearized models of calcium dynamics: Formal equivalence to the cable equation. *J. Neurosci.* **14**: 4705–4715.
 45. Harris, K. M., and Kater, S. B. (1994). Dendritic spines: Cellular specializations imparting both stability and flexibility to synaptic function. *Annu. Rev. Neurosci.* **17**: 341–371.
 46. Yuste, R., and Tank, D. (1996). Dendritic integration in mammalian neurons, a century after Cajal. *Neuron* **13**: 23–43.

Membrane Potential and Action Potential

David A. McCormick

The communication of information between neurons and between neurons and muscles or peripheral organs requires that signals travel over considerable distances. A number of notable scientists have contemplated the nature of this communication through the ages. In the second century AD, the great Greek physician Claudius Galen proposed that “humors” flowed from the brain to the muscles along hollow nerves. A true electrophysiological understanding of nerve and muscle, however, depended on the discovery and understanding of electricity itself. The precise nature of nerve and muscle action became clearer with the advent of new experimental techniques by a number of European scientists, including Luigi Galvani, Emil Du Bois-Reymond, Carlo Matteucci, and Hermann von Helmholtz, to name a few.^{1,2} Through the application of electrical stimulation to nerves and muscles, these early electrophysiologists demonstrated that the conduction of commands from the brain to muscle for the generation of movement was mediated by the flow of electricity along nerve fibers.

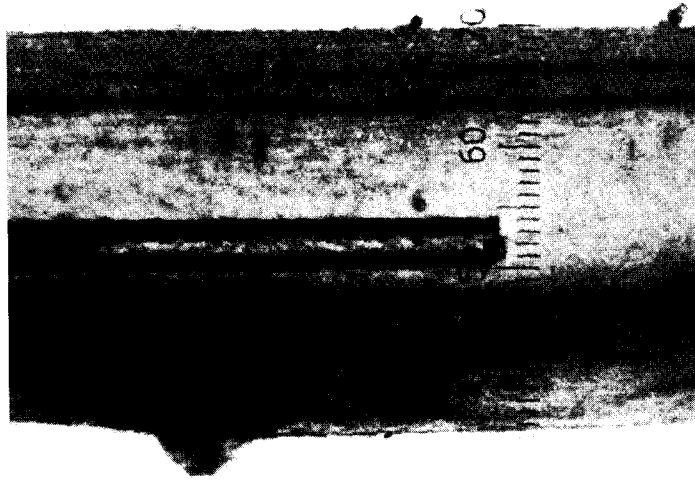
With the advancement of electrophysiological techniques, electrical activity recorded from nerves revealed that the conduction of information along the axon was mediated by the active generation of an electrical potential, called the **action potential**. But what precisely was the nature of these action potentials? To know this in detail required not only a preparation from which to obtain intracellular recordings but also one that could survive *in vitro*. The squid giant axon provided precisely such a preparation, as was first demonstrated by J. Z. Young in 1936.³ Many invertebrates contain unusually large

axons for the generation of escape reflexes; large axons conduct more quickly than small ones and so the response time for escape is reduced (see Chapter 5). The squid possesses an axon approximately 0.5 mm in diameter, large enough to be impaled by even a coarse micropipette (Fig. 6.1). By inserting a glass micropipette filled with a salt solution into the squid giant axon, Alan Hodgkin and Andrew Huxley demonstrated in 1939 that axons at rest are electrically **polarized** exhibiting a resting **membrane potential** of approximately -60 mV inside versus outside.^{4,5} In the generation of an action potential, the polarization of the membrane is removed (referred to as **depolarization**) and exhibits a rapid swing toward, and even past 0 mV (Fig. 6.1). This depolarization is followed by a rapid swing in the membrane potential to more negative values, a process referred to as **hyperpolarization**. The membrane potential following an action potential typically becomes even more negative than the original value of approximately -60 mV. This period of increased polarization is referred to as the **afterhyperpolarization** or the undershoot.

The development of electrophysiological techniques to the point that intracellular recordings could be obtained from the small cells of the mammalian nervous system revealed that action potentials in these neurons are generated through mechanisms similar to that of the squid giant axon.⁶⁻⁹

It is now known that action potential generation in nearly all types of neurons and muscle cells is accomplished through mechanisms similar to those first detailed in the squid giant axon by Hodgkin and Huxley. In this chapter, we consider the cellular

A



B

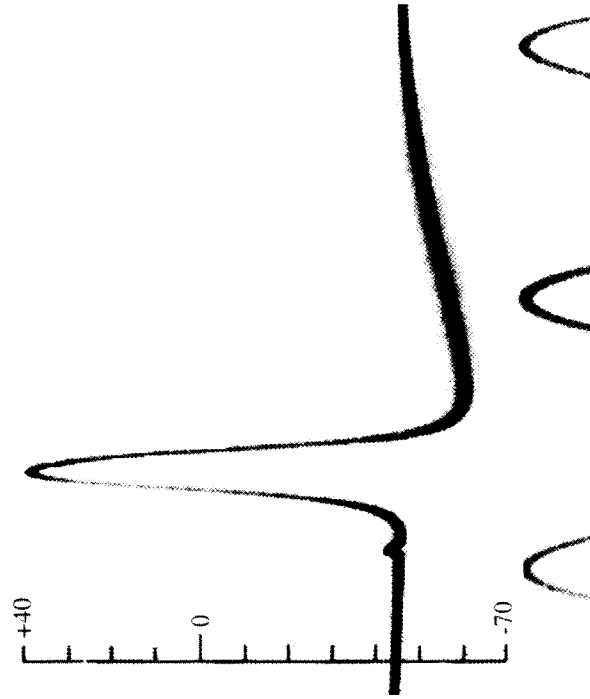


FIGURE 6.1 Intracellular recording of the membrane potential and action potential generation in the squid giant axon. (A) A glass micropipette, about $100\ \mu\text{m}$ in diameter, was filled with seawater and lowered into a squid giant axon that had been dissected free. The axon, about $0.5\ \text{mm}$ in diameter, was transilluminated from behind. (B) The nerve action potential. Note that the membrane potential becomes positive at the peak and that the repolarization is followed by an afterhyperpolarization. The sine wave at the bottom provides a scale for timing, with 2 ms between peaks. From Hodgkin and Huxley.⁴

mechanisms by which neurons and axons generate a resting membrane potential and how this membrane potential is briefly disrupted for the purpose of propagation of an electrical signal, the action potential.

THE MEMBRANE POTENTIAL

The Membrane Potential Is Generated by the Differential Distribution of Ions

Through the operation of ionic pumps and special ionic buffering mechanisms, neurons actively maintain precise internal concentrations of several important ions, including Na^+ , K^+ , Cl^- , and Ca^{2+} . The mechanisms by which they do so are illustrated in Figs. 6.2 and 6.3. The intracellular and extracellular concentrations of Na^+ , K^+ , Cl^- , and Ca^{2+} differ markedly (see Fig. 6.2); K^+ is actively concentrated inside the cell, and Na^+ , Cl^- , and Ca^{2+} are actively extruded to the extracellular space. However, this does not mean that the cell is filled only with positive charge; anions (denoted A^-) to which the plasma membrane is impermeant are also present inside the cell and almost balance the high concentration of K^+ . The osmolarity inside the cell is approximately equal to that outside the cell.

Electrical and Thermodynamic Forces Determine the Passive Distribution of Ions

Ions tend to move down their concentration gradients through specialized ionic pores, known as **ionic channels**, in the plasma membrane. Through simple laws of thermodynamics, the high concentration of K^+ inside glial cells, neurons, and axons results in a tendency for K^+ ions to diffuse down their concentration gradient and leave the cell or cell process (see Fig. 6.3). However, the movement of ions across the membrane also results in a redistribution of electrical charge. As K^+ ions move down their concentration gradient, the intracellular voltage becomes more negative, and this increased negativity results in an electrical attraction between the negative potential inside the cell and the positively charged, K^+ ions, thus offsetting the outward flow of K^+ ions. The membrane is **selectively permeable**; that is, it is impermeable to the large anions inside the cell, which cannot follow the potassium ions across the membrane. At some membrane potential, the “force” of the electrostatic attraction between the negative membrane potential inside the cell and the positively charged K^+ ions will exactly balance the thermal “forces” by which K^+ ions tend to flow down their concentration gradient (see Fig. 6.3). In this circum-

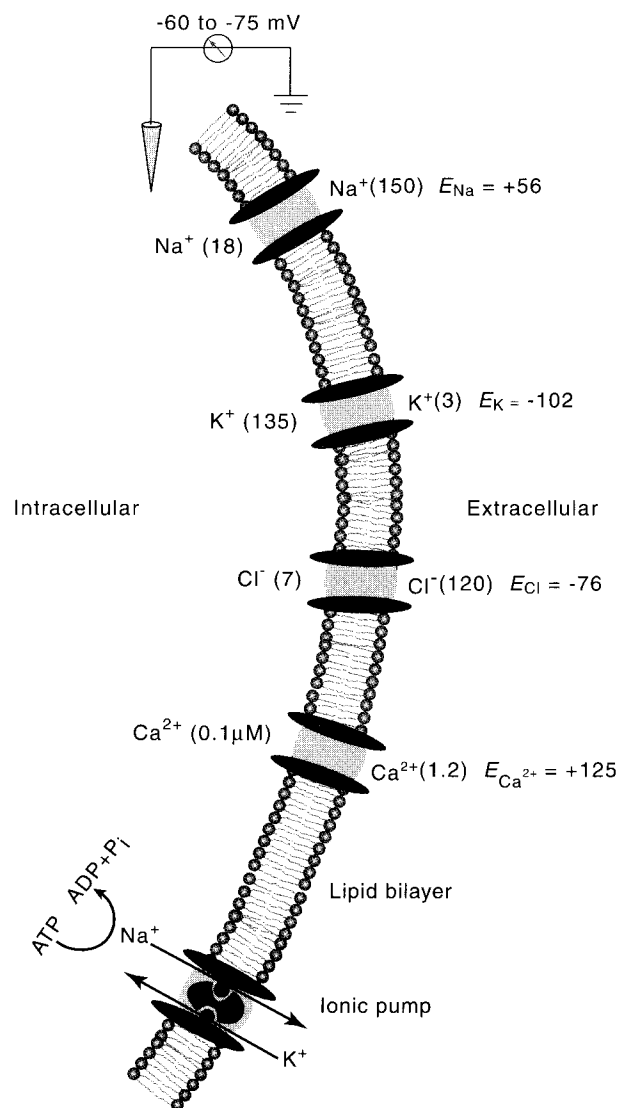


FIGURE 6.2 Differential distribution of ions inside and outside plasma membrane of neurons and neuronal processes, showing ionic channels for Na^+ , K^+ , Cl^- , and Ca^{2+} , as well as an electrogenic Na^+ - K^+ ionic pump (also known as Na^+ , K^+ -ATPase). Concentrations (in millimoles except that for intracellular Ca^{2+}) of the ions are given in parentheses; their equilibrium potentials (E) for a typical mammalian neuron are indicated.

stance, it is equally likely that a K^+ ion exits the cell by movement down the concentration gradient as it is that a K^+ ion enters the cell owing to the attraction between the negative membrane potential and the positive charge of this ion. At this membrane potential, there is no *net* flow of K^+ , and these ions are said to be in **equilibrium**. The membrane potential at which this occurs is known as the **equilibrium potential**. (See Box 6.1¹⁰ for the calculation of the equilibrium potential.)

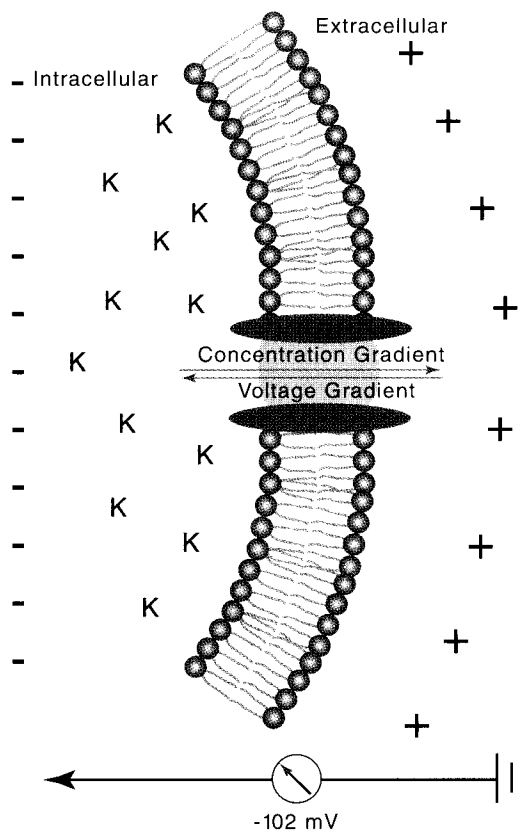


FIGURE 6.3 The equilibrium potential is influenced by the concentration gradient and the voltage difference across the membrane. Neurons actively concentrate K^+ inside the cell. These K^+ ions tend to flow down their concentration gradient from inside to outside the cell. However, the negative membrane potential inside the cell provides an attraction for K^+ ions to enter or remain within the cell. These two factors balance one another at the equilibrium potential, which in a typical mammalian neuron is -102 mV for K^+ .

To illustrate, let us consider the passive distribution of K^+ ions in the squid giant axon as studied by Hodgkin and Huxley. The K^+ concentration $[K^+]_i$ inside the squid giant axon is about 400 mM, whereas the $[K^+]_o$ outside the axon is about 20 mM (Table 6.1). Because $[K^+]_i$ is greater than $[K^+]_o$, potassium ions will tend to flow down their concentration gradient, taking positive charge with them. The equilibrium potential (at which the tendency for K^+ ions to flow down their concentration gradient will be exactly offset by the attraction for K^+ ions to enter the cell because of the negative charge inside the cell) at a room temperature of 20°C is

$$E_K = 58.2 \log_{10}(20/400) = -76 \text{ mV}.$$

Therefore, at a membrane potential of -76 mV, K^+ ions have an equal tendency to flow either into or out of the axon. The concentrations of K^+ in mammalian neurons and glial cells differ considerably from that

in the squid giant axon (see Table 6.1). By substituting 3.1 mM for $[K^+]_o$ and 140 mM for $[K^+]_i$ in the Nernst equation, with $T = 37^\circ\text{C}$, we obtain

$$E_K = 61.5 \log_{10}(3.1/140) = -102 \text{ mV}.$$

Movements of Ions Can Cause either Hyperpolarization or Depolarization

In mammalian cells, at membrane potentials positive to -102 mV, K^+ ions tend to flow out of the cell. Increasing the ability of K^+ ions to flow across the membrane—that is, increasing the **conductance** of the membrane to K^+ (g_K)—causes the membrane potential to become more negative, or **hyperpolarized**, owing to the exiting of positively charged ions from inside the cell (Fig. 6.4).

At membrane potentials negative to -102 mV, K^+ ions tend to flow into the cell; increasing the membrane conductance to K^+ causes the membrane potential to become more positive, or **depolarized**, owing to the flow of positive charge into the cell. The membrane potential at which the net current “flips” direction is referred to as the **reversal potential**. If the channels conduct only one type of ion (e.g., K^+ ions), then the reversal potential and the Nernst equilibrium potential for that ion coincide (see Fig. 6.4A). Increasing the membrane conductance to K^+ ions while the membrane potential is at the equilibrium potential for K^+ (E_K) does not change the membrane potential, because no net driving force causes K^+ ions to either exit or enter the cell. However, this increase in membrane conductance to K^+ decreases the ability of other species of ions to change the membrane potential, because any deviation of the potential from E_K increases the drive for K^+ ions to either exit or enter the cell, thereby drawing the membrane potential back toward E_K (see Fig. 6.4B).

The exiting and entering of the cell by K^+ ions during the generation of the membrane potential give rise to a curious problem. When K^+ ions leave the cell to generate a membrane potential, the concentration of K^+ changes both inside and outside the cell. Why does this change in concentration not alter the equilibrium potential, thus changing the tendency for K^+ ions to flow down their concentration gradient? The reason is that the number of K^+ ions required to leave the cell to achieve the equilibrium potential is quite small. For example, if a cell were at 0 mV and the membrane suddenly became permeable to K^+ ions, only about 10^{-12} mol of K^+ ions per square centimeter of membrane would move from inside to outside the cell in bringing the membrane potential to the equilibrium potential for K^+ . In a spherical cell of 25- μm diameter, this would

BOX 6.1

THE NERNST EQUATION

The equilibrium potential is determined by (1) the concentration of the ion inside and outside the cell, (2) the temperature of the solution, (3) the valence of the ion, and (4) the amount of work required to separate a given quantity of charge. The equation that describes the equilibrium potential was formulated by a German physical chemist named Walter Nernst in 1888¹⁰:

$$E_{\text{ion}} = RT/zF \cdot \ln[\text{ion}]_o/[\text{ion}]_i.$$

Here, E_{ion} is the membrane potential at which the ionic species is at equilibrium, R is the gas constant [8.315 joules per Kelvin per mole ($\text{J K}^{-1} \text{mol}^{-1}$)], T is the temperature in Kelvins ($T_{\text{Kelvin}} = 273.16 + T_{\text{Celsius}}$), F is Faraday's constant

[96,485 coulombs per mole (C mol^{-1})], z is the valence of the ion, and $[\text{ion}]_o$ and $[\text{ion}]_i$ are the concentrations of the ion outside and inside the cell, respectively. For a monovalent, positively charged ion (cation) at room temperature (20°C), substituting the appropriate numbers and converting natural log (\ln) into log base 10 (\log_{10}) result in the equation

$$E_{\text{ion}} = 58.2 \log_{10}[\text{ion}]_o/[\text{ion}]_i;$$

at a body temperature of 37°C , the Nernst equation is

$$E_{\text{ion}} = 61.5 \log_{10}[\text{ion}]_o/[\text{ion}]_i.$$

amount to an average decrease in intracellular K^+ of only about $4 \mu\text{M}$ (e.g., from 140 to 139.996 mM). However, there are instances when significant changes in the concentrations of K^+ may occur, particularly during the generation of pronounced activity, such as that related to an epileptic seizure. During the occurrence of a tonic-clonic generalized (grand mal) seizure, large numbers of neurons discharge throughout the cerebral cortex in a synchronized manner. This synchronous discharge of large numbers of neurons significantly increases the extracellular K^+ concentration, by as much as a couple of millimoles, resulting in a commensurate positive shift in the equilibrium potential for

K^+ .^{11,12} This shift in the equilibrium potential can increase the excitability of affected neurons and neuronal processes and thus promote the spread of the seizure activity. Fortunately, the extracellular concentration of K^+ is tightly regulated and kept at normal levels through uptake by glial cells as well as by diffusion through the fluid of the extracellular space.¹³

As is true for K^+ ions, each of the different ions to which biological membranes are permeable possesses an equilibrium potential that depends on the concentration of the ions inside and outside the cell. Thus, equilibrium potentials may vary between different cell types, such as those found in animals adapted to live in salt water versus mammalian neurons (see Table 6.1). In mammalian neurons, the equilibrium potential is approximately $+56 \text{ mV}$ for Na^+ , approximately -76 mV for Cl^- , and about $+125 \text{ mV}$ for Ca^{2+} (see Table 6.1 and Fig. 6.2). Thus, increasing the membrane conductance to Na^+ (g_{Na}) through the opening of Na^+ channels depolarizes the membrane potential toward $+56 \text{ mV}$; increasing the membrane conductance to Cl^- brings the membrane potential closer to -76 mV ; and finally increasing the membrane conductance to Ca^{2+} depolarizes the cell toward $+125 \text{ mV}$.

Na^+ , K^+ , and Cl^- Contribute to the Determination of the Resting Membrane Potential

If a membrane is permeable to only one ion and no electrogenic ionic pumps are operating (see next section), then the membrane potential is necessarily at

TABLE 6.1 Ion Concentrations and Equilibrium Potentials

	Inside (mM)	Outside (mM)	Equilibrium potential (mV)
Squid giant axon			
Na^+	50	440	+55
K^+	400	20	-76
Cl^-	40	560	-66
Ca^{2+}	$0.4 \mu\text{M}$	10	+145
Mammalian neuron			
Na^+	18	145	+56
K^+	135	3	-102
Cl^-	7	120	-76
Ca^{2+}	100 nM	1.2	+125

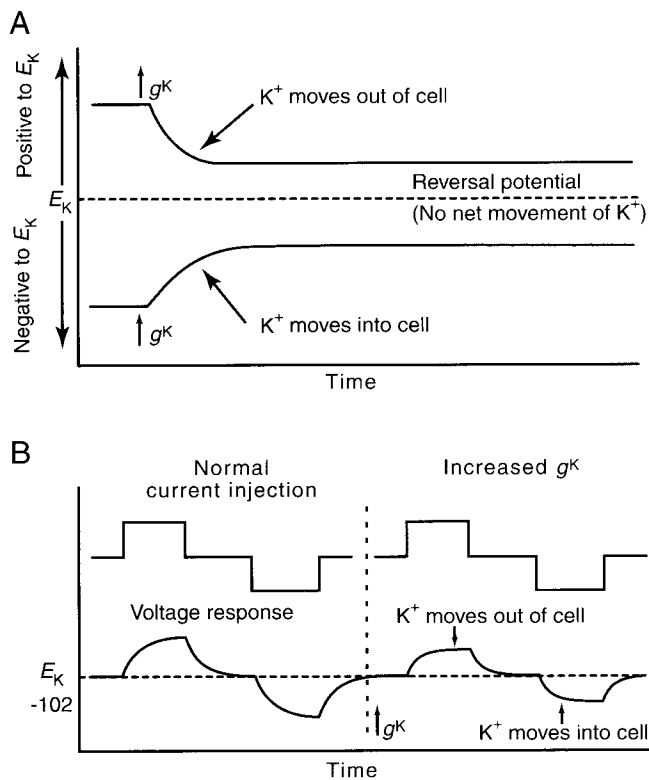


FIGURE 6.4 Increases in K^+ conductance can result in hyperpolarization, depolarization, or no change in membrane potential. (A) Opening K^+ channels increases the conductance of the membrane to K^+ , denoted g_K . If the membrane potential is positive to the equilibrium potential (also known as the reversal potential) for K^+ , then increasing g_K will cause some K^+ ions to leave the cell, and the cell will become hyperpolarized. If the membrane potential is negative to E_K when g_K is increased, then K^+ ions will enter the cell, therefore making the inside more positive (more depolarized). If the membrane potential is exactly E_K when g_K is increased, then there will be no net movement of K^+ ions. (B) Opening K^+ channels when the membrane potential is at E_K does not change the membrane potential; however, it reduces the ability of other ionic currents to move the membrane potential away from E_K . For example, a comparison of the ability of the injection of two pulses of current, one depolarizing and one hyperpolarizing, to change the membrane potential before and after opening K^+ channels reveals that increases in g_K noticeably decrease the responses of the cell.

the equilibrium potential for that ion. At rest, the plasma membrane of most cell types is not at the equilibrium potential for K^+ ions, indicating that the membrane is also permeable to other types of ions. For example, the resting membrane of the squid giant axon is permeable to Cl^- and Na^+ , as well as K^+ , owing to the presence of ionic channels that not only allow these ions to pass but also are open at the resting membrane potential. Because the membrane is permeable to K^+ , Cl^- , and Na^+ , the resting potential of the squid giant axon is not equal to E_K , E_{Na} , or E_{Cl} , but is somewhere in-between these three. A membrane permeable to

more than one ion has a steady-state membrane potential whose value is between those of the equilibrium potentials for each of the permeant ions (Box 6.2).^{14,15}

Different Types of Neurons Have Different Resting Potentials

Intracellular recordings from neurons in the mammalian CNS reveal that different types of neurons exhibit different resting membrane potentials. Indeed, some types of neurons do not even exhibit a true “resting” membrane potential; they spontaneously and continuously generate action potentials even in the total lack of synaptic input. In the visual system, intracellular recordings have shown that the photoreceptor cells of the retina—the rods and cones—have a membrane potential of approximately -40 mV at rest and are hyperpolarized when activated by light.¹⁶ Cells in the dorsal lateral geniculate nucleus, which receive axonal input from the retina and project to the visual cortex, have a resting membrane potential of approximately -70 mV during sleep and -55 mV during waking,^{17–19} whereas pyramidal neurons of the visual cortex have a resting membrane potential of about -75 mV.²⁰ Presumably, the resting membrane potentials of different cell types in the central and peripheral nervous system are highly regulated and are functionally important. For example, the depolarized membrane potential of photoreceptors presumably allows the membrane potential to move in both negative and positive directions in response to changes in light intensity. The hyperpolarized membrane potential of thalamic neurons during sleep (-70 mV) dramatically decreases the flow of information from the sensory periphery to the cerebral cortex,^{21,22} presumably to allow the cortex to be relatively undisturbed during sleep, and the 20-mV membrane potential between the resting potential and the action potential threshold in cortical pyramidal cells may permit the subthreshold computation and integration of multiple neuronal inputs in single neurons (see Chapters 5 and 13).

Ionic Pumps Actively Maintain Ionic Gradients

Because the resting membrane potential of a neuron is not at the equilibrium potential for any particular ion, ions constantly flow down their concentration gradients. This flux becomes considerably larger with the generation of electrical and synaptic potentials, because ionic channels are opened by these events. Although the absolute number of ions traversing the plasma membrane during each action potential or synaptic potential may be small in individual cells, the

BOX 6.2

THE GOLDMAN-HODGKIN-KATZ EQUATION

An equation developed by Goldman¹⁴ and later used by Alan Hodgkin and Bernard Katz¹⁵ describes the steady-state membrane potential for a given set of ionic concentrations inside and outside the cell and the relative **permeabilities** of the membrane to each of those ions:

$$V_m = RT/F \cdot \ln\{(p_K[K^+]_o + p_{Na}[Na^+]_o + p_{Cl}[Cl^-]_i) / (p_K[K^+]_i + p_{Na}[Na^+]_i + p_{Cl}[Cl^-]_o)\}.$$

The relative contribution of each ion is determined by its concentration differences across the membrane and the relative permeability (p_K , p_{Na} , p_{Cl}) of the membrane to each type of ion. If a membrane is permeable to only one ion, then the Goldman-Hodgkin-Katz equation reduces to the Nernst equation. In the squid giant axon, at resting membrane potential, the permeability ratios are

$$p_K : p_{Na} : p_{Cl} = 1.00 : 0.04 : 0.45.$$

The membrane of the squid giant axon, at rest, is most permeable to K^+ ions, less so to Cl^- , and least permeable to Na^+ . (Chloride appears to contribute considerably less to the determination of the resting potential of mammalian neurons.) These results indicate that the resting membrane potential is determined by the resting permeability of the membrane to K^+ , Na^+ , and Cl^- . In theory, this resting membrane potential may be anywhere between E_K (e.g., -76 mV) and E_{Na} ($+55$ mV). For the three ions at 20°C , the equation is

$$V_m = 58.2 \log_{10}\{(1 \cdot 20 + 0.04 \cdot 440 + 0.45 \cdot 40) / (1 \cdot 400 + 0.04 \cdot 50 + 0.45 \cdot 560)\} = -62 \text{ mV}.$$

This suggests that the squid giant axon should have a resting membrane potential of -62 mV. In fact, the resting membrane potential may be a few millivolts hyperpolarized to this value through the operation of the electrogenic Na^+-K^+ pump.

collective influence of a large neural network of cells, such as in the brain, and the presence of ion fluxes even at rest can substantially change the distribution of ions inside and outside neurons. Cells have solved this problem with the use of active transport of ions against their concentration gradients. The proteins that actively transport ions are referred to as **ionic pumps**, of which the Na^+-K^+ pump is perhaps the most thoroughly understood.²³⁻²⁶ The Na^+-K^+ pump is stimulated by increases in the intracellular concentration of Na^+ and moves Na^+ out of the cell while moving K^+ into it, achieving this task through the hydrolysis of ATP (see Fig. 6.2). Three Na^+ ions are extruded for every two K^+ ions transported into the cell. Owing to the unequal transport of ions, the operation of this pump generates a hyperpolarizing electrical potential and is said to be **electrogenic**. The Na^+-K^+ pump typically results in the membrane potential of the cell being a few millivolts more negative than it would be otherwise.

The Na^+-K^+ pump consists of two subunits, α and β , arranged in a tetramer $(\alpha\beta)_2$. The α subunit has a molecular mass of about 100 kDa and six hydrophobic regions capable of forming transmembrane helices.^{27,28} The β subunit is smaller (about 38 kDa) and has only one hydrophobic membrane-spanning region. The Na^+-K^+ pump is believed to operate through conformational changes that alternatively expose a Na^+ bind-

ing site to the interior of the cell (followed by the release of Na^+) and a K^+ binding site to the extracellular fluid (see Fig. 6.2). Such a conformation change may be due to the phosphorylation and dephosphorylation of the protein.

The membranes of neurons and glia contain multiple types of ionic pumps, used to maintain the proper distribution of each ionic species important for cellular signaling.^{29,30} Many of these pumps are operated by the Na^+ gradient across the cell, whereas others operate through a mechanism similar to that of the Na^+-K^+ pump (i.e., the hydrolysis of ATP). For example, the calcium concentration inside neurons is kept to very low levels (typically 50–100 nM) through the operation of both types of ionic pumps as well as special intracellular Ca^{2+} buffering mechanisms. Ca^{2+} is extruded from neurons through both a Ca^{2+}, Mg^{2+} -ATPase and a Na^+-Ca^{2+} exchanger. The Na^+-Ca^{2+} exchanger is driven by the Na^+ gradient across the membrane and extrudes one Ca^{2+} ion for each Na^+ ion allowed to enter the cell.

The Cl^- concentration in neurons is actively maintained at a low level through the operation of a chloride-bicarbonate exchanger, which brings in one ion of Na^+ and one ion of HCO_3^- for each ion of Cl^- extruded.^{31,32} Intracellular pH also can markedly affect neuronal excitability and is therefore tightly regulated, in part by a Na^+-H^+ exchanger that extrudes one proton for each Na^+ allowed to enter the cell.

Summary

The membrane potential is generated by the unequal distribution of ions, particularly K^+ , Na^+ , and Cl^- , across the plasma membrane. This unequal distribution of ions is maintained by ionic pumps and exchangers. K^+ ions are concentrated inside the neuron and tend to flow down their concentration gradient, leading to a hyperpolarization of the cell. At the equilibrium potential, the tendency of K^+ ions to flow out of the cell will be exactly offset by the tendency of K^+ ions to enter the cell owing to the attraction of the negative potential inside the cell. The resting membrane is also permeable to Na^+ and Cl^- and therefore the resting membrane potential is approximately -75 to -40 mV, in other words, substantially positive to E_K .

THE ACTION POTENTIAL

An Increase in Na^+ and K^+ Conductance Generates Action Potentials

Hodgkin and Huxley not only recorded the action potential with an intracellular microelectrode (see Fig. 6.1), but also went on to perform a remarkable series of experiments that qualitatively and quantitatively explained the ionic mechanisms by which the action potential is generated.^{33–37} As mentioned earlier, these investigators found that during the action potential, the membrane potential of the cell rapidly overshoots 0 mV and approaches the equilibrium potential for Na^+ . After the generation of the action potential, the membrane potential repolarizes and becomes more negative than before, generating an afterhyperpolarization. Kenneth Cole and Howard Curtis had previously shown that these changes in membrane potential during the generation of the action potential are associated with a large increase in conductance of the plasma membrane.³⁸ But to what does the membrane become conductive in order to generate the action potential? The prevailing hypothesis was that there was a nonselective increase in conductance causing the negative resting potential to increase toward 0 mV. Since publication of the experiments of E. Overton in 1902,³⁹ the action potential had been known to depend on the presence of extracellular Na^+ . Reducing the concentration of Na^+ in the artificial seawater bathing the axon resulted in a marked reduction in the amplitude of the action potential. On the basis of these and other data, Hodgkin and Katz proposed that the action potential is generated through a rapid increase in the conductance of the membrane to Na^+ ions. A quantitative

proof of this theory was lacking, however, because ionic currents could not be observed directly. The development of the **voltage-clamp** technique by Kenneth Cole at the Marine Biological Laboratory in Massachusetts resolved this problem and allowed quantitative measurement of the Na^+ and K^+ currents underlying the action potential⁴⁰ (Box 6.3).

Hodgkin and Huxley used the voltage-clamp technique to investigate the mechanisms of generation of the action potential in the squid giant axon. Axons and neurons have a threshold for the initialization of an action potential of about -45 to -55 mV. Increasing the voltage from -60 to 0 mV produces a large, but transient, flow of positive charge into the cell (known as **inward current**). This **transient** inward current is followed by a sustained flow of positive charge out of the cell (the **outward current**). By voltage-clamping the cell and substituting different ions inside or outside the axon or both, Hodgkin, Huxley, and colleagues demonstrated that the transient inward current is carried by Na^+ ions flowing into the cell and the sustained outward current is mediated by a sustained flux of K^+ ions moving out of the cell (Fig. 6.6).^{33–37,41}

The Na^+ and K^+ currents (I_{Na} and I_K , respectively) can be blocked, allowing each current to be examined in isolation (see Fig. 6.6B). Tetrodotoxin (TTX), a powerful poison found in the puffer fish *Spheroidees rubripes*,⁴² selectively blocks voltage-dependent Na^+ currents (the puffer fish remains a delicacy in Japan and must be prepared with the utmost care by the chef). Using TTX, one can selectively isolate I_K and examine its voltage dependence and time course (see Fig. 6.6B).

Clay Armstrong, Bertil Hille,⁴³ and others demonstrated that tetraethylammonium (TEA) is a useful pharmacological tool for selectively blocking I_K (see Fig. 6.6B). The use of TEA to examine the voltage dependence and time course of the Na^+ current underlying action-potential generation (see Fig. 6.6B) reveals some fundamental differences between the Na^+ and the K^+ currents. First, the inward Na^+ current *activates*, or “turns on,” much more rapidly than does the K^+ current (giving rise to the name “delayed rectifier” for this K^+ current). Second, the Na^+ current is transient; it *inactivates*, even if the membrane potential is maintained at 0 mV (see Fig. 6.6A). In contrast, the outward K^+ current, once activated, remains “on” as long as the membrane potential is clamped to positive levels; that is, the K^+ current does not inactivate; it is *sustained*. Remarkably, from one experiment, we see that the Na^+ current both rapidly *activates* and *inactivates*, whereas the K^+ current only slowly *activates*. These fundamental properties of the underlying Na^+ and K^+ channels allow the generation of action potentials.

BOX 6.3

THE VOLTAGE-CLAMP TECHNIQUE

In the voltage-clamp technique, two independent electrodes are inserted into the squid giant axon: one for recording the voltage difference across the membrane and the other for intracellularly injecting the current (Fig. 6.5). These electrodes are then connected to a feedback circuit that compares the measured voltage across the membrane with the voltage desired by the experimenter. If these two values differ, then current is injected into the axon to compensate for this difference. This continuous feedback cycle, in which the voltage is measured and current is injected, effectively "clamps" the membrane at a particular voltage. If ionic channels were to open, then the resultant flow of ions into or out of the axon would be compensated for by the injection of positive or negative current into the axon through the current-injection electrode. The current injected through this electrode is necessarily equal to the current flowing through the ionic channels. It is this injected current that is measured by the experimenter. The benefits of the voltage-clamp technique are twofold. First, the current injected into the axon to keep the membrane potential "clamped" is necessarily equal to the current flowing through the ionic channels in the membrane, thereby giving a direct measurement of this current. Second, ionic currents are both voltage and time dependent; they become active at certain membrane potentials and do so at a particular rate. Keeping the voltage constant in the voltage clamp allows these two variables to be separated; the voltage dependence and the kinetics of the ionic currents flowing through the plasma membrane can be directly measured.

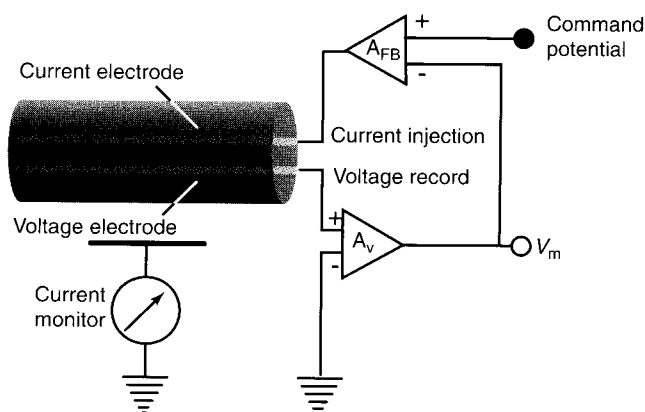


FIGURE 6.5 Voltage-clamp technique. The voltage-clamp technique keeps the voltage across the membrane constant so that the amplitude and time course of ionic currents can be measured. In the two-electrode voltage-clamp technique, one electrode measures the voltage across the membrane while the other injects current into the cell to keep the voltage constant. The experimenter sets a voltage to which the axon or neuron is to be stepped (the command potential). Current is then injected into the cell in proportion to the difference between the present membrane potential and the command potential. This feedback cycle occurs continuously, thereby clamping the membrane potential to the command potential. By measuring the amount of current injected, the experimenter can determine the amplitude and time course of the ionic currents flowing across the membrane.

Hodgkin and Huxley³³⁻³⁶ proposed that the K^+ channels possess a voltage-sensitive "gate" that opens by the depolarization and closes by the subsequent repolarization of the membrane potential. This process of "turning on" and "turning off" the K^+ current came to be known as **activation** and **deactivation**. The Na^+ current also exhibits voltage-dependent activation and deactivation (see Fig. 6.6), but the Na^+ channels also become inactive despite maintained depolarization. Thus, the Na^+ current not only activates and deactivates, but also exhibits a separate process known as **inactivation**, whereby the channels become blocked even though they are activated. The removal of this inactivation is achieved by removal of the depolarization and is a process known as **deinactivation**. Thus, the Na^+ channels possess two voltage-sensitive pro-

cesses: *activation–deactivation* and *inactivation–deinactivation*. The kinetics of these two properties of Na^+ channels are different: inactivation takes place at a slower rate than activation.

The functional consequence of the two mechanisms is that Na^+ ions are allowed to flow across the membrane only when the current is activated but not inactivated. Accordingly, Na^+ ions do not flow at resting membrane potentials, because the activation gate is closed (even though the inactivation gate is not). Upon depolarization, the activation gate opens, allowing Na^+ ions to flow into the cell. However, this depolarization also results in the closure (at a slower rate) of the inactivation gate, which then blocks the flow of Na^+ ions. Upon repolarization of the membrane potential, the activation gate once again closes and the inactiva-

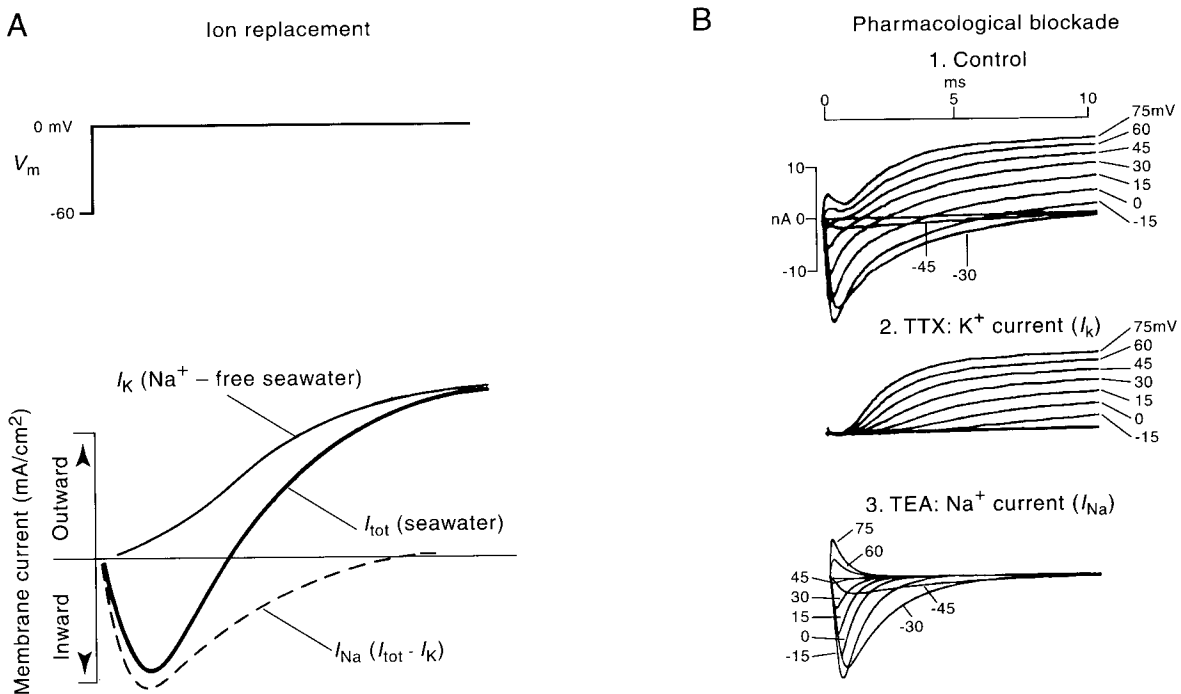


FIGURE 6.6 Voltage-clamp analysis reveals the ionic currents underlying action potential generation. (A) Increasing the potential from -60 to 0 mV across the membrane of the squid giant axon activates an inward current followed by an outward current. If the Na^+ in seawater is replaced by choline (which does not pass through Na^+ channels), then increasing the membrane potential from -60 to 0 mV results in only the outward current, which corresponds to I_K . Subtracting I_K from the recording in normal seawater illustrates the amplitude-time course of the inward Na^+ current, I_{Na} . Note that I_K activates more slowly than I_{Na} and that I_{Na} inactivates with time. (B) These two ionic currents can also be isolated from one another through the use of pharmacological blockers. (1) Increasing the membrane potential from -45 to $+75$ mV in 15 -mV steps reveals the amplitude-time course of the inward Na^+ and outward K^+ currents. (2) After the block of I_{Na} with the poison tetrodotoxin (TTX), increasing the membrane potential to positive levels activates I_K only. (3) After the block of I_K with tetraethylammonium (TEA), increasing the membrane potential to positive levels activates I_{Na} only. Part A, from Hodgkin and Huxley³³; part B from Hille.⁴¹

tion gate once again opens, preparing the axon for the generation of the next action potential (Fig. 6.7). Depolarization allows ionic current to flow by virtue of *activation* of the channel. The rush of Na^+ ions into the cell further depolarizes the membrane potential and more Na^+ channels become activated, forming a positive feedback loop that rapidly (within $100 \mu\text{s}$ or so) brings the membrane potential toward E_{Na} . However, the depolarization associated with the generation of the action potential also inactivates Na^+ channels, and, as a larger and larger percentage of Na^+ channels become inactivated, the rush of Na^+ into the cell diminishes. This inactivation of the Na^+ channels and the activation of K^+ channels result in the repolarization of the action potential. This repolarization deactivates the Na^+ channels. Then, the inactivation of the channel is slowly removed, and the channels are ready, once again, for the generation of another action potential (see Fig. 6.7).

By measuring the voltage sensitivity and kinetics of these two processes, activation-deactivation and inactivation-deinactivation of the Na^+ current, as well as the activation-deactivation of the delayed rectifier K^+ current, Hodgkin and Huxley generated a series of mathematical equations that quantitatively described the generation of the action potential (the calculation of the propagation of a single action potential required an entire week of cranking a mechanical calculator). According to these early experimental and computational neuroscientists, the action potential is generated as follows. Depolarization of the membrane potential increases the probability of Na^+ channels being in the activated, but not yet inactivated, state. At a particular membrane potential, the resulting inflow of Na^+ ions tips the balance of the net ionic current from outward to inward (remember that depolarization will also increase K^+ and Cl^- currents by moving the membrane potential away from E_K and E_{Cl}). At this membrane

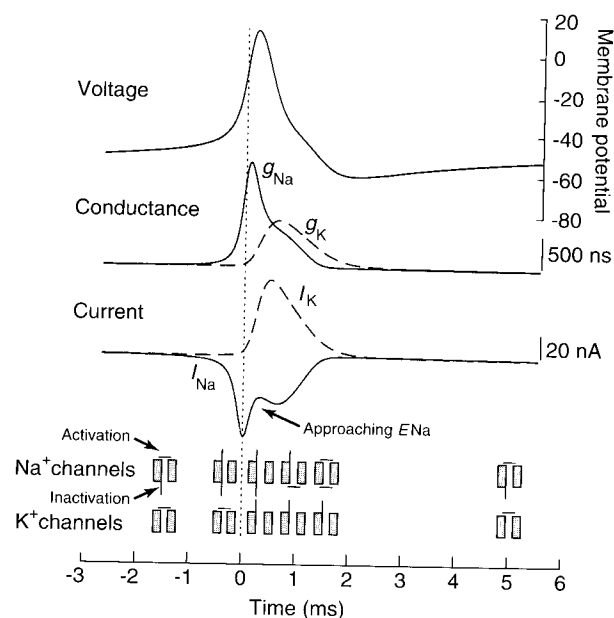


FIGURE 6.7 The generation of the action potential is associated with an increase in membrane Na^+ conductance and Na^+ current followed by an increase in K^+ conductance and K^+ current. Before action potential generation, Na^+ channels are neither activated nor inactivated (illustrated at the bottom of the figure). Activation of the Na^+ channels allows Na^+ ions to enter the cell, depolarizing the membrane potential. This depolarization also activates K^+ channels. After activation and depolarization, the inactivation particle on the Na^+ channels closes and the membrane potential repolarizes. The persistence of the activation of K^+ channels (and other membrane properties) generates an afterhyperpolarization. During this period, the inactivation particle of the Na^+ channel is removed and the K^+ channels close. From Huguenard and McCormick.⁶¹

potential, known as the action potential threshold (typically about -55 mV), the movement of Na^+ ions into the cell depolarizes the axon, and opens more Na^+ channels, causing yet more depolarization of the membrane; repetition of this process yields a rapid, positive feedback loop that brings the axon close to E_{Na} . However, even as more and more Na^+ channels are becoming activated, some of these channels are also inactivating and therefore no longer conducting Na^+ ions. In addition, the delayed rectifier K^+ channels also are opening, owing to the depolarization of the membrane potential, and allowing positive charge to exit the cell. At some point, close to the peak of the action potential, the inward movement of Na^+ ions into the cell is exactly offset by the outward movement of K^+ ions out of the cell. After this point, the outward movement of K^+ ions dominates, and the membrane potential is repolarized, corresponding to the fall of the action potential. The persistence of the K^+ current for a few milliseconds following the generation of the action potential generates the afterhyperpolarization. During

this afterhyperpolarization, which is lengthened by the membrane time constant, the inactivation of the Na^+ channels is removed, preparing the axon for generation of the next action potential (see Fig. 6.7).

The occurrence of an action potential is not associated with substantial changes in the intracellular or extracellular concentrations of Na^+ or K^+ , as we saw earlier for the generation of the resting membrane potential. For example, the generation of a single action potential in a $25\text{-}\mu\text{m}$ -diameter hypothetical spherical cell should increase the intracellular concentration of Na^+ by only approximately $6\text{ }\mu\text{M}$ (from about 31 to 31.006 mM). Thus, the action potential is an electrical event generated by a change in the distribution of charge across the membrane and not by a marked change in the intracellular or extracellular concentration of Na^+ or K^+ .

Refractory Periods Prevent “Reverberation”

The ability of depolarization to activate an action potential varies as a function of the time since the last generation of an action potential, owing to the inactivation of Na^+ channels and the activation of K^+ channels. Immediately after the generation of an action potential, another action potential usually cannot be generated regardless of the amount of current injected into the axon. This period corresponds to the **absolute refractory period** and is largely mediated by the inactivation of Na^+ channels. The **relative refractory period** follows the absolute refractory period during the action potential afterhyperpolarization. This few-millisecond period is characterized by a requirement for the increased injection of ionic current into the cell to generate another action potential and results from the persistence of the outward K^+ current. The practical implication of refractory periods is that action potentials are not allowed to “reverberate” between the soma and the axon terminals.

The Speed of Action Potential Propagation Is Affected by Myelination

Axons may be either myelinated or unmyelinated. Invertebrate axons or small vertebrate axons are typically unmyelinated, whereas larger vertebrate axons are often myelinated. As described in Chapter 4, sensory and motor axons of the peripheral nervous system are myelinated by specialized cells (Schwann cells) that form a spiral wrapping of multiple layers of myelin around the axon (Fig. 6.8). Several Schwann cells wrap around an axon along its length; between the ends of successive Schwann cells are small gaps (nodes of Ranvier). In the central nervous system, a single **oligo-**

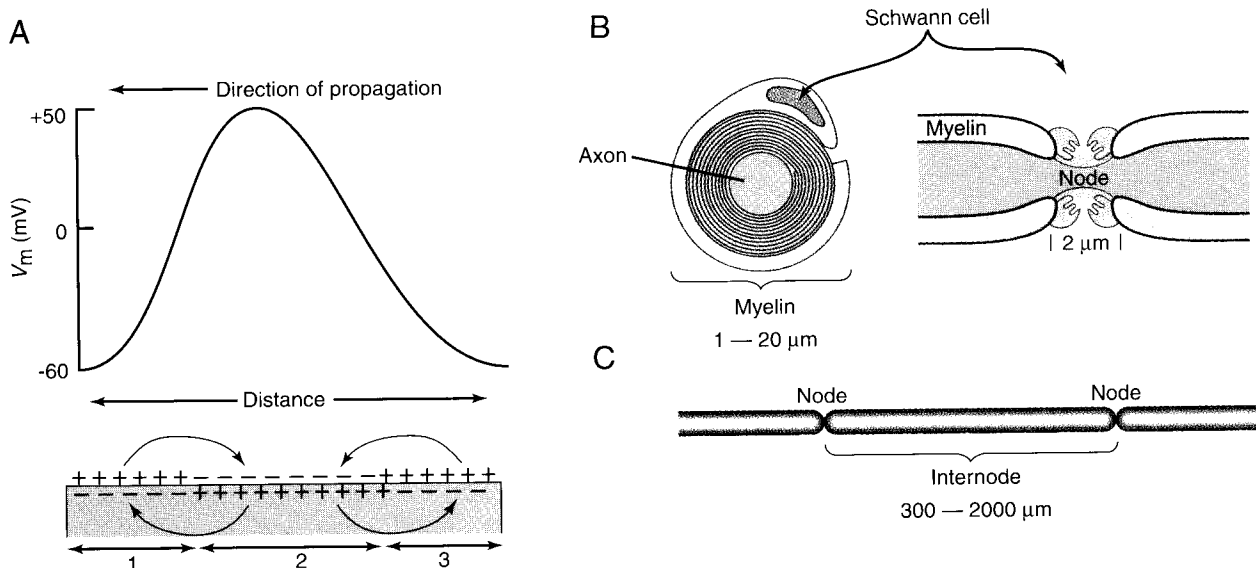


FIGURE 6.8 Propagation of the action potential in unmyelinated and myelinated axons. (A) Action potentials propagate in unmyelinated axons through the depolarization of adjacent regions of membrane. In the illustrated axon, region 2 is undergoing depolarization during the generation of the action potential, while region 3 has already generated the action potential and is now hyperpolarized. The action potential will propagate further by depolarizing region 1. (B) Vertebrate myelinated axons have a specialized Schwann cell that wraps around them in many spiral turns. The axon is exposed to the external medium at the nodes of Ranvier (Node). (C) Action potentials in myelinated fibers are regenerated at the nodes of Ranvier, where there is a high density of Na^+ channels. Action potentials are induced at each node through the depolarizing influence of the generation of an action potential at an adjacent node, thereby increasing the conduction velocity.

dendrocyte, a special type of glial cell, typically ensheaths several axonal processes.⁴⁴

In unmyelinated axons, the Na^+ and K^+ channels taking part in action potential generation are distributed along the axon, and the action potential propagates along the length of the axon through local depolarization of each neighboring patch of membrane, causing that patch of membrane also to generate an action potential (see Fig. 6.8). In myelinated axons, on the other hand, the Na^+ channels are concentrated at the nodes of Ranvier.⁴⁵ The generation of an action potential at each node results in the depolarization of the next node and subsequently the generation of an action potential with an internode delay of only about 20 μ s (see Chapter 5), referred to as **saltatory conduction** (from the Latin *saltare*, “to leap”). Growing evidence indicates that, between the nodes of Ranvier and underneath the myelin covering, K^+ channels may play a role in determining the resting membrane potential and the repolarization of the action potential. A cause of some neurological disorders, such as multiple sclerosis and Guillain–Barre syndrome, is the demyelination of axons, resulting in a block of conduction of the action potentials (see Chapter 3).

Ion Channels Are Membrane-Spanning Proteins with Water-Filled Pores

The generation of ionic currents useful for the propagation of action potentials requires the movement of significant numbers of ions across the membrane in a relatively short time. The rate of ionic flow during the generation of an action potential is far too high to be achieved by an active transport mechanism and results instead from the opening of ion channels. Although the existence of ionic channels in the membrane has been postulated for decades, their properties and structure have only recently become known in detail. The powerful combination of electrophysiological and molecular techniques has greatly enhanced our knowledge of the structure–function relations of ionic channels^{46–51} (Box 6.4).

Various neural toxins were particularly useful in the initial isolation of ionic channels. For example, three subunits (α , β_1 , β_2) of the voltage-dependent Na^+ channel were isolated with the use of a derivative of a scorpion toxin.^{49,52} The α subunit of the Na^+ channel is a large glycoprotein with a molecular mass of 270 kDa, whereas the β_1 and β_2 subunits are smaller poly-

peptides of molecular masses 39 and 37 kDa, respectively (Fig. 6.9). The α subunit forms the water-filled pore of the ionic channel, whereas the β subunits have some other role, such as in the regulation or structure of the native channel.

The α subunit of the Na^+ channel contains four internal repetitions (see Fig. 6.9B). Hydrophobicity analysis of these four components reveals that each contains six hydrophobic domains that may span the membrane as an α -helix. Of these six membrane-spanning components, the fourth (S4) has been proposed to be critical to the voltage sensitivity of the Na^+ channels. Voltage-sensitive gating of Na^+ channels is accomplished by the redistribution of ionic charge ("gating charge") in the Na^+ channel.⁵³ Positive charges in the S4 region may act as voltage sensors such that an increase in the positivity of the inside of the cell results in a conformational change of the ionic channel. In support of this hypothesis, site-directed mutagenesis of the S4 region of the Na^+ channel to reduce the positive charge of this portion of the pore also reduces the voltage sensitivity of activation of the ionic channel.⁴⁹

The mechanisms of inactivation of ionic channels have been analyzed with a combination of molecular and electrophysiological techniques. The most convincing hypothesis is that inactivation is achieved by a block of the inner mouth of the aqueous pore. Ionic channels are inactivated without detectable movement of ionic current through the membrane; thus inactivation is probably not directly gated by changes in the membrane potential alone. Rather, inactivation may be triggered or facilitated as a secondary consequence of activation. Site-directed mutagenesis or the use of antibodies has shown that the part of the molecule between regions III and IV may be allowed to move to block the cytoplasmic side of the ionic pore after the conformational change associated with activation.⁵⁴⁻⁵⁶

Neurons of the Central Nervous System Exhibit a Wide Variety of Electrophysiological Properties

The first intracellular recordings of action potentials in mammalian neurons by Sir John Eccles and colleagues revealed a remarkable similarity to those of the squid giant axon and gave rise to the assumption that the electrophysiology of neurons in the CNS was really rather simple: when synaptic potentials brought the membrane potential positive to action potential threshold, action potentials were produced through an increase in Na^+ conductance followed by an increase in K^+ conductance, as in the squid giant axon. The assumption, therefore, was that the complicated pat-

terns of activity generated by the brain during the resting, sleeping, or active states were brought about as an interaction of the very large numbers of neurons present in the mammalian CNS.^{6,57} However, intracellular recordings of invertebrate neurons revealed that different cell types exhibit a wide variety of different electrophysiological behaviors, indicating that neurons may be significantly more complicated than the squid giant axon.⁵⁸⁻⁶⁰ The elucidation of the basic electrophysiology and synaptic physiology of different types of neurons and neuronal pathways within the mammalian CNS was facilitated by the *in vitro* slice technique, in which thin (~ 0.5 mm) slices of brain can be maintained for several hours. Intracellular recordings from identified cells revealed that neurons of the mammalian nervous system, such as those of invertebrate networks, can generate complex patterns of action potentials entirely through intrinsic ionic mechanisms and without synaptic interaction with other cell types. For example, Rodolfo Llinás and colleagues discovered that Purkinje cells of the cerebellum can generate high-frequency trains (>200 Hz) of Na^+ - and K^+ -mediated action potentials interrupted by Ca^{2+} spikes in the dendrites,^{61,62} whereas a major afferent to these neurons, the inferior olivary cell, can generate rhythmic sequences of broad action potentials only at low frequencies (<15 Hz) through an interaction between various Ca^{2+} , Na^+ , and K^+ conductances^{63,64} (Fig. 6.10). These *in vitro* recordings confirmed a major finding obtained with earlier intracellular recordings *in vivo*: each morphologically distinct class of neuron in the brain exhibits distinct electrophysiological features.⁶⁵ Just as cortical pyramidal cells are morphologically distinct from cerebellar Purkinje cells, which are distinct from thalamic relay cells, the electrophysiological properties of each of these different cell types also are markedly distinct.

Although no uniform classification scheme has been formulated in which all the different types of neurons of the brain can be classified, a few characteristic patterns of activity seem to recur. The first general class of action potential generation is characterized by those cells that generate trains of action potentials one spike at a time. The more prolonged the depolarization of these cells, the more prolonged their discharge. The more intensely these cells are depolarized, the higher the frequency of action potential generation. This type of relatively linear behavior is typical for brainstem and spinal cord motor neurons functioning in muscle contraction. A modification of this basic pattern of "regular firing" is characterized by the generation of trains of action potentials that exhibit a marked tendency to slow down in frequency with time, a process known as spike frequency adaptation. Examples of

BOX 6.4

ION CHANNELS AND DISEASE

Cells cannot survive without functional ion channels. It is therefore not surprising that an ever increasing number of diseases have been found to be associated with defective ion channel function. There are a number of different mechanisms by which this may occur.

1. Mutations in the coding region of ion channel genes may lead to gain or loss of channel function, either of which may have deleterious consequences. For example, mutations producing enhanced activity of the epithelial Na^+ channel are responsible for Liddle syndrome, an inherited form of hypertension, whereas other mutations in the same protein that cause reduced channel activity give rise to hypotension. The most common inherited disease in Caucasians is also an ion channel mutation. This disease is cystic fibrosis (CF), which results from mutations in the epithelial chloride channel, known as CFTR. The most common mutation, the deletion of a phenylalanine at position 508, results in defective processing of the protein and prevents it from reaching the surface membrane. CFTR regulates chloride fluxes across epithelial cell membranes, and this loss of CFTR activity leads to reduced fluid secretion in the lung, resulting in potentially fatal lung infections.

2. Mutations in the promoter region of the gene may cause under- or overexpression of a given ion channel.

3. Other diseases result from defective regulation of channel activity by cellular constituents or extracellular ligands. This defective regulation may be caused by mutations in the genes encoding the regulatory molecules themselves or defects in the pathways leading to their production. Some forms of maturity-onset diabetes of the young (MODY) may be attributed to such a mechanism. ATP-sensitive potassium (K-ATP) channels play a key role in the glucose-induced insulin secretion from pancreatic β cells, and their defective regulation is responsible for two forms of MODY.

4. Autoantibodies to channel proteins may cause disease by down-regulating channel function—often by causing internalization of the channel protein itself. Well-known examples are myasthenic gravis, which results from antibodies to skeletal muscle acetylcholine channels, and Eaton Lambert myasthenic syndrome, in which patients produce antibodies against presynaptic Ca channels.

5. Finally, a number of ion channels are secreted by cells as toxic agents. They insert into the membrane of the target cell and form large nonselective pores, leading

to cell lysis and death. The hemolytic toxin produced by the bacterium *Staphylococcus aureus* and the toxin secreted by the protozoan *Entamoeba histolytica*, which causes amebic dysentery, are examples.

Natural mutations in ion channels have been invaluable for studying the relationship between channel structure and function. In many cases, genetic analysis of a disease has led to the cloning of the relevant ion channel. The first K channel to be identified (*Shaker*), for example, came from the cloning of the gene that caused *Drosophila* to shake when exposed to ether. Likewise, the gene encoding the primary subunit of a cardiac potassium channel (*KVLQT1*) was identified by positional cloning in families carrying mutations that caused a cardiac disorder known as long QT syndrome (see below). Conversely, the large number of studies on the relationship between Na channel structure and function have greatly assisted our understanding of how mutations in Na channels produce their clinical phenotypes.

Many diseases are genetically heterogeneous, and the same clinical phenotype may be caused by mutations in different genes. Long QT syndrome is a relatively rare inherited cardiac disorder that causes abrupt loss of consciousness, seizures, and sudden death from ventricular arrhythmia in young people. Mutations in three different genes, two types of cardiac muscle K channels (*HERG* and *KVLQT1*) and the cardiac muscle sodium channel (*SCN1A*), give rise to long QT syndrome. The disorder is characterized by a long QT interval in the electrocardiogram, which reflects the delayed repolarization of the cardiac action potential. As might therefore be expected, the mutations in the cardiac Na channel gene that cause long QT syndrome enhance the Na current (by reducing Na channel inactivation), while those in the potassium channel genes cause loss of function and reduce the K current.

Mutations in many different types of ion channels have been shown to cause human diseases. In addition to the examples listed above, mutations in water channels cause nephrogenic diabetes insipidus; mutations in gap junction channels cause Charcot-Marie-Tooth disease (a form of peripheral neuropathy) and hereditary deafness; mutations in the skeletal muscle Na channel cause a range of disorders known as the periodic paralyses; mutations in intracellular Ca-release channels cause malignant hyperthermia (a disease in which inhalation anaesthetics trigger a potentially fatal rise in body temperature); and muta-

tions in neuronal voltage-gated Ca channels cause migraine and episodic ataxia. The list increases daily. As is the case with all single gene disorders, the frequency of these diseases in the general population is very low. However, the insight they have provided into the relationship between ion channel structure and function, and into the physiological role of the different ion channels, has been

invaluable. As William Harvey said in 1657 "nor is there any better way to advance the proper practice of medicine than to give our minds to the discovery of the usual form of nature, by careful investigation of the rarer forms of disease."

Frances M. Ashcroft

cells that discharge in this manner are cortical and hippocampal pyramidal cells.^{20,66,67}

In addition to these regular firing cells, many neurons in the central nervous system exhibit the intrinsic propensity to generate rhythmic bursts of action potentials (see Fig. 6.10). Examples of such neurons are thalamic relay neurons, inferior olivary neurons, and some types of cortical and hippocampal pyramidal cells.^{18,19,63,64,68} In these cells, clusters of action potentials can occur together when the membrane is brought above firing threshold. These clusters of action potentials are typically generated through the activation of specialized Ca^{2+} currents that, through their slower kinetics, allow the membrane potential to be depolarized for a sufficient period to result in the generation of a burst of regular, Na^{+} - and K^{+} -dependent action potentials (discussed in the next section).

Yet another general category of neurons in the brain comprises cells that generate relatively short duration (<1 ms) action potentials and can discharge at relatively high frequencies (>300 Hz). Such electrophysiological properties are often found in neurons that release the inhibitory amino acid γ -aminobutyric acid^{61,62} (see Fig. 6.10) and some types of interneurons in the cerebral cortex, thalamus, and hippocampus.^{20,69,70} Finally, the last general category of neurons consists of those that spontaneously generate action potentials at relatively slow frequencies (e.g., 1–10 Hz). This type of electrophysiological behavior is often associated with neurons that release neuromodulatory transmitters, such as acetylcholine, norepinephrine, serotonin, and histamine.^{71–73} Neurons that release these neuromodulatory substances often innervate wide regions of the brain and appear to set the "state" of the different neural networks of the CNS, in a manner similar to the modulation of the different organs of the body by the sympathetic and parasympathetic nervous systems.^{22,74}

Each of these unique intrinsic patterns of activity in the nervous system is due to the presence of a distinct mixture and distribution of different ionic currents in the cells. As in the classical studies of the squid giant

axon, these different ionic currents have been characterized, at least in part, with voltage-clamp and pharmacological techniques, and the basic electrophysiological properties have been replicated with computational simulations^{75–77} (see Figs. 6.7 and 6.12).

Neurons Have Multiple Active Conductances

The search for the electrophysiological basis of the varying intrinsic properties of different types of neurons of vertebrates and invertebrates revealed a wide variety of ionic currents. Each type of ionic current is characterized by several features: (1) the type of ions conducted by the underlying ionic channels (e.g., Na^{+} , K^{+} , Ca^{2+} , Cl^{-} , or mixed cations), (2) their voltage and time dependence, and (3) their sensitivity to second messengers. In vertebrate neurons, two distinct Na^{+} currents have been identified and five distinct Ca^{2+} currents and a plethora of distinct K^{+} currents are known (Table 6.2; Fig. 6.11). In the following sections, we briefly review these classes of ionic currents and their ionic channels, relating them to the different patterns of behavior mentioned earlier for neurons in the mammalian CNS.

Na^{+} Currents Are Both Transient and Persistent

Depolarization of many different types of vertebrate neurons results not only in the activation of the rapidly activating and inactivating Na^{+} current (I_{NaT}) underlying action potential generation but also in the rapid activation of a Na^{+} current that does not inactivate and is therefore known as the "persistent" Na^{+} current (I_{NaP}).^{65,78–80} The threshold for activation of the persistent Na^{+} current is typically about -65 mV—that is, below the threshold for the generation of action potentials. This property gives this current the interesting ability to enhance or facilitate the response of the neuron to depolarizing, yet subthreshold, inputs. For example, synaptic events that depolarize the cell will activate I_{NaP} , resulting in an extra influx of positive charge and

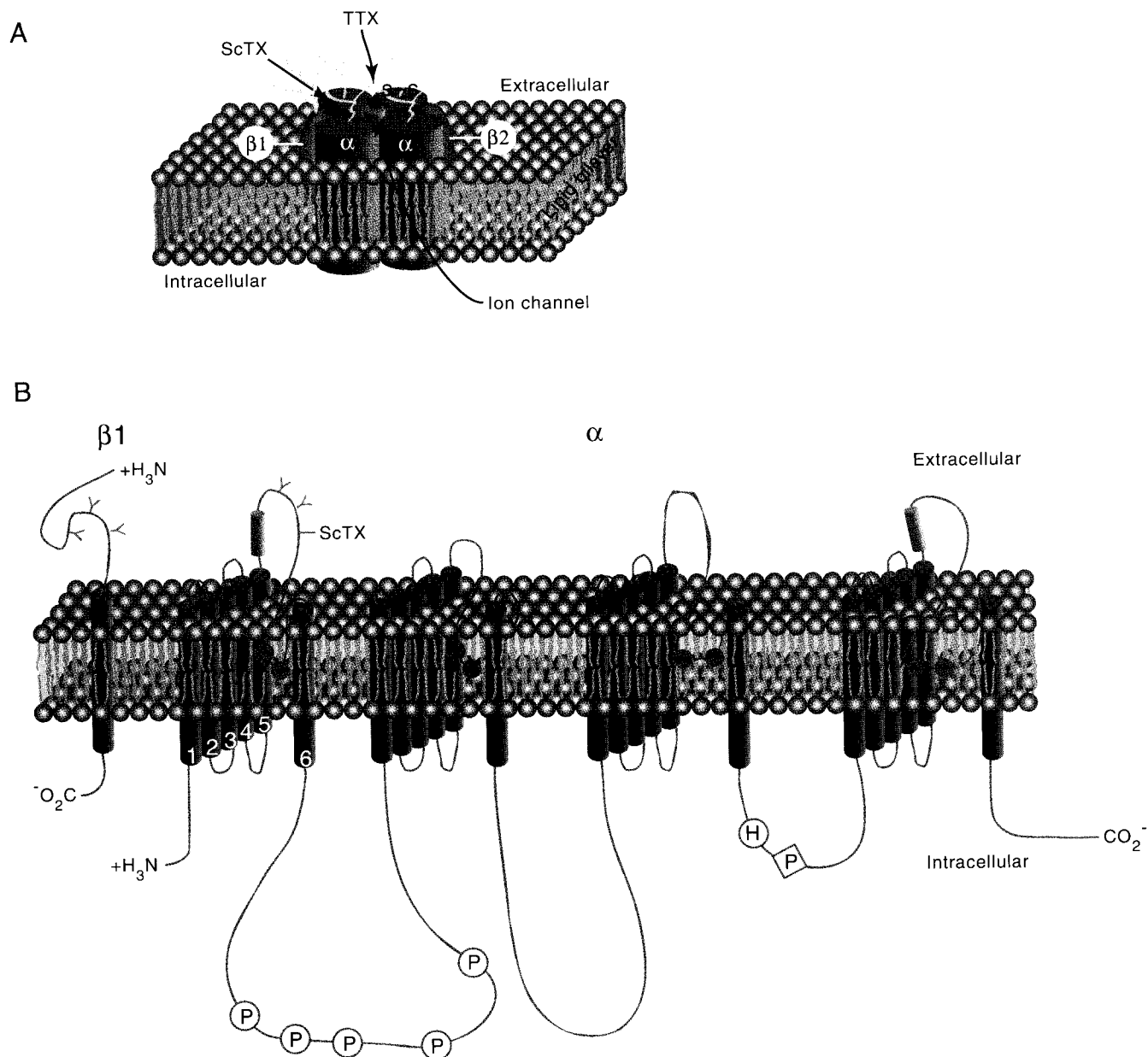


FIGURE 6.9 Structure of the sodium channel. (A) Cross section of a hypothetical sodium channel consisting of a single transmembrane α subunit in association with a $\beta 1$ subunit and a $\beta 2$ subunit. The α subunit has receptor sites for α -scorpion toxins (ScTX) and tetrodotoxin (TTX). (B) Primary structures of α and $\beta 1$ subunits of sodium channel illustrated as transmembrane folding diagrams. Cylinders represent probable transmembrane α -helices.

therefore a larger depolarization than otherwise would occur. Likewise, hyperpolarizations may result in deactivation of I_{NaP} , again resulting in larger hyperpolarizations than would otherwise occur. In this manner, the persistent Na^+ current may play an important regulatory function in the control of the functional responsiveness of the neuron to synaptic inputs and may

contribute to the dynamic coupling of the dendrites to the soma.

Persistent activation of I_{NaP} may also contribute to another electrophysiological feature of neurons—namely, the generation of **plateau potentials**.⁶⁵ A plateau potential refers to the ability of many different types of neurons to generate, through intrinsic ionic

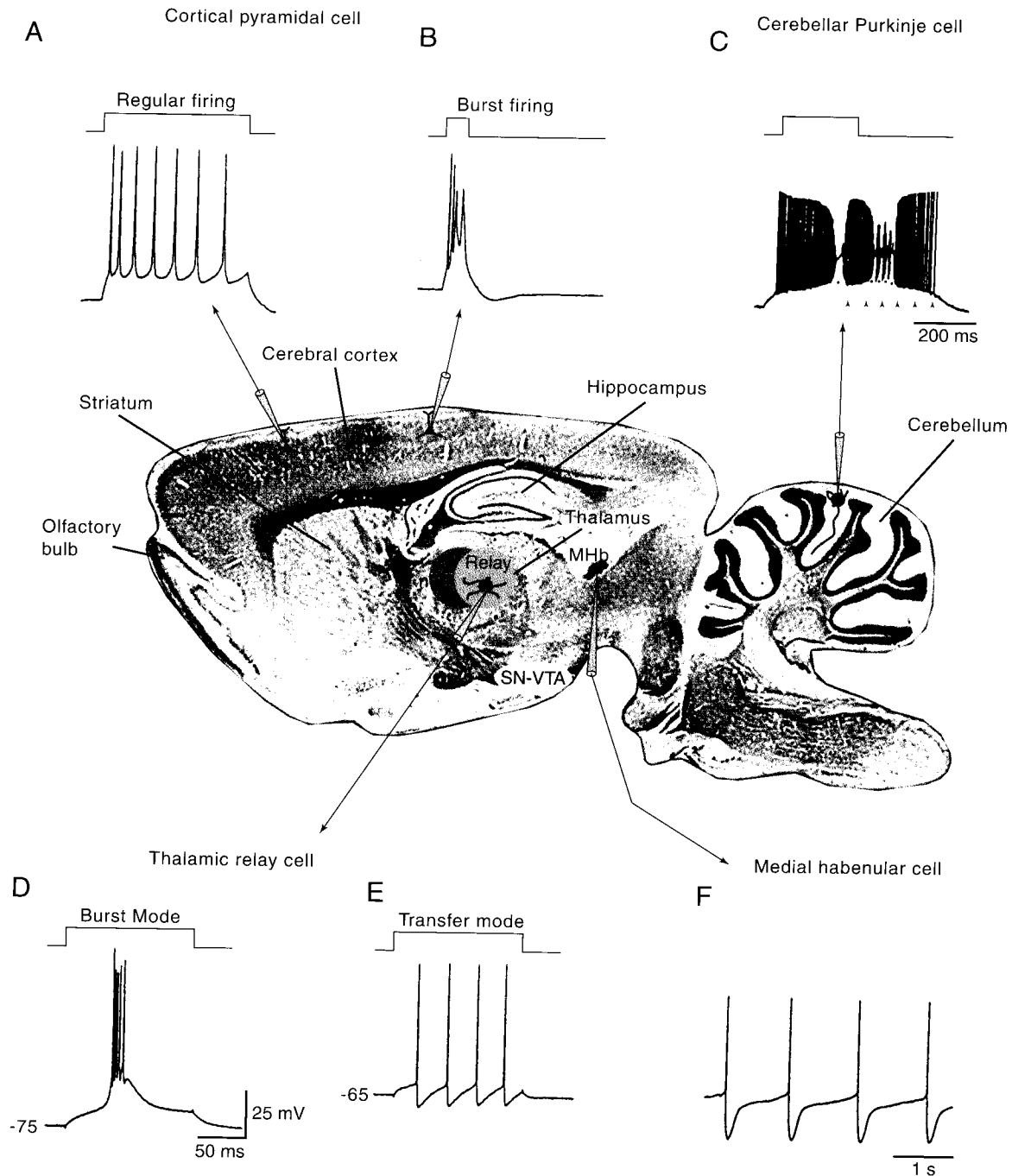


FIGURE 6.10 Neurons in the mammalian brain exhibit widely varying electrophysiological properties. (A) Intracellular injection of a depolarizing current pulse in a cortical pyramidal cell results in a train of action potentials that slow down in frequency. This pattern of activity is known as "regular firing." (B) Some cortical cells generated bursts of three or more action potentials, even when depolarized only for a short period of time. (C) Cerebellar Purkinje cells generate high-frequency trains of action potentials in their cell bodies that are disrupted by the generation of Ca^{2+} spikes in their dendrites. These cells can also generate "plateau potentials" from the persistent activation of Na^+ conductances (arrowheads). (D) Thalamic relay cells may generate action potentials either as bursts (D) or as tonic trains of action potentials (E) owing to the presence of a large low-threshold Ca^{2+} current. (F) Medial habenular cells generate action potentials at a steady and slow rate, in a "pacemaker" fashion.

TABLE 6.2 Neuronal Ionic Currents

Current	Description	Function
Na⁺ currents		
$I_{Na,t}$	Transient; rapidly activating and inactivating	Action potentials
$I_{Na,p}$	Persistent; noninactivating	Enhances depolarization; contributes to steady-state firing
Ca²⁺ currents		
I_T , low threshold	Transient; rapidly inactivating; threshold negative to -65 mV	Underlies rhythmic burst firing
I_L , high threshold	Long-lasting; slowly inactivating; threshold around -20 mV	Underlies Ca ²⁺ spikes that are prominent in dendrites; involved in synaptic transmission
I_N	Neither; rapidly inactivating; threshold around -20 mV	Underlies Ca ²⁺ spikes that are prominent in dendrites; involved in synaptic transmission
I_P	Purkinje; threshold around -50 mV	
K⁺ currents		
I_K	Activated by strong depolarization	Repolarization of action potential
I_C	Activated by increases in $[Ca^{2+}]_i$	Action potential repolarization and interspike interval
I_{AHP}	Slow afterhyperpolarization; sensitive to increases in $[Ca^{2+}]_i$	Slow adaptation of action potential discharge; the block of this current by neuromodulators enhances neuronal excitability
I_A	Transient; inactivating	Delayed onset of firing; lengthens interspike interval; action potential repolarization
I_M	Muscarine sensitive; activated by depolarization; noninactivating	Contributes to spike frequency adaptation; the block of this current by neuromodulators enhances neuronal excitability
I_h	Depolarizing (mixed cation) current that is activated by hyperpolarization	Contributes to rhythmic burst firing and other rhythmic activities
$I_{K,leak}$	Contributes to neuronal resting membrane potential	Block of this current by neuromodulators can result in a sustained change in membrane potential

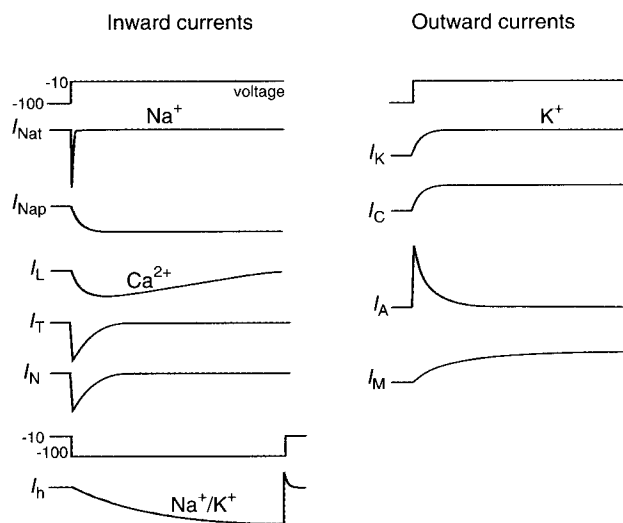


FIGURE 6.11 Voltage dependence and kinetics of different ionic currents in the mammalian brain. Depolarization of the membrane potential from -100 to -10 mV results in the activation of currents entering or leaving neurons.

mechanisms, a prolonged (from tens of milliseconds to seconds) depolarization and action potential discharge in response to a short-lasting depolarization (see Fig. 6.10C). One can wonder whether such plateau potentials contribute to persistent firing in neurons during the performance of visual memory tasks, as has been found in some types of neurons in the frontal neocortex and superior colliculus of behaving primates.⁸¹

K⁺ Currents Vary in Their Voltage Sensitivity and Kinetics

Potassium currents that contribute to the electrophysiological properties of neurons are numerous and exhibit a wide range of voltage-dependent and kinetic properties.^{51,82–84} Perhaps the simplest K⁺ current is that characterized by Hodgkin and Huxley: this K⁺ current, I_K , rapidly activates on depolarization and does not inactivate (see Fig. 6.11). Other K⁺ currents activate with depolarization but also inactivate with time. For example, the rapid activation and inactivation of I_A give this current a transient appearance (see Fig. 6.11),

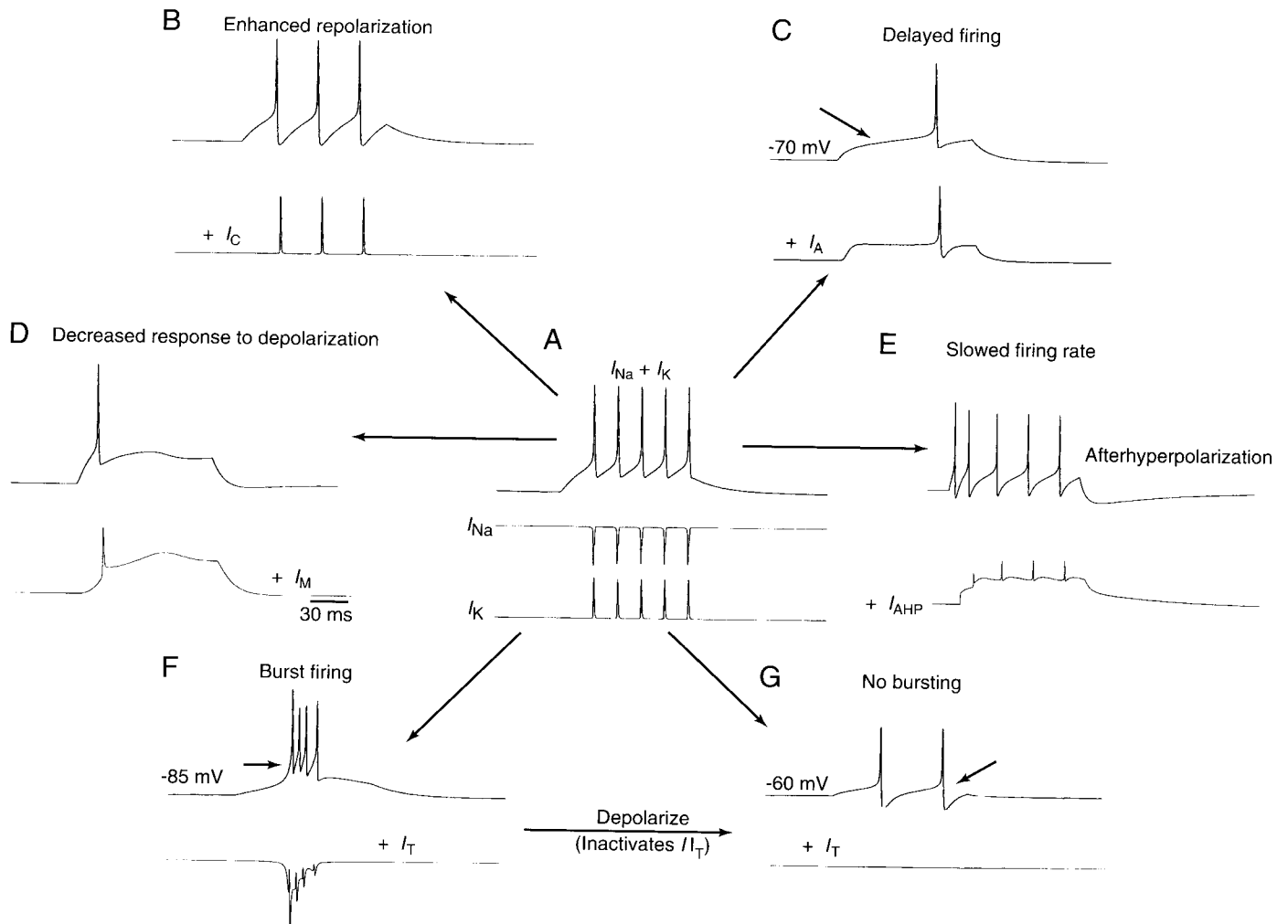


FIGURE 6.12 Simulation of the effects of the addition of various ionic currents to the pattern of activity generated by neurons in the mammalian CNS. (A) The repetitive impulse response of the classical Hodgkin-Huxley model (voltage recordings above, current traces below). With only I_{Na} and I_K , the neuron generates a train of five action potentials in response to depolarization. Addition of I_C (B) enhances action potential repolarization. Addition of I_A (C) delays the onset of action potential generation. Addition of I_M (D) decreases the ability of the cell to generate a train of action potentials. Addition of I_{AHP} (E) slows the firing rate and generates a slow afterhyperpolarization. Finally, addition of the transient Ca^{2+} current I_T results in two states of action potential firing: (F) burst firing at -85 mV and (G) tonic firing at -60 mV. From Huguenard and McCormick.⁶¹

and I_A is believed to be important in controlling the rate of action potential generation, particularly at low frequencies^{85,86} (Fig. 6.12). Like the Na^+ channel, I_A channels are inactivated by the plugging of the inner mouth of the pore through the movement of an inactivation particle.^{87,88}

Another broad class of K^+ channels consists of those that are sensitive to changes in the intracellular concentration of Ca^{2+} .^{89,90} These K^+ currents are collectively referred to as I_{KCa} (see Fig. 6.11). Still other K^+ channels are not only activated by voltage but also modulated by activation of various modulatory neurotransmitter

receptors (e.g., I_M ; see Fig. 6.11). Between these classic examples of K^+ currents are a variety of other types that have not been fully characterized, including K^+ currents that vary from one another in their voltage sensitivity, kinetics, and response to various second messengers.

Recent molecular biological studies of voltage-sensitive K^+ channels, first done in *Drosophila* and later in mammals, have revealed the presence of four distinct gene families, *Shaker*, *Shab*, *Shaw*, and *Shal*,⁵¹ that correspond to the newer nomenclature of Kv1, Kv2, Kv3, and Kv4 subfamilies.⁹¹ These genes generate a wide

variety of different K^+ channels through alternative RNA splicing and gene duplication. Functional expression of these different K^+ channels reveals remarkable variation in the rate of inactivation, such that *Shaker* channels are typically rapidly inactivating (A-current like), *Shal* channels inactivate more slowly, *Shab* channels inactivate very slowly, and *Shaw* channels typically do not inactivate, similar to I_K . These studies indicate that each type of neuron in the nervous system is likely to contain a unique set of functional voltage-sensitive K^+ channels, perhaps selected, modified, and placed in particular spatial locations in the cell in a manner to facilitate the unique role of that cell type in neuronal processing.

An additional current that also regulates the responsiveness of neurons to depolarizing inputs is the voltage-sensitive K^+ current known as the M-current (Figs. 6.11 and 6.12D). By investigating the ionic mechanisms by which the release of acetylcholine from preganglionic neurons in the brain results in prolonged changes in the excitability of neurons of the sympathetic ganglia, David Brown and Paul Adams⁹² discovered a unique K^+ current that slowly (over tens of milliseconds) turns on with depolarization of the neuron (see Fig. 6.12D). The slow activation of this K^+ current results in a decrease in the responsiveness of the cell to depolarization, and therefore regulates how the cell responds to excitation. This K^+ current, like I_{AHP} , is reduced by the activation of a wide variety of receptors, including muscarinic receptors, for which it is named. Reduction of I_M results in a marked increase in responsiveness of the affected cell to depolarizing inputs and again may contribute to the mechanisms by which neuromodulatory systems control the state of activity in cortical and hippocampal networks.^{74,93,94}

Ca^{2+} Currents Control Electrophysiological Properties and Ca^{2+} -Dependent Second-Messenger Systems

Ionic channels that conduct Ca^{2+} are present in all neurons. These channels are special in that they serve two important functions. First, Ca^{2+} channels are present throughout the different parts of the neuron (dendrites, soma, synaptic terminals) and contribute greatly to the electrophysiological properties of these processes.^{65,95,96} Second, Ca^{2+} channels are unique in that Ca^{2+} is an important second messenger in neurons, and entry of Ca^{2+} into the cell can affect numerous physiological functions, including neurotransmitter release, synaptic plasticity, neurite outgrowth during development, and even gene expression.

On the bases of their voltage sensitivity, their kinetics of activation and inactivation, and their ability to be blocked by various pharmacological agents, Ca^{2+}

currents can be separated into at least four separate categories, three of which are I_T ("transient"), I_L ("long lasting"), and I_N ("neither"),^{97,98} illustrated in Fig. 6.11A. A fourth, I_P , is found in the Purkinje cells of the cerebellum, as well as in many different cell types of the CNS.⁹⁹ The wide variety of genes involved in the production of Ca^{2+} channels ensures that more Ca^{2+} currents are yet to be characterized.^{100,101}

Neurons Possess Multiple Subtypes of High-Threshold Ca^{2+} Currents

High-voltage-activated Ca^{2+} channels are activated at membrane potentials positive to approximately -40 mV and include the currents I_L , I_N , and I_P . The L-type calcium currents exhibit a high threshold for activation (about -10 mV) and give rise to rather persistent, or long-lasting, ionic currents (see Fig. 6.11A). Dihydropyridines, Ca^{2+} channel antagonists, are clinically useful for their effects on the heart and vascular smooth muscle (e.g., for the treatment of arrhythmias, angina, and migraine headaches) and selectively block L-type Ca^{2+} channels.^{102,103} In contrast with I_L , I_N is not blocked by dihydropyridines; rather it is selectively blocked by a toxin found in Pacific cone shells (ω -conotoxin-GVIA). The N-type Ca^{2+} channels have a threshold for activation of about -20 mV, inactivate with maintained depolarization, and are modulated by a variety of neurotransmitters. In some cell types, I_N has a role in the Ca^{2+} -dependent release of neurotransmitters at presynaptic terminals.¹⁰⁴ The P-type calcium channel is distinct from N and L types in that it is not blocked by either dihydropyridines or ω -conotoxin-GVIA but is blocked by a toxin (ω -agatoxin-IVA) present in the venom of the Funnel web spider.^{99,103} This type of calcium channel activates at relatively high thresholds and does not inactivate. Prevalent in Purkinje cells as well as other cell types, as mentioned earlier, the P-type Ca^{2+} channel participates in the generation of dendritic Ca^{2+} spikes, which can strongly modulate the firing pattern of the neuron in which it resides (see Fig. 6.10C).

Collectively, the high-threshold-activated Ca^{2+} channels contribute to the generation of action potentials in mammalian neurons. The activation of Ca^{2+} currents adds somewhat to the depolarizing part of the action potential, but, more importantly, these channels allow Ca^{2+} to enter the cell and this has the secondary consequence of activation of various Ca^{2+} -activated K^+ currents⁹⁰ and protein kinases (see Chapter 10). As mentioned earlier, the activation of these K^+ currents modifies the pattern of action potentials generated in the cell (see Figs. 6.10 and 6.12).

High-threshold Ca^{2+} channels are similar to the Na^+ channel in that they are composed of a central $\alpha 1$ sub-

unit that forms the aqueous pore and several regulatory or auxiliary subunits. As in the Na^+ channel, the primary structure of the $\alpha 1$ subunit of the Ca^{2+} channel consists of four homologous domains (I–IV), each containing six regions (S1–S6) that may generate transmembrane α -helices. The genes for at least five different Ca^{2+} channel α subunits have been cloned ($\alpha 1\text{A}$ – E), and the properties of the products of these genes indicate that I_L is likely to correspond to $\alpha 1\text{C}$ and $\alpha 1\text{D}$, whereas I_N corresponds to $\alpha 1\text{B}$ and I_P may be related to $\alpha 1\text{A}$.^{101,103}

Low-Threshold Ca^{2+} Currents Generate Bursts of Action Potentials

Low-threshold Ca^{2+} currents (see Fig. 6.11A) often take part in the generation of rhythmic bursts of action potentials (see Figs. 6.10 and 6.12). The low-threshold Ca^{2+} current is characterized by a threshold for activation of about -65 mV, which is below the threshold

for generation of typical Na^+ – K^+ -dependent action potentials (-55 mV). This current inactivates with maintained depolarization. Owing to these properties, the role of low-threshold Ca^{2+} currents differs markedly from that of the high-threshold Ca^{2+} currents. Through activation and inactivation of the low-threshold Ca^{2+} current, neurons can generate slow (about 100 ms) Ca^{2+} spikes, which can result, owing to their prolonged duration, in the generation of a high-frequency “burst” of short-duration Na^+ – K^+ action potentials (see Fig. 6.10 and Box 6.5).^{105–109}

In the mammalian brain, this pattern is especially well exemplified by the activity of thalamic relay neurons; in the visual system, these neurons receive direct input from the retina and transmit this information to the visual cortex. During periods of slow wave sleep, the membrane potential of these relay neurons is relatively hyperpolarized, resulting in the removal of inactivation (deinactivation) of the low-threshold Ca^{2+} current. This deinactivation allows these cells to spon-

BOX 6.5

JELLYFISH—WHAT A NERVE!

Research on jellyfish provides an intriguing insight into how the properties and distribution of ion channels within a nerve membrane can affect the behavior of the whole animal. *Aglantha digitale* can swim slowly when feeding or quickly if escaping predators just through the “behavior” of a single muscle sheet coupled to a simply organized nervous system.

The jellyfish does this through an unusual form of signaling. Each “giant” motor nerve axon not only has voltage-dependent sodium channels and three types of potassium channel, but also crucial T-type calcium channels. *Aglantha* motor axons are unusual because they develop two entirely different propagating action potentials.¹⁰⁵ The T-type calcium channels contribute to a low-amplitude calcium-dependent spike that propagates along the motor axon without gaining amplitude or decrementing in the way that electrotonic potentials do.¹⁰⁶ The motor axon makes direct synaptic contact with the muscle epithelium that makes up the bell of the jellyfish and so the propagating calcium spike induces the weak contractions responsible for propulsion during the regular slow swimming the animal performs when feeding.

Aglantha lives in the colder waters of the world at a depth of about 100 m. Studied in their natural habitat, they are seen to avoid predators by generating an altogether stronger form of swimming. In the laboratory this “escape” swimming can be reproduced by stimulating

vibration-sensitive receptors at the base of the bell of the animal.¹⁰⁷ The strong synaptic depolarization that this stimulus induces in each of the eight giant motor axons drives its membrane potential beyond the peak of the calcium spike and induces a full-sized sodium action potential. As the sodium spike propagates more rapidly than the slow swim calcium spike, there is a coordinated contraction of the body wall that drives the animal forward.

Sodium and calcium spikes like those seen in *Aglantha* have been recorded from a variety of sites in the mammalian CNS.^{64,108} However, unlike in *Aglantha*, the peak of the calcium spike always exceeds the threshold of the sodium spike and the two impulses form a single complex signal. Patch-clamp analysis of *Aglantha* axons has revealed a family of potassium channels that are responsible for setting thresholds and repolarizing each of the two different impulses. Each potassium channel class has an identical unitary conductance and appears to be organized in a mosaic fashion over the surface of the axon.¹⁰⁹ Sodium and T-type calcium channels are clustered together into well-defined “hot spots.” George Mackie and I have suggested that the mosaic organization facilitates the turnover of ion channels; channels inserted into the membrane in clusters age together and are eliminated together.

Robert W. Meech

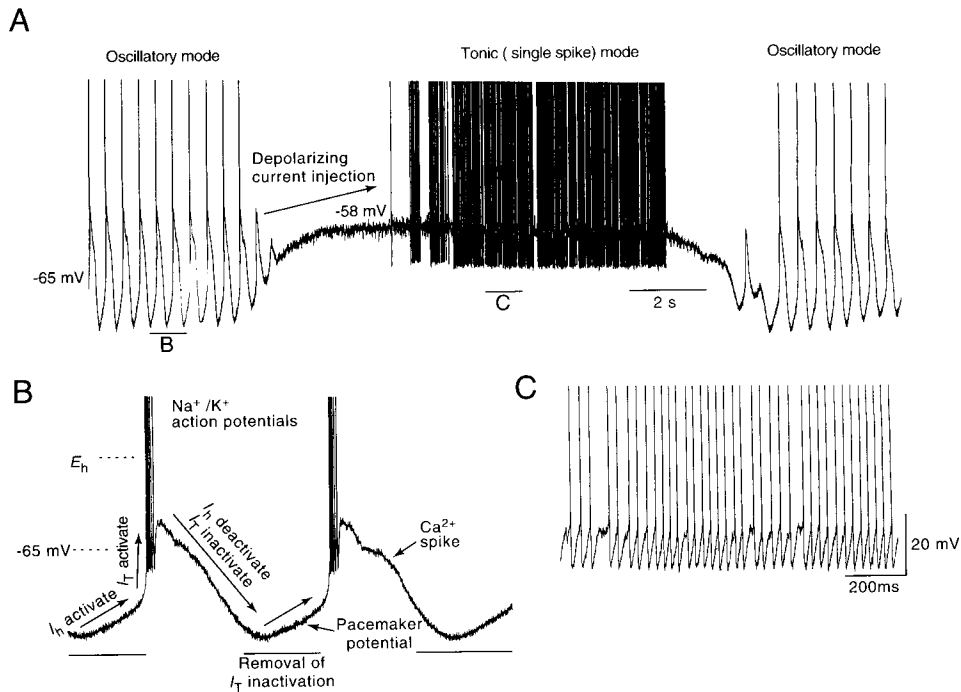


FIGURE 6.13 Two different patterns of activity generated in the same neuron, depending on membrane potential. (A) The thalamic neuron spontaneously generates rhythmic bursts of action potentials owing to the interaction of the Ca^{2+} current I_T and the inward “pacemaker” current I_h . Depolarization of the neuron changes the firing mode from rhythmic burst firing to tonic action potential generation in which spikes are generated one at a time. Removal of this depolarization reinstates the rhythmic burst firing. This transition from rhythmic burst firing to tonic activity is similar to that which occurs in the transition from sleep to waking. (B) Expansion of detail of rhythmic burst firing. (C) Expansion of detail of tonic firing. From McCormick and Pape.¹¹⁰

taneously generate low-threshold Ca^{2+} spikes and bursts of from two to five action potentials (Fig. 6.13).¹¹⁰ The large number of thalamic relay cells bursting during sleep in part gives rise to the spontaneous synchronized activity that early investigators were so surprised to find during recordings from the brains of sleeping animals.¹¹¹ It has even proved possible to maintain one of the sleep-related brain rhythms (spindle waves) intact in slices of thalamic tissue maintained *in vitro*, owing to the generation of this rhythm by the interaction of a local network of thalamic cells and their electrophysiological properties.¹¹²

The transition to waking or the period of sleep when dreams are prevalent (rapid eye movement sleep) is associated with a maintained depolarization of thalamic relay cells to membrane potentials ranging from about -60 to -55 mV. The low-threshold Ca^{2+} current is inactivated and therefore the burst discharges are abolished. In this way, the properties of a single ionic current (I_T) help to explain in part the remarkable changes in brain activity taking place in the transition from sleep to waking (Fig. 6.13).

Low-threshold Ca^{2+} channels were recently cloned and shown to have some similarities to other Ca^{2+} channels.¹¹⁷ Evidence suggests that some antiepileptic drugs may exert their therapeutic actions through a reduction in I_T . This is especially true of the drugs useful in the treatment of generalized absence (petit mal) seizures, which are known to rely on the thalamus for their generation.¹¹³

Hyperpolarization-Activated Ionic Currents Are Involved in Rhythmic Activity

In most types of neurons, hyperpolarization negative to approximately -60 mV activates an ionic current, known as I_h , that conducts both Na^+ and K^+ ions (see Fig. 6.11A). This current typically has very slow kinetics, turning on with a time constant on the order of tens of milliseconds to seconds. Because the channels underlying this current allow the passage of both Na^+ and K^+ ions, the reversal potential of I_h is typically about -35 mV—between E_{Na} and E_{K} . Because this current is activated by hyperpolarization below approxi-

mately -60 mV, it is typically dominated by the inward movement of Na^+ ions and is therefore depolarizing. For what purpose could neurons use a depolarizing current that activates when the cell is hyperpolarized? A clue comes from cardiac cells in which this current, known as I_f for "funny," is important for determining heart rate.¹¹⁴ Activation of I_f results in a slow depolarization of the membrane potential between adjacent cardiac action potentials. The more that I_f is activated, the faster the membrane depolarizes between beats and therefore the sooner the threshold for the next action potential is reached and the next beat is generated. In this manner, the amplitude, or sensitivity to voltage, of I_f can modify heart rate. Interestingly, the sensitivity of I_f to voltage is adjusted by the release of noradrenaline and acetylcholine; the activation of β -adrenoceptors by noradrenaline increases I_f and therefore increases the heart rate, whereas the activation of muscarinic receptors decreases I_f , thereby decreasing the heart rate.^{115,116} This continual adjustment of I_f results from a "push-pull" arrangement between β -adrenergic and muscarinic cholinergic receptors and is mediated by the adjustment of intracellular levels of cyclic AMP. Indeed, the recent cloning of H-channels reveals that its structure is similar to that of cyclic nucleotide gated channels.¹¹⁸

Could I_h play a role in neurons similar to that of I_f in the heart? Possibly. Synchronized rhythmic oscillations in the membrane potential of large numbers of neurons, in some respects similar to those of the heart, are characteristic of the mammalian brain. Oscillations of this type are particularly prevalent in thalamic relay neurons during some periods of sleep, as mentioned earlier. Intracellular recordings from these thalamic neurons reveal that they often generate rhythmic "bursts" of action potentials mediated by the activation of a slow spike that is generated through the activation of the low-threshold, or transient, Ca^{2+} current, I_T ^{76,110} (see Fig. 6.13). Between the occurrence of each low-threshold Ca^{2+} spike is a slowly depolarizing membrane potential generated by activation of the mixed Na^+ - K^+ current I_h , as with I_f in the heart. The amplitude, or voltage sensitivity, of I_h adjusts the rate at which the thalamic cells oscillate, and, as with the heart, this sensitivity is adjusted by the release of modulatory neurotransmitters (see Fig. 6.13). In a sense, the thalamic neurons are "beating" in a manner similar to that of the heart.

Summary

An action potential is generated by the rapid influx of Na^+ ions followed by a slightly slower efflux of K^+ ions. Although the generation of an action potential

does not disrupt the concentration gradients of these ions across the membrane, the movement of charge is sufficient to generate a large and brief deviation in the membrane potential. Propagation of the action potential along the axon allows communication of the output of the cell to its synapses. Neurons possess many different types of ionic channels in their membranes, allowing complex patterns of action potentials to be generated and complex synaptic computations to occur within single neurons.

References

1. Brazier, M. A. B. (1959). The historical development of neurophysiology. In *Handbook of Physiology* (J. Field, ed.), Sect. 1, Vol. 1, pp. 1–58. Am. Physiol. Soc., Washington, DC.
2. Brazier, M. A. B. (1988). *A History of Neurophysiology in the 19th Century*. Raven Press, New York.
3. Young, J. Z. (1936). The giant nerve fibers and epistellar body of cephalopods. *Q. J. Microsc. Sci.* **78**: 367.
4. Hodgkin, A. L., and Huxley, A. F. (1939). Action potentials recorded from inside a nerve fiber. *Nature (London)* **144**: 710–711.
5. Hodgkin, A. L. (1976). Chance and design in electrophysiology: An informal account of certain experiments on nerve carried out between 1934 and 1952. *J. Physiol. (London)* **263**: 1–21.
6. Brock, L. G., Coombs, J. S., and Eccles, J. C. (1952). The recording of potentials from motoneurons with an intracellular electrode. *J. Physiol. (London)* **117**: 431–460.
7. Buser, P., and Albe-Fessard, D. (1953). Premiers résultats d'une analyse l'activité électrique du cortex cérébral du Chat par microélectrodes intracellulaires. *C. R. Hebd. Seances Acad. Sci.* **236**: 1197–1199.
8. Tasaki, I., Polley, E. H., and Orrego, F. (1954). Action potentials from individual elements in cat geniculate and striate cortex. *J. Neurophysiol.* **17**: 454–474.
9. Phillips, C. G. (1956). Intracellular records from betz cells in the cat. *Q. J. Exp. Physiol.* **41**: 58–69.
10. Nernst, W. (1888). On the kinetics of substances in solution. Translated from *Z. Phys. Chem.* **2**: 613–622, 634–637. In *Cell Membrane Permeability and Transport* (G. R. Kepner, ed.), pp. 174–183. Dowden, Hutchinson & Ross, Stroudsburg, PA, 1979.
11. Hotson, J. R., Sybert, G. W., and Ward, A. A. (1973). Extracellular potassium concentration changes during propagated seizures in neocortex. *Exp. Neurol.* **38**: 20–26.
12. Prince, D. A., Lux, H. D., and Neher, E. (1973). Measurements of extracellular potassium activity in cat cortex. *Brain Res.* **50**: 489–495.
13. Kuffler, S. W., and Nicholls, J. G. (1966). The physiology of neuroglia cells. *Ergeb. Physiol.* **57**: 1–90.
14. Goldman, D. F. (1943). Potential, impedance, and rectification in membranes. *J. Gen. Physiol.* **27**: 37–60.
15. Hodgkin, A. L., and Katz, B. (1949). The effect of sodium ions on the electrical activity of the giant axon of the squid. *J. Physiol. (London)* **108**: 37–77.
16. Tomita, T. (1965). Electrophysiological study of the mechanisms subserving color coding in the fish retina. *Cold Spring Harbor Symp. Quant. Biol.* **30**: 559–566.
17. Hirsch, J. C., Fourment, A., and Marc, M. E. (1983). Sleep-related variations of membrane potential in the lateral geniculate body relay neurons of the cat. *Brain Res.* **259**: 308–312.
18. Jahnson, H., and Llinás, R. (1984). Electrophysiological proper-

- ties of guinea-pig thalamic neurons: an *in vitro* study. *J. Physiol. (London)* **349**: 205–226.
19. Jahnsen, H., and Llinás, R. (1984). Ionic basis for the electrosensiveness and oscillatory properties of guinea-pig thalamic neurons *in vitro*. *J. Physiol. (London)* **349**: 227–247.
 20. McCormick, D. A., Connors, B. W., Lighthall, J. W., and Prince, D. A. (1985). Comparative electrophysiology of pyramidal and sparsely spiny neurons of the neocortex. *J. Neurophysiol.* **54**: 782–806.
 21. Livingstone, M. S., and Hubel, D. H. (1981). Effects of sleep and arousal on the processing of visual information in the cat. *Nature (London)* **291**: 554–561.
 22. Steriade, M., and McCarley, R. W. (1990). *Brainstem Control of Wakefulness and Sleep*. Plenum, New York.
 23. Hodgkin, A. L., and Keynes, D. (1955). Active transport of cations in giant axons from *Sepia* and *Loligo*. *J. Physiol. (London)* **128**: 28–60.
 24. Skou, J. C. (1957). The influence of some cations on an adenosine triphosphatase from peripheral nerves. *Biochim. Biophys. Acta* **23**: 394–401.
 25. Thomas, R. C. (1972). Electrogenic sodium pump in nerve and muscle cells. *Physiol. Rev.* **52**: 563–594.
 26. Skou, J. C. (1988). Overview: The Na,K pump. In *Methods in Enzymology* (S. Fleischer and B. Fleischer, eds.), Vol. 156, pp. 1–25. Academic Press, Orlando, FL.
 27. Mercer, R. W. (1993). Structure of the Na,K-ATPase. *Int. Rev. Cytol.* **137C**: 139–168.
 28. Horisberger, J.-D., Lemas, V., Kraehenbühl, J.-P., and Rossier, B. C. (1991). Structure–function relationship of Na,K-ATPase. *Annu. Rev. Physiol.* **53**: 565–584.
 29. Pedersen, P. L., and Carafoli, E. (1987). Ion motive ATPases. I. Ubiquity, properties, and significance to cell function. *Trends Biochem. Sci.* **12**: 146–150.
 30. Läuger, P. (1991). *Electrogenic Ion Pumps*. Sinauer, Sunderland, MA.
 31. Reithmeier, R. A. F. (1994). Mammalian exchangers and co-transporters. *Curr. Opin. Cell Biol.* **6**: 583–594.
 32. Thompson, S. M., Deisz, R. A., and Prince, D. A. (1988). Relative contributions of passive equilibrium and active transport to the distribution of chloride in mammalian cortical neurons. *J. Neurophysiol.* **60**: 105–124.
 33. Hodgkin, A. L., and Huxley, A. F. (1952). Currents carried by sodium and potassium ions through the membrane of the giant axon of *Loligo*. *J. Physiol. (London)* **116**: 449–472.
 34. Hodgkin, A. L., and Huxley, A. F. (1952). The components of membrane conductance in the giant axon of *Loligo*. *J. Physiol. (London)* **116**: 473–496.
 35. Hodgkin, A. L., and Huxley, A. F. (1952). The dual effect of membrane potential on sodium conductance in the giant axon of *Loligo*. *J. Physiol. (London)* **116**: 497–506.
 36. Hodgkin, A. L., and Huxley, A. F. (1952). A quantitative description of membrane current and its application to conduction and excitation in nerve. *J. Physiol. (London)* **117**: 500–544.
 37. Hodgkin, A. L., Huxley, A. F., and Katz, B. (1952). Measurement of current-voltage relations in the membrane of the giant axon of *Loligo*. *J. Physiol. (London)* **116**: 424–448.
 38. Cole, K. S., and Curtis, H. J. (1939). Electric impedance of the squid giant axon during activity. *J. Gen. Physiol.* **22**: 649–670.
 39. Overton, E. (1902). Beiträge zur allgemeinen Muskel- und Nervenphysiologie. II. Ueber die Urentbehrrlichkeit von Natrium- (oder Lithium-) Ionen für den Contractionsact des Muskel. *Pfluegers Arch. Gesamte Physiol. Menschen Tiere* **92**: 346–386.
 40. Cole, K. S. (1949). Dynamic electrical characteristics of the squid axon membrane. *Arch. Sci. Physiol.* **3**: 253–258.
 41. Hille, B. (1977). Ionic basis of resting potentials and action potentials. In *Handbook of Physiology* (E. R. Kandel, ed.), Sect. 1, Vol. 1, pp. 99–136. Am. Physiol. Soc., Bethesda, MD.
 42. Kao, C. T. (1966). Tetrodotoxin, saxotoxin and their significance in the study of excitation phenomena. *Pharmacol. Rev.* **18**: 997–1049.
 43. Armstrong, C. M., and Hille, B. (1972). The inner quaternary ammonium ion receptor in potassium channels of the node of Ranvier. *J. Gen. Physiol.* **59**: 388–400.
 44. Bunge, R. P. (1968). Glial cells and the central myelin sheath. *Physiol. Rev.* **48**: 197–251.
 45. Ritchie, J. M., and Rogart, R. B. (1977). Density of sodium channels in mammalian myelinated nerve fibers and nature of the axonal membrane under the myelin sheath. *Proc. Natl. Acad. Sci. U.S.A.* **74**: 211–215.
 46. Miller, C. (1989). Genetic manipulation of ion channels: A new approach to structure and mechanism. *Neuron* **2**: 1195–1205.
 47. Anderson, O. S., and Koeppe, R. E., II (1992). Molecular determinants of channel function. *Physiol. Rev.* **72**(Suppl.): S89–S158.
 48. Catterall, W. A. (1988). Structure and function of voltage-sensitive ion channels. *Science* **242**: 50–61.
 49. Catterall, W. A. (1992). Cellular and molecular biology of voltage-gated sodium channels. *Physiol. Rev.* **72**(4, Suppl.): S15–S48.
 50. Catterall, W. A. (1995). Structure and function of voltage-gated ion channels. *Annu. Rev. Biochem.* **64**: 493–531.
 51. Salkoff, L., Baker, K., Butler, A., Covarrubias, M., Pak, M. D., and Wei, A. (1992). An essential “set” of K⁺ channels conserved in flies, mice, and humans. *Trends Neurosci.* **15**: 161–166.
 52. Beneski, D. A., and Catterall, W. A. (1980). Covalent labeling of protein components of the sodium channel with a photoactivable derivative of scorpion toxin. *Proc. Natl. Acad. Sci. U.S.A.* **77**: 639–643.
 53. Armstrong, C. M. (1992). Voltage-dependent ionic channels and their gating. *Physiol. Rev.* **72**(Suppl.): 5–13.
 54. Vassilev, P. M., Scheuer, T., and Catterall, W. A. (1988). Identification of an intracellular peptide segment involved in sodium channel inactivation. *Science* **241**: 1658–1661.
 55. Vassilev, P., Scheuer, T., and Catterall, W. A. (1989). Inhibition of inactivation of single sodium channels by a site-directed antibody. *Proc. Natl. Acad. Sci. U.S.A.* **86**: 8147–8151.
 56. Stuhmer, W., Conti, F., Suzuki, H., Wang, X., Noda, M., Yahadi, N., Kobu, H., and Numa, S. (1989). Structural parts involved in activation and inactivation of the sodium channel. *Nature (London)* **339**: 597–603.
 57. Eccles, J. C. (1957). *The Physiology of Nerve Cells*. Johns Hopkins University Press, Baltimore, MD.
 58. Alving, B. O. (1968). Spontaneous activity in isolated somata of *Aplysia* pacemaker neurons. *J. Gen. Physiol.* **51**: 29–45.
 59. Arvanitaki, A., and Chalazonitis, N. (1961). Slow waves and associated spiking in nerve cells of *Aplysia*. *Bull. Inst. Oceanogr. Monaco* **58**: 1–15.
 60. Jacklet, J. W. (1989). *Neuronal and Cellular Oscillators*. Dekker, New York.
 61. Llinás, R., and Sugimori, M. (1980). Electrophysiological properties of *in vitro* Purkinje cell somata in mammalian cerebellar slices. *J. Physiol. (London)* **305**: 171–195.
 62. Llinás, R., and Sugimori, M. (1980). Electrophysiological properties of *in vitro* Purkinje cell dendrites in mammalian cerebellar slices. *J. Physiol. (London)* **305**: 197–213.
 63. Llinás, R., and Yarom, Y. (1981). Electrophysiology of mammalian inferior olivary neurones *in vitro*: Different types of voltage-dependent ionic conductances. *J. Physiol. (London)* **315**: 569–584.

64. Llinás, R., and Yarom, Y. (1981). Properties and distribution of ionic conductances generating electroresponsiveness of mammalian inferior olivary neurones *in vitro*. *J. Physiol. (London)* **315**: 569–584.
65. Llinás, R. R. (1988). The intrinsic electrophysiological properties of mammalian neurons: Insights into central nervous system function. *Science* **242**: 1654–1664.
66. Madison, D. V., and Nicoll, R. A. (1984). Control of repetitive discharge of rat CA1 pyramidal neurons *in vitro*. *J. Physiol. (London)* **354**: 319–331.
67. Pennefather, P., Lancaster, B., Adams, P. R., and Nicoll, R. A. (1985). Two distinct Ca-dependent K currents in bullfrog sympathetic ganglion cells. *Proc. Natl. Acad. Sci. U.S.A.* **82**: 3040–3044.
68. Wang, Z., and McCormick, D. A. (1993). Control of firing mode of corticotectal and corticopontine layer V burst-generating neurons by norepinephrine, acetylcholine, and 1S,3R-ACPD. *J. Neurosci.* **13**: 2199–2216.
69. Schwartzkroin, P. A., and Mathers, L. H. (1978). Physiological and morphological identification of a nonpyramidal hippocampal cell type. *Brain Res.* **157**: 1–10.
70. Pape, H.-C., and McCormick, D. A. (1995). Electrophysiological and pharmacological properties of interneurons in the cat dorsal lateral geniculate nucleus. *Neuroscience* **68**: 1105–1125.
71. Vandermaelen, C. P., and Aghajanian, G. K. (1983). Electrophysiological and pharmacological characterization of serotonergic dorsal raphe neurons recorded extracellularly and intracellularly in rat brain slices. *Brain Res.* **289**: 109–119.
72. Williams, J. T., North, R. A., Shefner, S. A., Nishi, S., and Egan, T. M. (1984). Membrane properties of rat locus coeruleus neurones. *Neuroscience* **13**: 137–156.
73. Reiner, P. B., and McGeer, E. G. (1987). Electrophysiological properties of cortically projecting histamine neurons of the rat hypothalamus. *Neurosci. Lett.* **73**: 43–47.
74. McCormick, D. A. (1992). Neurotransmitter actions in the thalamus and cerebral cortex and their role in neuromodulation of thalamocortical activity. *Prog. Neurobiol.* **39**: 337–388.
75. Belluzzi, O., and Sacchi, O. (1991). A five-conductance model of the action potential in the rat sympathetic neurone. *Prog. Biophys. Mol. Biol.* **55**: 1–30.
76. McCormick, D. A., and Huguenard, D. A. (1992). A model of the electrophysiological properties of thalamocortical relay neurons. *J. Neurophysiol.* **68**: 1384–1400.
77. Huguenard, J., and McCormick, D. A. (1994). *Electrophysiology of the Neuron*. Oxford University Press, New York.
78. Hotson, J. R., Prince, D. A., and Schwartzkroin, P. A. (1979). Anomalous inward rectification in hippocampal neurons. *J. Neurophysiol.* **42**: 889–895.
79. Stafstrom, C. E., Schwindt, P. C., and Crill, W. E. (1982). Negative slope conductance due to a persistent subthreshold sodium current in cat neocortical neurons *in vitro*. *Brain Res.* **236**: 221–226.
80. Alzheimer, C., Schwindt, P. C., and Crill, W. E. (1993). Modal gating of Na⁺ channels as a mechanism of persistent Na⁺ current in pyramidal neurons from rat and cat sensorimotor cortex. *J. Neurosci.* **13**: 660–673.
81. Goldman-Rakic, P. S. (1995). Cellular basis of working memory. *Neuron* **14**: 477–485.
82. Jan, L. Y., and Jan, Y. N. (1990). How might the diversity of potassium channels be generated? *Trends Neurosci.* **13**: 415–419.
83. Storm, J. F. (1990). Potassium currents in hippocampal pyramidal cells. *Prog. Brain Res.* **83**: 161–187.
84. Johnston, D., and Wu, S. M.-S. (1995). *Foundations of Cellular Neurophysiology*. MIT Press, Cambridge, MA.
85. Connor, J. A., and Stevens, C. F. (1971). Voltage clamp studies of a transient outward membrane current in gastropod neural somata. *J. Physiol. (London)* **213**: 21–30.
86. Connor, J. A., and Stevens, C. F. (1971). Prediction of repetitive firing behaviour from voltage clamp data on an isolated neurone soma. *J. Physiol. (London)* **213**: 31–53.
87. Hoshi, T., Zagotta, W. N., and Aldrich, R. W. (1990). Biophysical and molecular mechanisms of Shaker potassium channel inactivation. *Science* **250**: 533–538.
88. Zagotta, W. N., Hoshi, T., and Aldrich, R. W. (1990). Restoration of inactivation in mutants of Shaker potassium channels by a peptide derived from ShB. *Science* **250**: 568–571.
89. Blatz, A. L., and Magleby, K. L. (1987). Calcium-activated potassium channels. *Trends Neurosci.* **11**: 463–467.
90. Latorre, R., Oberhauser, A., Labarca, P., and Alvarez, O. (1989). Varieties of calcium-activated potassium channels. *Annu. Rev. Physiol.* **51**: 385–399.
91. Chandy, K. G., and Gutman, G. A. (1995). Voltage-gated potassium channel genes. In *Ligand- and Voltage-Gated Channels* (A. North, ed.), pp. 1–72. CRC Press, Boca Raton, FL.
92. Brown, D. A., and Adams, P. R. (1980). Muscarinic suppression of a novel voltage sensitive K⁺ current in a vertebrate neurone. *Nature (London)* **283**: 673–676.
93. Nicoll, R. A. (1988). The coupling of neurotransmitter receptors to ion channels in the brain. *Science* **241**: 545–551.
94. Nicoll, R. A., Malenka, R. C., and Kauer, J. A. (1990). Functional comparison of neurotransmitter receptor subtypes in mammalian central nervous system. *Physiol. Rev.* **70**: 513–565.
95. Regehr, W. G., and Tank, D. W. (1994). Dendritic calcium dynamics. *Curr. Opin. Neurobiol.* **4**: 373–382.
96. Markram, H., Helm, P. J., and Sakmann, B. (1995). Dendritic calcium transients evoked by single back-propagating action potentials in rat neocortical pyramidal neurons. *J. Physiol. (London)* **485**: 1–20.
97. Nowycky, M. C., Fox, A. P., and Tsien, R. W. (1985). Three types of neuronal calcium channel with different calcium agonist sensitivity. *Nature (London)* **316**: 440–443.
98. Carbonne, E., and Lux, H. D. (1984). A low voltage-activated, fully inactivating Ca channel in vertebrate sensory neurones. *Nature (London)* **310**: 501–502.
99. Llinás, R., Sugimori, M., Hillman, D. E., and Cherksey, B. (1992). Distribution and functional significance of the P-type, voltage-dependent Ca²⁺ channels in the mammalian nervous system. *Trends Neurosci.* **15**: 351–355.
100. Tsien, R. W., Ellinor, P. T., and Horne, W. A. (1991). Molecular diversity of voltage-dependent Ca²⁺ channels. *Trends Pharmacol. Sci.* **12**: 349–354.
101. Birnbaumer, L., Campbell, K. P., Catterall, W. A., Harpold, M. M., Hofmann, F., Horne, W. A., Mori, Y., Schwartz, A., Snutch, T. P., Tanabe, T., and Tsien, R. W. (1994). The naming of voltage-gated calcium channels. *Neuron* **13**: 505–506.
102. Bean, B. P. (1989). Classes of calcium channels in vertebrate cells. *Annu. Rev. Physiol.* **51**: 367–384.
103. Stea, A. Soong, T. W., and Snutch, T. P. (1995). Voltage-gated calcium channels. In *Ligand and Voltage-Gated Ion Channels* (A. North, ed.), pp. 113–152. CRC Press, Boca Raton, FL.
104. Wheeler, D. B., Randall, A., and Tsien, R. W. (1994). Roles of N-type and Q-type Ca²⁺ channels in supporting hippocampal synaptic transmission. *Science* **264**: 107–111.
105. Mackie, G. O., and Meech, R. W. (1985). Separate sodium and calcium spikes in the same axon. *Nature (London)* **313**: 791–793.
106. Meech, R. W., and Mackie, G. O. (1995). Synaptic events underlying the production of calcium and sodium spikes in motor giant axons of *Aglaantha digitale*. *J. Neurophysiol.* **74**: 1662–1669.

107. Arnett, S., Mackie, G. O., and Meech, R. W. (1988). Hair-cell mechanoreception in the jellyfish *Aglantha digitale*. *J. Exp. Biol.* **135**: 329–342.
108. Llinas, R., and Jahnsen, H. (1982). Electrophysiology of mammalian thalamic neurones *in vitro*. *Nature (London)* **297**: 406–408.
109. Meech, R. W., and Mackie, G. O. (1993). Potassium channel family in giant motor axons of *Aglantha digitale*. *Neurophysiology* **69**: 894–901.
110. McCormick, D. A., and Pape, H.-C. (1990). Properties of a hyperpolarization-activated cation current and its role in rhythmic oscillation in thalamic relay neurones. *J. Physiol. (London)* **431**: 291–318.
111. Steriade, M., McCormick, D. A., and Sejnowski, T. (1993). Thalamic oscillations in the sleep and aroused brain. *Science* **262**: 679–685.
112. von Krosigk, M., Bal, T., and McCormick, D. A. (1993). Cellular mechanisms of a synchronized oscillation in the thalamus. *Science* **261**: 361–364.
113. Coulter, D. A., Huguenard, J. R., and Prince, D. A. (1990). Differential effects of petit mal anticonvulsants and convulsants on thalamic neurones: Calcium current reduction. *Br. J. Pharmacol.* **100**: 800–806.
114. DiFrancesco, D. (1985). The cardiac hyperpolarizing-activated current, I_h : Origins and developments. *Prog. Biophys. Mol. Biol.* **46**: 163–183.
115. DiFrancesco, D. (1993). Pacemaker mechanisms in cardiac tissue. *Annu. Rev. Physiol.* **55**: 455–472.
116. DiFrancesco, D., Ducouret, P., and Robinson, R. B. (1989). Muscarinic modulation of cardiac rate at low acetylcholine concentrations. *Science* **243**: 669–671.
117. Perez-Reyes, E., Cribbs, L. L., Daud, A., Lacerda, A. E., Barclay, J., Williamson, M. P., Fox, M., Rees, M. and Lee, J.-H. (1998). Molecular characterization of a neuronal low-voltage-activated T-type calcium channel. *Nature* **391**: 896–900.
118. Ludwig, A., Zong, X., Jeglitsch, M., Hofmann, F., and Biel, M. (1998). A family of hyperpolarization-activated mammalian cation channels. *Nature* **393**: 587–591.

Release of Neurotransmitters

Robert S. Zucker, Dimitri M. Kullmann, and Mark Bennett

The synapse is the point of functional contact between one neuron and another. It is the primary place at which information is transmitted from neuron to neuron in the central nervous system or from neuron to target (gland or muscle) in the periphery. The simplest way for one cell to inform another of its activity is by direct electrical interaction, in which the current generated extracellularly from the action potential in the first cell passes through neighboring cells. Owing to the shunting of current by the highly conductive extracellular fluid, a 100-mV action potential may generate only 10–100 μ V in a neighboring neuron. This coupling can be improved if neighboring cells are joined by a specialized conductive pathway through gap junctions (see Chapter 11); even then, a presynaptic spike is not likely to generate more than about 1 mV postsynaptically, unless the presynaptic process is nearly as large or larger than the postsynaptic process. This biophysical constraint limits the number of presynaptic cells that can converge on and influence a postsynaptic cell, and such electrical connections can normally only be excitatory and short-lasting, are bidirectional in transmission, and show little plasticity or modifiability. They have limited potential for complex computation, but can be useful when a postsynaptic neuron must be activated with high reliability and speed or when concurrent activity in a large number of presynaptic afferents must be signaled.

ORGANIZATION OF THE CHEMICAL SYNAPSE

Most interneuronal communication relies on the use of a chemical intermediary, or **transmitter**, secreted subsequent to action potentials by presynaptic cells to

influence the activity of postsynaptic cells. In chemical transmission, a single action potential in a small presynaptic terminal can generate a large **postsynaptic potential** (PSP) (as large as tens of millivolts). This is accomplished by the release of thousands to hundreds of thousands of molecules of transmitter that can bind to postsynaptic **receptor molecules** and open (or close) as many ion channels in about 1 ms. There is room for many afferents (often thousands) to interact and influence a postsynaptic neuron, and the effect can be either excitatory or inhibitory, depending on the ions that permeate the channels operated by the receptor. The resulting responses are either **excitatory postsynaptic potentials** (EPSPs) or **inhibitory postsynaptic potentials** (IPSPs), depending on whether they drive the cell toward a point above or below its firing threshold. Different afferents can have different effects, with different strengths and kinetics, on each other as well as on postsynaptic cells. These differences depend on the identity of the transmitter(s) released and the receptors present (see Chapters 8 and 9). Chemical synapses are often modified by prior activity in the presynaptic neuron. Chemical synapses are also particularly subject to modulation of presynaptic ion channels by substances released by the postsynaptic or neighboring neurons. This flexibility is essential for the complex processing of information that neural circuits must accomplish, and it provides an important locus for modifiability of neural circuits underlying adaptive processes such as learning (Chapters 55 and 56).

Transmitter Release Is Quantal

One of the first applications of the microelectrode was the discovery that transmitter release is *quantal* in nature.¹ Transmitter is released spontaneously in

multimolecular packets called **quanta** in the absence of presynaptic electrical activity. Each packet generates a small postsynaptic signal—either a **miniature excitatory** or a **miniature inhibitory postsynaptic potential** (MEPSP or MIPSP, respectively, or just MPSP); under voltage clamp, a miniature excitatory or an inhibitory postsynaptic current (MEPSC or MIPSC, respectively, or just MPSC) is generated. An action potential tremendously, but very briefly, accelerates the rate of secretion of quanta and synchronizes them to evoke a PSP. Vertebrate skeletal neuromuscular junctions are frequently used as model synapses, because both receptors and nerve terminals are relatively accessible for anatomical, electrophysiological, and biochemical studies. At the neuromuscular junction, the motor nerve forms a cluster of small unmyelinated processes that lie in shallow

gutters in the muscle to form a structure called an **end plate**, and PSPs, PSCs, MPSPs, and MPSCs are called **end-plate potentials** (EPPs), **end-plate currents** (EPCs), **miniature end-plate potentials** (MEPPs), and **miniature end-plate currents** (MEPCs), respectively.

Why is transmission quantized? Neural circuits must process complex and quickly changing information fast enough to generate timely appropriate responses. This requires rapid transmission across synapses. Fast-acting chemical synapses accomplish this by concentrating transmitter in membrane-bound structures, 50 nm in diameter, called **synaptic vesicles** and docking these vesicles at specialized sites called **active zones** along the presynaptic membrane (Fig. 7.1A). Vesicles not docked at the membrane are clustered behind it and associated with cytoskeletal ele-

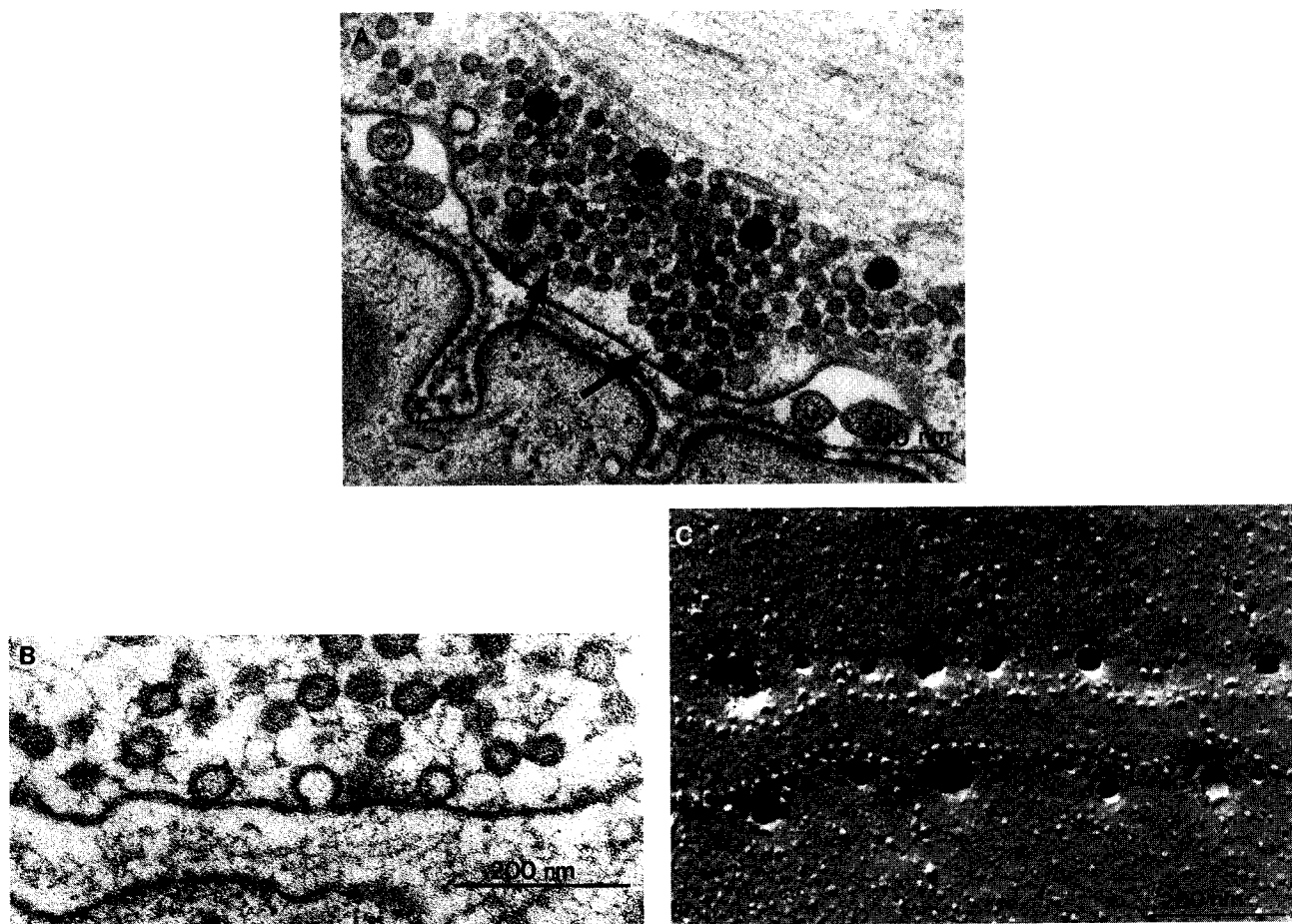


FIGURE 7.1 Ultrastructural images of synaptic vesicle exocytosis. Synapses from frog sartorius neuromuscular junctions were quick-frozen milliseconds after stimulation in 4-aminopyridine to broaden action potentials and enhance transmission. (A) A thin section from which water was replaced with organic solvents (*freeze substitution*) and fixed in osmium tetroxide, showing vesicles clustered in the active zone, some docked at the membrane (arrows). (B) Shortly (5 ms) after stimulation, vesicles were seen to fuse with the plasma membrane. (C) After freezing, presynaptic membranes were *freeze-fractured* and a platinum replica was made of the external face of the cytoplasmic membrane leaflet. Vesicles fuse about 50 nm from rows of intramembranous particles thought to include Ca^{2+} channels. Parts A and B from Heuser²; part C from Heuser and Reese.⁴ Part B reproduced from the *Journal of Cell Biology*, 1981, 88, pp. 564–580.

BOX 7.1

EVIDENCE THAT A QUANTUM IS A VESICLE

Transmitter is released from vesicles:

1. All chemically transmitting synaptic terminals contain presynaptic vesicles.⁸
2. Synaptic vesicles concentrate and store transmitter.⁹
3. Rapid freezing of neuromuscular junctions during stimulation shows vesicle exocytosis occurring at the moment of transmitter release.¹⁰
4. Intravesicular proteins appear on the external terminal surface after secretion.^{11,12}
5. Retarding the filling of vesicles by using transport inhibitors (e.g., vesamicol for acetylcholine) or by reducing the transvesicular pH gradient generates a class of small MEPPs that probably represent partially filled vesicles; drugs that enhance vesicle loading increase MEPP size.¹³⁻¹⁵
6. Quantal size is independent of membrane potential or cytoplasmic acetylcholine concentration altered osmotically.¹⁶
7. Synaptic vesicles formed by endocytosis load with extracellular electron-dense and fluorescent dyes (horseradish peroxidase and FM1-43, respectively) after nerve stimulation; the dye is released by subsequent stimulation.^{17,18}
8. False transmitters synthesized from choline derivatives load slowly into cholinergic vesicles; they are

coreleased with acetylcholine in proportion to their concentrations in vesicles.¹⁹

9. Clostridial toxins that interfere with the synaptic vesicle-plasma membrane interaction block neurosecretion.²⁰

One quantum is one vesicle:

1. The number of acetylcholine molecules in isolated vesicles corresponds to the number of molecules released in a quantum.⁵⁻⁷
2. When release is enhanced and the collapse of vesicle fusion images is prolonged by treatment with the potassium channel blocker 4-aminopyridine to broaden action potentials, the number of vesicle fusions observed corresponds to the number of quanta released by an action potential.²¹ Under these special circumstances, several vesicles are released at each active zone (Fig. 7.1C).
3. The number of vesicles present in nerve terminals corresponds to the total store of releasable quanta. When endocytosis is blocked by the temperature-sensitive *Drosophila* mutant *shibiri*²³ or pharmacologically²² and the motor nerve is stimulated to exhaustion, the number of quanta released corresponds to the original number of presynaptic vesicles.

ments.² Action potentials release transmitter by depolarizing the presynaptic membrane and opening Ca^{2+} channels that are strategically colocalized with the synaptic vesicles in the active zone.³ The local intense rise in Ca^{2+} concentration triggers the fusion of docked vesicles with the plasma membrane (called **exocytosis**; Figs. 7.1B and 7.1C⁴) and the release of their contents into the narrow **synaptic cleft** (about 100 nm wide) separating the presynaptic terminal from high concentrations of postsynaptic receptors. The fusion of one vesicle releases about 5000 transmitter molecules within a millisecond⁵⁻⁷ and generates the quantal response recorded postsynaptically. No membrane carrier can release so much transmitter this fast, nor can a pore or channel unless some mechanism exists to concentrate the transmitter behind the pore, which may be regarded as the function of synaptic vesicles. Evidence that transmitter is released from vesicles and that one quantum is due to exocytosis of a vesicle is summarized in Box 7.1.⁸⁻²³

At neuromuscular junctions, transmitter from one vesicle diffuses across the synaptic cleft in 2 μs and reaches a concentration of about 1 mM at the postsynaptic receptors.²⁴ These receptors bind transmitter rapidly, opening from 1000 to 2000 postsynaptic ion channels²⁵ (two molecules of transmitter must bind simultaneously to receptors to open each channel—see Chapter 14). Each channel has a 25-pS conductance and remains open for about 1.5 ms, admitting a net inflow of 35,000 positive ions. A single action potential in a motor neuron can release 300 quanta within about 1.5 ms along a junction that contains about 1000 active zones. The resulting postsynaptic depolarization, which begins after a **synaptic delay** of about 0.5 ms and reaches a peak of tens of millivolts, is typically sufficient to generate an action potential in the muscle fiber.

At fast central synapses, postsynaptic cells make contact with presynaptic axon swellings called **varicosities** when they occur along fine axons and **boutons**

when they are located at the tips of terminals. Each varicosity or bouton contains one active zone or a few of them. The postsynaptic process is often on a fine dendritic branch or tiny spine with a length of a few micrometers, having a very high input resistance and capable of generating active propagating responses. At inhibitory GABAergic synapses and excitatory glutamatergic synapses,^{26,27} each action potential releases from 5 to 10 quanta, and each quantum released elevates transmitter concentration^{28–30} in the cleft to about 1 mM and activates about 30 ion channels. At excitatory synapses, this release may be sufficient to generate EPSPs of 1 mV or less in amplitude, clearly subthreshold for generating action potentials. But central neurons often receive thousands of inputs, each of which has a “vote” on how the cell should respond. No input has absolute, or even majority, control over postsynaptic cell activity, but the matching of quantal size to input resistance ensures that inputs are reasonably effective. Consequently, at synapses onto larger central neurons with lower input resistances, quanta open between 100 and 1000 postsynaptic channels.

Synaptic Vesicles Are Recycled

A constant supply of vesicles filled with transmitter must be available for release from the nerve terminal at all times. Maintaining this supply requires the efficient recycling of synaptic vesicles. For this purpose, two partly overlapping cycles are utilized: one for the components of the synaptic vesicle membrane and another for the vesicle contents (transmitter substances). The cycles overlap from the time of transmitter packaging into vesicles until exocytosis. The cycles are distinct during the stages in which vesicle membrane and transmitter are recovered for reuse. The various steps of these cycles are common to all chemical synapses and are summarized in Fig. 7.2.

Vesicle Membrane Cycle

The components of the synaptic vesicle membrane are initially synthesized in the cell body before being transported to nerve terminals by fast axoplasmic transport^{31,32} (see Chapter 4). Within the nerve terminal, the synaptic vesicles are loaded with transmitter and either anchored to each other and actin filaments³³ or targeted to plasma membrane docking sites at active zones. These docking sites are also rich in clusters of high-voltage-activated Ca^{2+} channels^{3,34} (mainly N-type, P-type, and Q-type Ca^{2+} channels, depending on the synapse^{35,36}; see Chapter 6). Depolarization of the plasma membrane by an invading action potential opens these voltage-dependent Ca^{2+} channels to admit Ca^{2+} ions in the neighborhood of docked vesicles. The

local high concentration of Ca^{2+} resulting from the opening of multiple Ca^{2+} channels triggers exocytosis. After exocytosis, some vesicles may rapidly reclose, whereas others fuse fully with the plasma membrane.^{37,38} The latter are recovered by **endocytosis**, a budding off of the vesicular membrane to form a new “coated” vesicle covered by the protein *clathrin*. Endocytosis may also be regulated by presynaptic $[\text{Ca}^{2+}]$.^{39,40} Recovered vesicular membrane often fuses to form large membranous sacs, called *endosomes* or *cisternae*, from which new synaptic vesicles are formed. Molecular mechanisms of the vesicle cycle of exo- and endocytosis are discussed later in this chapter.

Transmitter Cycle

The steps of the transmitter cycle vary with the type of transmitter. Some transmitters are synthesized from precursors in the cytoplasm before transport into synaptic vesicles, whereas other transmitters are synthesized in synaptic vesicles from transported precursors. Peptide transmitters are synthesized exclusively in the cell body and are not locally recycled. At most synapses, a transporter that harnesses the energy in the proton gradient across the vesicular membrane functions to concentrate transmitter (or transmitter precursors) in vesicles.⁹ The pH gradient arises from the action of a vacuolar proton ATPase that uses the energy of ATP hydrolysis to transport protons into vesicles. After exocytosis, released transmitter diffuses across the synaptic cleft and rapidly binds to receptors. As transmitter falls off receptors, it is typically recovered from the synaptic cleft by sodium-dependent uptake transporters (see Chapters 8 and 9). At cholinergic

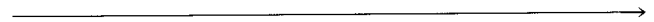
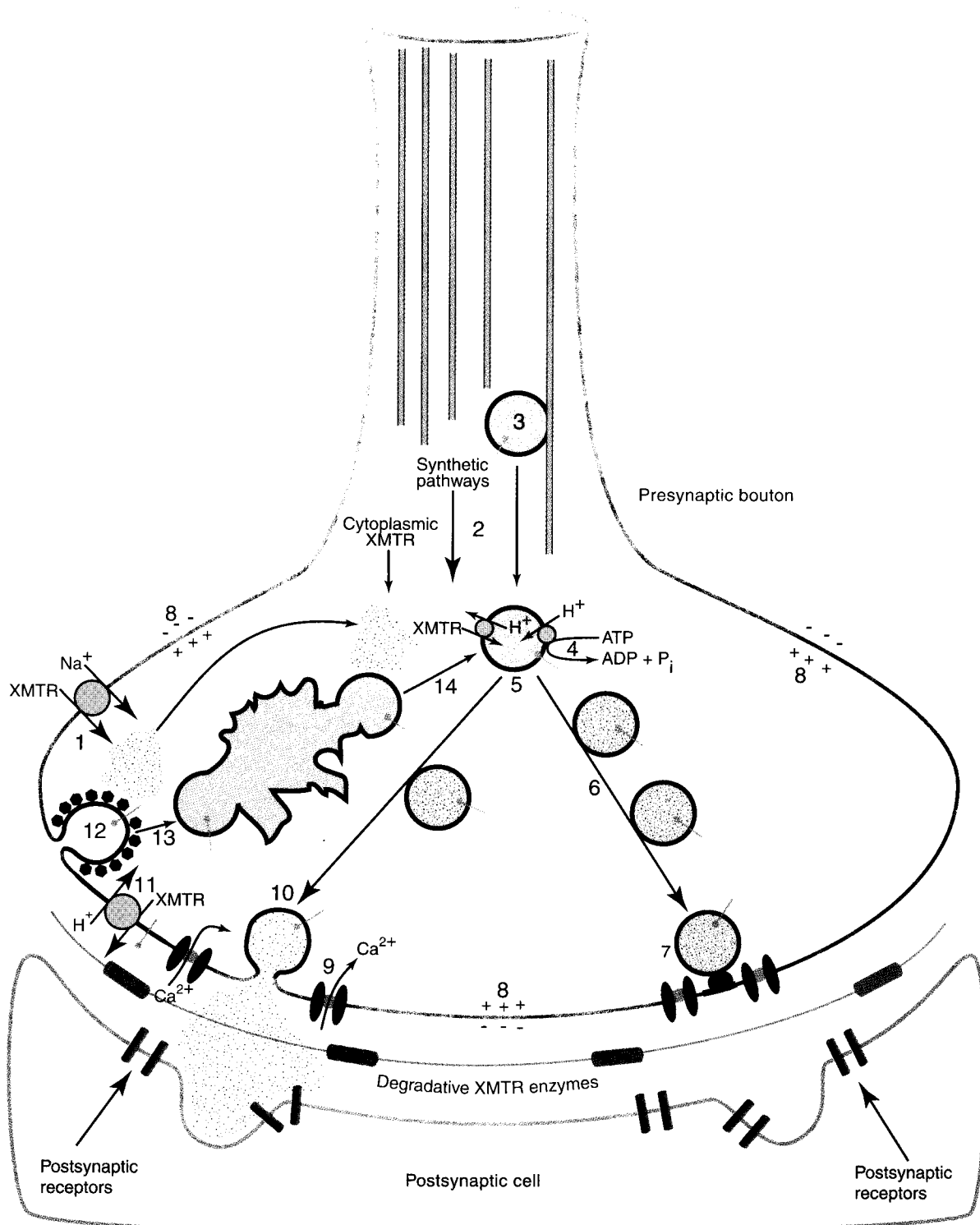


FIGURE 7.2 Steps in the life cycle of synaptic vesicles: (1) Na^+ -dependent uptake of transmitter (XMTR) or XMTR precursors into the cytoplasm, (2) synthesis of XMTR, (3) delivery of vesicle membrane containing specialized transmembrane proteins by axoplasmic transport on microtubules, (4) production of transvesicular H^+ gradient by vacuolar ATPase, (5) concentration of XMTR in vesicles by H^+ /XMTR antiporter, (6) synapsin I-dependent anchoring of vesicles to actin filaments near active zones, (7) releasable vesicles docked in active zones near Ca^{2+} channels, (8) depolarization of nerve terminal and presynaptic bouton by action potential, (9) opening of Ca^{2+} channels and formation of regions of local high $[\text{Ca}^{2+}]$ (“ Ca^{2+} microdomains”) in active zones, (10) triggering of exocytosis of docked vesicles comprising quantal units of XMTR release by overlapping Ca^{2+} microdomains, (11) nonquantal leakage of XMTR through vesicle membrane fused with plasma membrane and exposure of vesicle proteins to synaptic cleft, (12) recovery of vesicle membrane by dynamin-dependent endocytosis of clathrin-coated vesicles, (13) fusion of coated vesicles with endosomal cisternae, (14) formation of synaptic vesicles from endosomes. Also shown are postsynaptic receptors with multiple XMTR binding sites and extracellular XMTR-degradative enzymes in synaptic cleft.



BOX 7.2

EVIDENCE FOR SOME OF THE EVENTS IN THE
LIFE HISTORY OF VESICLES

Numbers refer to the steps in Fig. 7.2.

1. Uptake of transmitter or transmitter precursors is prevented by specific inhibitors, such as *hemicholinium-3* block of choline uptake at cholinergic synapses, ultimately leading to failure of synaptic transmission.⁴¹
2. Cholinergic synapses can be identified by the presence of the synthetic enzyme choline acetyltransferase, GABAergic synapses by the enzyme *glutamic acid decarboxylase*, adrenergic synapses by the enzyme *dopamine β -hydroxylase*, and so forth.⁴²
3. Vesicular transport into nerve terminals is blocked by inhibitors of axoplasmic transport such as antibodies to the microtubule motor protein *kinesin*.^{31,32}
- 4, 5. The storage of transmitter in vesicles can be blocked by inhibitors of vacuolar ATPase, such as *bafilomycin A₁*, or of an H⁺-dependent transporter, such as *vesamicol* for acetylcholine.⁴³
6. Dephosphorylation of synapsin I inhibits vesicle movements and transmission, whereas its phosphorylation by Ca²⁺-calmodulin-dependent kinase II protects against this inhibition.^{33,44}
7. Toxins from *Clostridium* bacteria, which proteolyze the vesicular protein *synaptobrevin* or plasma mem-

brane proteins *SNAP-25* and *syntaxin*, block exocytosis, whereas mutants deficient in the vesicle protein *synaptotagmin* and injection of peptides derived from synaptotagmin show defects in evoked transmitter release (more details later in this chapter).

8. Block of action potential propagation by local application of *tetrodotoxin* prevents transmission, and depolarization by elevating potassium in the bath accelerates MPSP frequency, as long as Ca²⁺ is present in the medium.¹
- 9, 10. N- and P-type calcium channel antagonists, such as ω -conotoxin and ω -agatoxin IVA, prevent Ca²⁺ influx and block transmission at many synapses.^{35,36}
11. Cholinergic synapses show a nonquantal leak of acetylcholine that is enhanced after stimulation; it is blocked by vesamicol, the vesicular acetylcholine transport inhibitor, indicating that the leak is due to transport through vesicular membrane fused with the plasma membrane.⁴⁵
12. Endocytosis is blocked at high temperature in the *shibiri* mutant of *Drosophila*, which affects the protein *dynamin* in endocytosis of coated vesicles.^{46,47}

Morphological evidence for steps 13 and 14 in Fig. 7.2 is given in the text.

synapses, acetylcholine is hydrolyzed to acetate and choline by the enzyme acetylcholinesterase present in the synaptic cleft. This enzyme is saturated by the initial gush of transmitter following exocytosis but can keep up with its subsequent slower release from receptors. The choline so produced is recovered by a presynaptic choline transporter and made available for the synthesis of new transmitter.

Much of the evidence for the steps outlined in Fig. 7.2 comes from ultrastructural and pharmacological experiments. Some of this evidence is outlined in Boxes 7.2^{41–47} and 7.3.⁴⁸

Summary

Chemical synapses are ideally suited to permit one neuron to rapidly and effectively excite or inhibit the activity of another cell. A diversity of transmitters and receptors guarantees a multiplicity of postsynaptic

responses. The opportunity for presynaptic and postsynaptic interactions between inputs provides for marvelously complex computational capabilities. The packaging of transmitter into vesicles and its release in quanta enable a single action potential to secrete hundreds of thousands of molecules of transmitter almost instantaneously at a synapse onto another cell. Neurochemical and ultrastructural studies have provided a rich picture of the life cycle of synaptic vesicles from their exocytosis at active zones to their recovery by endocytosis, their refilling with transmitter, and redocking at release sites.

EXCITATION-SECRETION COUPLING

Shortly after an action potential invades presynaptic terminals at fast synapses, the synchronous release of

many quanta of transmitter generates the postsynaptic potential. Since the work of Locke⁴⁹ in 1894, the presence of calcium in the external medium has been known to be a requirement for transmission. What is the central role of Ca^{2+} in triggering neurosecretion?

Calcium Triggers Release of Transmitters at Internal Sites

Calcium was originally believed to act at an external site to enable neurons to release transmitter. The pioneering work of Bernard Katz¹ and his co-workers showed that Ca^{2+} acts intracellularly. This conclusion is based on many lines of evidence:

1. Calcium must be present only at the moment of invasion of the nerve terminal by an action potential for transmitter to be released.
2. Calcium entry is retarded by a large presynaptic depolarization, and transmitter release is delayed until the voltage gradient is reversed at the end of the pulse, whereupon Ca^{2+} enters and release occurs as an off-EPSP until Ca^{2+} channels close. Sodium influx is not necessary for secretion, and K^+ ions have no role.
3. Elevation of intracellular $[\text{Ca}^{2+}]$ accelerates the spontaneous release of quanta of transmitter.^{50,51} Stimulation in a Ca^{2+} -free medium reduces intracellular $[\text{Ca}^{2+}]$ and MEPP frequency.
4. The presence of Ca^{2+} channels in presynaptic terminals is shown by the ability to stimulate local action potentials that trigger release in a high- $[\text{Ca}^{2+}]$ medium when Na^+ action potentials are blocked with tetrodotoxin and K^+ channels are blocked with tetraethylammonium.
5. Divalent cations that permeate Ca^{2+} channels, such as Ba^{2+} and Sr^{2+} , support transmitter release, although only weakly. Cations that block Ca^{2+} channels, such as Co^{2+} and Mn^{2+} , block transmission⁵²; Mg^{2+} reduces transmission, perhaps by screening fixed surface charge and effectively hyperpolarizing the nerve.⁵³
6. Transmission depends nonlinearly on $[\text{Ca}^{2+}]$ in the bath, varying with the fourth power of $[\text{Ca}^{2+}]$, whereas Ca^{2+} influx remains a linear function of

BOX 7.3

HISTOLOGICAL TRACERS CAN BE USED TO FOLLOW VESICLE RECYCLING

An elegant picture of the life history of synaptic vesicles comes from studies using electron-dense or fluorescent markers of intracellular regions that have been in contact with the extracellular space. *Horseradish peroxidase* (HRP) is an enzyme that catalyzes the oxidation of diaminobenzidine, forming an electron-dense product that can easily be identified in tissues fixed with osmium tetroxide for electron microscopy; FM1-43 is an amphipathic styryl dye that becomes highly fluorescent on partitioning into cell membranes. When frog muscles were soaked in HRP and the motor neurons were stimulated at 10 Hz for 1 min, the enzyme appeared in coated vesicles in nerve terminals in regions outside active zones. After more prolonged stimulation, most of the HRP collected in endosomal cisternae, owing to the fusion of endocytotic vesicles with these organelles. When the HRP was washed out and the neurons were rested for an hour before fixation, HRP appeared in small clear synaptic vesicles in active zones. When rested neurons were stimulated again before fixation, this time in the absence of HRP, the filled vesicles gradually disappeared owing to their release by exo-

cytosis.¹⁷ Another study traced the uptake of FM1-43 into living motor nerve terminals with the use of confocal fluorescence microscopy. High-frequency stimulation for just 15 s in FM1-43 was marked by uptake of dye into nerve terminals. More prolonged stimulation followed by a period of rest without the dye in the bath resulted in the persistent staining of synaptic vesicles in active zones. Subsequent stimulation at 10 Hz gradually destained the terminals in minutes; destaining required the presence of Ca^{2+} in the medium and represented exocytosis of stained vesicles. After about 1 min, the rate of destaining decreased as the vesicle pool began to be diluted with unstained vesicles newly recovered by endocytosis.¹⁸ Exposing dissociated hippocampal neurons to FM1-43 at various times after stimulation showed that endocytosis proceeded for about 1 min after exocytosis. Cells loaded with dye and then restimulated began to destain about 30 s after endocytosis, which is a measure of the time needed for recycling of recovered vesicles into the pool of releasable vesicles.⁴⁸ These experiments provide a dynamic view of the life cycle of synaptic vesicles.

$[Ca^{2+}]$, indicating a high degree of Ca^{2+} cooperativity in triggering exocytosis.⁵²

7. At giant synapses in the stellate ganglion of squid, voltage-clamp recording of the presynaptic Ca^{2+} current reveals a close correspondence between Ca^{2+} influx and transmitter release, including an association between the off-EPSP and a delay in Ca^{2+} current until the end of large pulses (called a tail current).⁵⁴
8. Action potentials trigger no phasic release of transmitter when Ca^{2+} influx is blocked, even when presynaptic Ca^{2+} is tonically elevated by photolysis of photosensitive Ca^{2+} chelators; however, the elevated presynaptic $[Ca^{2+}]$ accelerates the frequency of MEPPs.⁵⁵

Vesicles Are Released by Calcium Microdomains

Single action potentials generate a Ca^{2+} rise of about 10 nM, which lasts a few seconds.^{56,57} This increment in $[Ca^{2+}]$ is a small fraction of the typical resting $[Ca^{2+}]$ of 100 nM. How can such a tiny change in $[Ca^{2+}]$ trigger a massive synchronous release of quanta, and why is secretion so brief compared with the duration of the $[Ca^{2+}]$ change?

As mentioned earlier, postsynaptic responses begin only 0.5 ms after an action potential invades nerve terminals. This synaptic delay includes the time taken for Ca^{2+} channels to begin to open after the peak of the action potential (300 μ s),⁵⁴ leaving only about 200 μ s after that for transmitter secretion and the start of a postsynaptic response. At this time, Ca^{2+} has barely begun to diffuse away from Ca^{2+} channel mouths. In an aqueous solution, $[Ca^{2+}]$ would be mainly confined to within 1 μ m of channel mouths—estimated roughly from the solution of the diffusion equation for a brief influx of M moles of Ca^{2+} ,

$$[Ca^{2+}] = M/8(\pi Dt)^{3/2} \exp(-r^2/4Dt),$$

where t is time after the influx, r is distance from the channel mouth, and D is the diffusion constant for Ca^{2+} , $6 \times 10^{-6} \text{ cm}^2 \text{ s}^{-1}$. In the cytoplasm, Ca^{2+} diffusion is retarded by intracellular organelles and the presence of millimolar concentrations of fast-acting protein-associated Ca^{2+} -binding sites with an average dissociation constant of a few micromolar. Together, these effects restrict Ca^{2+} microdomains to about 50 nm around channel mouths.

Furthermore, the 200 μ s preceding the postsynaptic response must include not only the time required for Ca^{2+} to reach its target but also the time required for Ca^{2+} to bind and initiate exocytosis and for transmitter

to diffuse across the synaptic cleft, bind to receptors, and begin to open channels. Thus, the presynaptic Ca^{2+} targets must be located within a few tens of nanometers of Ca^{2+} channel mouths. Neuromuscular junctions that are fast frozen during the act of secretion show vesicle fusion images in freeze-fracture planes of the presynaptic membrane about 50 nm from intramembranous particles thought to be Ca^{2+} channels (see Fig. 7.1C). Solution of the diffusion equation for a steady point source of Ca^{2+} influx in the presence of a nearly immobile fast-binding Ca^{2+} buffer reveals that approximately 100 μ s after a Ca^{2+} channel opens, $[Ca^{2+}]$ increases to more than 10 μ M at 50 nm from its source and to over 100 μ M at a distance of 10 nm.⁵⁸

This calculation considers only what happens in the neighborhood of a single open Ca^{2+} channel. However, when individual Ca^{2+} channels are labeled with biotinylated ω -conotoxin tagged with colloidal gold particles, more than 100 channels per active zone are seen in terminals of chick parasympathetic ganglia.³⁴ Any vesicle docked at such an active zone is likely to be surrounded by as many as 10 Ca^{2+} channels within a 50-nm distance. Even though not all these channels will open during each action potential, more than one channel is likely to open, so a vesicle will be influenced by Ca^{2+} entering through several nearby channels. At the squid giant synapse, more than 50 channels open in each $\sim 0.6\text{-}\mu\text{m}^2$ active zone, whereas 10 channels open within the more compact active zones of frog saccular hair cells.^{58,59} The Ca^{2+} microdomains of these channels overlap at single vesicles, and they cooperate in triggering secretion of a vesicle. Calculations of diffusion of Ca^{2+} ions from arrays of Ca^{2+} channels in the presence of a saturable buffer indicate that the $[Ca^{2+}]$ at sites where neurotransmitter release is triggered is likely to reach 100–200 μ M (Fig. 7.3).

Three indications that $[Ca^{2+}]$ in fact reaches very high levels in active zones during action potentials are:

1. $[Ca^{2+}]$ levels of over 100 μ M have been measured in presynaptic submembrane regions of squid giant synapses likely to be active zones by using the low-affinity Ca^{2+} -sensitive photoprotein *n*-aequorin-J.⁶⁰
2. Estimates of $[Ca^{2+}]$ based on the activity of Ca^{2+} -activated K^+ channels in active zones of mechanosensory hair cells are similar.⁶¹
3. Transmitter release is blocked only by presynaptic injection of at least millimolar concentrations of fast high-affinity Ca^{2+} chelators, indicating that release is triggered locally by high concentrations of Ca^{2+} .⁶²

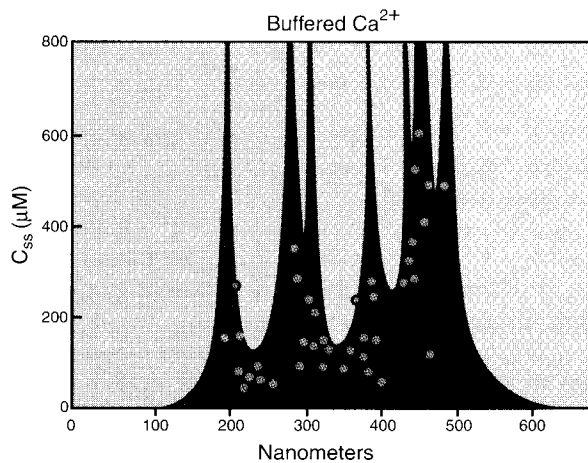


FIGURE 7.3 Computer simulations of steady-state $[Ca^{2+}]$ (designated C_{ss}) just below the plasma membrane in an active zone in frog saccular hair cells that have been depolarized for 100 μs . Open circles represent Ca^{2+} -activated K^+ channels, whose activity confirmed the high levels of $[Ca^{2+}]$. Docked vesicles are likely to be located in the troughs between rows of Ca^{2+} channels located at the peaks of the $[Ca^{2+}]$ profile. From Roberts.⁵⁸

Vesicle Exocytosis Is Normally Triggered by Overlapping Ca^{2+} Channel Microdomains of High $[Ca^{2+}]$

Although release of a quantum of transmitter subsequent to the opening of a single presynaptic Ca^{2+} channel has been observed,⁶³ exocytosis may normally be due to Ca^{2+} entering through clusters of Ca^{2+} channels in active zones and contributing to local high $[Ca^{2+}]$ at docked vesicles:

1. When transmitter release is increased under voltage clamp with pulses of increasing amplitude, a third-order power law relation exists between presynaptic Ca^{2+} current and postsynaptic response.⁶⁴ If each vesicle were released by Ca^{2+} entering through a single Ca^{2+} channel, then increasing depolarizations should recruit additional channel openings and proportionally more vesicle releases.⁶⁵ However, if Ca^{2+} channel microdomains from neighboring clustered Ca^{2+} channels overlap at docked vesicles, the $[Ca^{2+}]$ at each vesicle will rise with increasing depolarization as more channels are recruited, and some cooperativity of Ca^{2+} action in triggering secretion will be expressed.⁶⁶
2. In some neurons, more than one Ca^{2+} channel type contributes to secretion.^{35,36} When contributions of each channel type are isolated pharmacologically, their combined effects add nonlinearly,

much as would be predicted by a fourth-order cooperativity, indicating that the Ca^{2+} microdomains of different channels overlap and summate within individual active zones.

3. When transmitter release is increased by prolonging presynaptic depolarizations (e.g., by broadening action potentials with K^+ channel blockers), more channels are not likely to be opened simultaneously. Rather, as channels that open early in the action potential close, others open; so the pattern of presynaptic Ca^{2+} microdomains is not so much intensified as prolonged, leading to a more nearly linear relation between increases in Ca^{2+} influx and transmitter release.⁵⁷
4. Large depolarizations admit little Ca^{2+} as they approach the Ca^{2+} equilibrium potential; they are therefore accompanied by a reduced Ca^{2+} current and reduced transmitter release during a pulse. However, large depolarizations can release more transmitter than can small depolarizations evoking a given macroscopic Ca^{2+} current.^{54,67} This apparent voltage dependence of transmitter release may be due to the different spatial profiles of $[Ca^{2+}]$ in the active zone, with greater overlap of $[Ca^{2+}]$ from the larger number of more closely apposed open Ca^{2+} channels during large depolarizations.⁶⁶

The Exocytosis Trigger Must Have Fast, Low-Affinity, Cooperative Ca^{2+} Binding

The brevity of the synaptic delay implies not only that Ca^{2+} acts near Ca^{2+} channels to evoke exocytosis but also that Ca^{2+} must bind to its receptor extremely rapidly. This is confirmed by the finding that presynaptic injection of relatively slow Ca^{2+} buffers such as ethylene glycol bis(β -aminoethyl ether) N,N' -tetraacetic acid (EGTA) have almost no effect on transmitter release to single action potentials. Only millimolar concentrations of fast Ca^{2+} buffers such as 1,2-bis(2-aminophenoxy)ethane- N,N,N',N' -tetraacetic acid (BAPTA), with on-rates of about $5 \times 10^8 M^{-1} s^{-1}$, can capture Ca^{2+} ions before they bind to the secretory trigger,⁶² indicating that the on-rate of Ca^{2+} binding to this trigger is similarly fast. At a rate of $5 \times 10^8 M^{-1} s^{-1}$, 100 μM $[Ca^{2+}]$ reaches equilibrium with its target in about 50 μs .

From the dependence of transmitter release on external $[Ca^{2+}]$, we know that at least four Ca^{2+} ions cooperate in the release of a vesicle. The off-rate of Ca^{2+} dissociation from these sites also must be fast, at least $10^3 s^{-1}$, to account for the rapid termination of transmitter release (0.25-ms time constant) after Ca^{2+}

channels close and Ca^{2+} microdomains collapse. The high temperature sensitivity of the time course of transmitter release ($Q_{10} \approx 3$) indicates that exocytosis is rate limited by a step with a high energy barrier.⁵⁹ This step is likely to be the process of exocytosis itself. If Ca^{2+} binding is not rate limiting, its dissociation rate must be substantially faster than 10^3 s^{-1} . This means that the affinity of the secretory trigger for Ca^{2+} is low, with a dissociation constant (K_D) above $10 \mu\text{M}$.

The Ca^{2+} -binding trigger is not saturated under normal conditions, because increasing $[\text{Ca}^{2+}]$ in the bath increases release. Furthermore, because of the speed with which Ca^{2+} binds to its sites, this reaction will nearly equilibrate during the typical 0.5–1.0 ms that $[\text{Ca}^{2+}]$ remains high before Ca^{2+} channels close at the end of an action potential. If $[\text{Ca}^{2+}]$ reaches $100 \mu\text{M}$ or more in equilibrium with unsaturated release sites, the affinity of at least some of those sites binding Ca^{2+} must be similar to $100 \mu\text{M}$ or lower.

These predictions are consistent with experiments in which neurosecretion is triggered by photolysis of caged Ca^{2+} chelators such as DM-nitrophen. Partial flash photolysis of partially Ca^{2+} -loaded DM-nitrophen generates a $[\text{Ca}^{2+}]$ "spike" of a duration similar to the lifetime of Ca^{2+} microdomains around Ca^{2+} channels opened by an action potential.⁶⁸ This spike results in a postsynaptic response that closely resembles the normal EPSC at crayfish neuromuscular junctions, confirming that no presynaptic depolarization is necessary to obtain high levels of phasic transmitter release. As expected, secretion resembled a fourth-power function of peak $[\text{Ca}^{2+}]$. The peak presynaptic $[\text{Ca}^{2+}]$ needed for normal-amplitude postsynaptic responses was about $75 \mu\text{M}$. This concentration is somewhat less than the level thought to normally trigger neurosecretion; however, in the photolysis experiments, all docked vesicles, not just those nearest Ca^{2+} channels that open, were uniformly activated.

In similar experiments on retinal bipolar neurons from fish,⁶⁹ fully loaded DM-nitrophen was photolyzed to produce a stepped increase in $[\text{Ca}^{2+}]$ while secretion was monitored as an increase in membrane capacitance, a measure of cell membrane area increased by fusion of vesicles. Calcium ion concentration had to be raised by more than $20 \mu\text{M}$ before a fast phase of secretion developed. The sharp Ca^{2+} dependence of release and short synaptic delays were fitted by a model with a high degree of positive Ca^{2+} cooperativity, in which four successive Ca^{2+} ions bind with affinities increasing (or K_D decreasing) from 140 to $9 \mu\text{M}$, followed by a Ca^{2+} -independent rate-limiting step. These biophysical experiments provide a fairly detailed characterization of the Ca^{2+} receptor responsible for transmitter release.

Calcium Ions Must Mobilize Vesicles to Docking Sites at Slowly Transmitting Synapses

Most peptidergic synapses and some synapses releasing biogenic amines display kinetics remarkably different from those of fast synapses. In these slower synapses, single action potentials often have no discernible postsynaptic effect. During repetitive stimulation, postsynaptic responses rise slowly, often with a delay of seconds from the beginning of stimulation, and persist for just as long after stimulation ceases. Such slow responses are due to many factors: the postsynaptic receptors may have intrinsically sluggish second messengers or G proteins (Chapter 10); the postsynaptic receptors are often distant from release sites, so extracellular diffusion takes significant time; and release starts after the beginning of stimulation and continues after stimulation stops. Given these limitations, it is not surprising that single quanta are never discernible, either as spontaneous PSPs or as components of evoked responses.

The ultrastructural anatomy of presynaptic terminals of slowly transmitting synapses also is different from that of fast synapses. Transmitter is stored in large, dense core vesicles scattered randomly throughout the cytoplasm; vesicles do not tend to cluster at active zones or to line up at the membrane, docked and ready for release. Nevertheless, there is no doubt that transmitter is released from vesicles, because it is both stored and often synthesized in them, and they can be seen to undergo exocytosis during high-frequency stimulation causing high rates of release.⁷⁰

A High-Affinity Calcium-Binding Step Controls Secretion of Slow Transmitters

Calcium ions are required for excitation–secretion coupling in slow synapses, but the dependence of release on $[\text{Ca}^{2+}]$ is linear, in contrast with fast synapses.⁷¹ Furthermore, because few vesicles are predocked at active zones, most of those released by repetitive activity are not exposed to the local high $[\text{Ca}^{2+}]$ near Ca^{2+} channels. Thus, an important event triggered by Ca^{2+} influx in action potentials is likely to be the translocation of dense core vesicles to plasma membrane release sites, followed by exocytosis. This process has a very different dependence on $[\text{Ca}^{2+}]$ than does the release of docked vesicles. Measurements of $[\text{Ca}^{2+}]$ during stimulation indicate that release correlates well with $[\text{Ca}^{2+}]$ levels in the low micromolar range above a minimum, or threshold, level of a few hundred nanomolar.^{72,73}

A striking difference between the release of fast

transmitters, such as GABA and glutamate, and peptide transmitters, such as cholecystokinin, was found in studies of **synaptosomes**, isolated nerve terminals prepared from homogenized brain tissue by differential centrifugation.⁷⁴ When terminals were depolarized to admit Ca^{2+} through Ca^{2+} channels, the amino acid transmitters GABA and glutamate were released at much lower levels of bulk cytoplasmic $[\text{Ca}^{2+}]$ than when Ca^{2+} was admitted more uniformly and gradually across the membrane by use of the Ca^{2+} -transporting ionophore ionomycin. Peptides were released at the same low levels of $[\text{Ca}^{2+}]$ no matter which method was used to elevate $[\text{Ca}^{2+}]$. Thus, only amino acids were sensitive to the difference in $[\text{Ca}^{2+}]$ gradients imposed by the two methods and were preferentially released by local high submembrane $[\text{Ca}^{2+}]$ caused by depolarization. Apparently, peptides are released by a high-affinity rate-limiting step not especially sensitive to submembrane $[\text{Ca}^{2+}]$ levels.

Slow and Fast Transmitters May Be Coreleased from the Same Neuron Terminal

Some neurons have both small synaptic vesicles containing acetylcholine or glutamate and large, dense core vesicles containing neuropeptides.⁷⁵ Often, the two transmitters act on different targets. Single action potentials release only the fast transmitter, so different patterns of activity can have very different relative effects on the targets. For example, postganglionic parasympathetic nerves to the salivary gland release acetylcholine, which stimulates salivation, and vasoactive intestinal peptide, which stimulates vasodilation. Many examples of the corelease of multiple transmitters have been described.

Summary

Ca^{2+} acts as an intracellular messenger tying the electrical signal of presynaptic depolarization to the act of neurosecretion. At fast synapses, Ca^{2+} enters through clusters of channels near docked synaptic vesicles in active zones. It acts at extremely short distances (tens of nanometers) in remarkably little time (200 μs) and at very high local concentrations ($\geq 100 \mu\text{M}$), in calcium microdomains, by binding cooperatively to a low-affinity receptor with fast kinetics to trigger exocytosis. Some transmitters, such as peptides and some biogenic amines, are stored in larger, dense core vesicles not docked at the plasma membrane in active zones. Release of these transmitters, as well as their diffusion to postsynaptic targets and their postsynaptic actions, is much slower than that of transmitters such as acetylcholine and amino acids at fast synapses. Re-

lease of slow transmitters depends linearly on $[\text{Ca}^{2+}]$ and may be governed by a Ca^{2+} -sensitive rate-limiting step different from that triggering exocytosis of docked vesicles at fast synapses.

MOLECULAR MECHANISMS OF TRANSMITTER RELEASE

The primary function of the synaptic vesicle is transmitter exocytosis. This function is accomplished by the rapid, calcium-regulated fusion of the synaptic vesicle membrane with the presynaptic plasma membrane. After exocytosis, the components of the synaptic vesicle membrane are selectively recovered from the plasma membrane by endocytosis and recycled within the nerve terminal to generate new synaptic vesicles. This local recycling pathway, known as the **exo-endocytic cycle**, provides a mechanism by which neurons can maintain a constant supply of synaptic vesicles in the nerve terminal without reliance on the biosynthetic machinery in the cell body (which at some synapses can be more than 1 m away). The recycling capacity of the nerve terminal is thus essential for the consistent release of neurotransmitter in response to stimulation conditions of variable frequency and duration. The primary steps of the synaptic vesicle exo-endocytic cycle (illustrated in Fig. 7.2) include:

- Transmitter uptake from the cytoplasm
- Cytoskeletal and intervesicular anchoring
- Plasma membrane docking
- Membrane fusion (exocytosis)
- Endocytosis and recycling

Each step of the synaptic vesicle exo-endocytic cycle takes place at a site at which calcium or other second messengers may directly regulate or indirectly modulate transmitter secretion. Modulation of the strength or efficacy of synaptic signaling, commonly known as **synaptic plasticity**, plays an important role both in the development of synaptic connections and in the functioning of the mature nervous system. The synaptic vesicle exo-endocytic cycle is a prime target for such modulation. The combined use of biochemical, molecular genetic, and biophysical techniques is leading to an understanding of the molecular mechanisms that underlie the synaptic vesicle exo-endocytic cycle and the regulation of transmitter secretion.

Synaptic Vesicles Can Be Purified and Biochemically Characterized

How does one investigate the mechanisms that underlie transmitter release? A biochemical approach,